TECHNISCHE UNIVERSITÄT
ILMENAU

Self-Optimized Energy Saving Using Cell Fingerprinting for Future Radio Access Networks

PhD Thesis

by

Elke Roth-Mandutz

Reviewers

Prof. Dr.-Ing. habil. Andreas Mitschele-Thiel

Prof. Dr.-Ing. habil. Armin Zimmermann

Prof. Dr.-Ing. Jens Mückenheim

A dissertation to obtain the academic degree Doktoringenieur (Dr.-Ing.)
Faculty of Computer Science and Automation, TU Ilmenau

submitted on: 06.11.2015
defended on: 22.06.2016

urn:nbn:de:gbv:ilm1-2016000323

TECHNISCHE UNIVERSITÄT
ILMENAU

Self-Optimized Energy Saving Using Cell Fingerprinting for Future Radio Access Networks

Dissertation

von

Elke Roth-Mandutz

Gutachter

Prof. Dr.-Ing. habil. Andreas Mitschele-Thiel

Prof. Dr.-Ing. habil. Armin Zimmermann

Prof. Dr.-Ing. Jens Mückenheim

Dissertation zur Erlangung des akademischen Grades Doktoringenieur (Dr.-Ing.)
Fakultät für Informatik und Automatisierung, TU Ilmenau

eingereicht am: 06.11.2015
verteidigt am: 22.06.2016

urn:nbn:de:gbv:ilm1-2016000323

Abstract

Environmental sustainability and the strongly raising energy bill of network operators demand the implementation of energy reduction strategies in future radio access systems. The sharp rise in energy consumption is mostly caused by the exponential increase of data traffic in cellular networks demanding the deployment of a huge number of additional base stations (BSs). As the BS consumes the largest share of the energy in a cellular network, they offer a high energy saving potential. Energy consumption can be reduced in a self-organized way by adapting the network capacity in response to the instantaneous traffic demand. Thus, cells are deactivated and reactivated in line with the changing traffic demand. Cell deactivation can be implemented as a straight forward process. Each cell can easily determine, when its traffic has significantly reduced.

In this thesis, we concentrate on the complex problem of how to identify cells to be reactivated in situations of rising traffic demand. Reliable cell identification under any given traffic condition is the key for the implementation of the self-optimized energy saving approach. We propose the use of the fingerprint method, to identify the best fitting cell to take over the increasing traffic volume from highly loaded neighbor cells.

The first step is to generate the cell individual fingerprints, while all cells are active. Cells are found to be characterized by the received signal strength (RSS) measured by mobile device as observed in the neighbors cells. Consequently, a fingerprint consists of the list of neighbor cells and the associated RSS metrics that map the neighbor cell RSS distributions.

The second step is to identify and subsequently activate the most suitable sleeping cell(s) to relieve the active cell in overload. Initially, the overloaded cell requests a high data rate demanding mobile to measure the RSS of the active neighbor cells. This measurement sample is matched with each cell fingerprint representing a sleeping cell. The cell fingerprint that corresponds best to the sample is expected to provide the best radio conditions for the traffic volume demanding mobile. We validate the accuracy of the matching algorithm by considering different traffic situations. Results show that the accuracy increases with traffic load and number of metrics used for the matching, both of which provide more matching events.

Finally, a simple model is created to evaluate the energy saving potential of cell fingerprinting. Input for the model is the hit rate of the most suitable cell achieved during the preceding cell fingerprinting simulation studies. The saving potential approaches closely the optimum results, if the most suitable cell would have been known.

Although the practical applicability of the cell fingerprint approach is demonstrated on an LTE network simulator for energy saving, it is a generic approach. It is designed for all current generations of radio access network technologies and works for any cell identification application in cellular networks.

Zusammenfassung

Ökologische Nachhaltigkeit, aber auch die stark steigenden Energiekosten, verlangen nach neuen Strategien zur Senkung des Stromverbrauchs zukünftiger Mobilfunksysteme. Der drastische Anstieg des Stromverbrauchs zellularer Netze wird weitgehend durch die hohe Anzahl zusätzlicher Basisstationen (BS) verursacht, die zur Übertragung des exponentiell wachsenden Datenvolumens benötigt werden. Die BS bietet als größter Stromverbraucher eines Mobilfunknetzes ein sehr hohes Einsparungspotential. Durch selbstorganisierte Verfahren kann die zur Verfügung gestellte Netzkapazität kontinuierlich an die aktuell benötigte Kapazität angepasst werden, indem Funkzellen deaktiviert und, bei Bedarf, reaktiviert werden. Das Deaktivieren der Zellen kann als relativ einfacher Prozess implementiert werden, da jede Zelle die Abnahme des Datenverkehrs selbstständig erkennen kann.

Die zentrale Fragestellung dieser Arbeit ist, wie die geeignete, inaktive Zelle identifiziert und somit reaktiviert werden kann, sobald zusätzliche Netzkapazität erforderlich ist. Voraussetzung dafür ist es, zuverlässig unter jeder beliebigen Verkehrsbedingung die Identifizierung der am besten geeigneten, inaktiven Zelle zu gewährleisten. Dafür wird das Fingerprinting-Verfahren eingesetzt.

Der erste Schritt ist dabei die Generierung eines individuellen Datensatzes (Fingerabdrucks) jeder Zelle. Dafür messen die mobilen Endgeräte im gesamten Zellbereich die Empfangsfeldstärke der Nachbarzellen. Dementsprechend besteht der Fingerabdruck einer Zelle aus der Liste der Nachbarzellen und Metriken, die die Verteilung der Empfangsfeldstärke der jeweiligen Nachbarzelle abbilden.

Als zweiter Schritt wird die inaktive Zelle, die am besten geeignet ist das zunehmende Datenvolumen zu übernehmen, identifiziert und anschließend reaktiviert. Dafür fordert die überlastete Zelle zunächst Endgeräte mit hoher Datenlast auf, die Empfangsfeldstärke der aktiven Nachbarzellen zu messen. Diese Messwerte werden mit den Fingerabdrücken jeder inaktiven Nachbarzelle abgeglichen. Es wird angenommen, dass die inaktive Zelle deren Fingerabdruck am besten mit den Messwerten des Endgeräts übereinstimmt, die besten Funkbedingungen für mobile Endgeräte mit hohem Datenvolumen zur Verfügung stellt. Anschließend wird die Matching-Genauigkeit bei variierendem Datenaufkommen im Netz verifiziert. Die erzielten Ergebnisse zeigen, dass die Genauigkeit die passende Zelle zu identifizieren, sowohl von der Anzahl aktiver Nachbarzellen als auch von der Anzahl und Art der eingesetzten Matching-Metriken abhängt.

Zum Abschluss wird basierend auf einem vereinfachten Modell das Einsparungspotential berechnet, das durch Einsatz der Fingerprinting-Methode erreicht werden kann. Als Input werden die in den vorangegangenen Simulationsstudien ermittelten Genauigkeiten eingesetzt, mit denen die richtige Zelle unter vorgegebenen Verkehrsbedingungen identifiziert werden konnte. Das Einsparungspotential nähert sich dabei der maximal möglichen Stromeinsparung an, die erzielt würde, falls die richtige Zelle bekannt wäre.

Obwohl der Fingerprinting-Ansatz durch Simulationen mit einem LTE-Funknetz demonstriert wurde, handelt es sich um einen generischen Ansatz, der für alle derzeitigen Generationen von Mobilfunksystemen und unterschiedliche Anwendungen einsetzbar ist.

To Bernhard, Felix, and Senta
and to my parents Irmgard and Maximilian Roth

"All our dreams can come true, if we have the courage to pursue them."

Walt Disney

Acknowledgement

I would like to take the opportunity, to thank all the people for their outstanding support I received during my entire PhD work. This PhD thesis was carried out within the Integrated Communication Systems group as part of the International Graduate School of Mobile Communications. It was mostly financed by a doctoral sponsorship of the Bavarian universities of applied science for women with qualified professional experience.

I would like to express my most sincere thanks to my advisor Prof. Andreas Mitschele-Thiel for the guidance and mentorship he provided to me from the very beginning, when he encouraged me to start, through the completion of this work. At the same time, I thank Prof. Armin Zimmermann and Prof. Jens Mückenheim for all their valuable advices and time to review my thesis.

As a member of the SON-team, using the Alcatel-Lucent simulator for our studies, I would like to thank Siegfried Klein and Dr. Edgar Kühn from Alcatel-Lucent Bell Labs, Germany for their support with the simulator libraries and for reviewing my publications. In the same light, I would like to thank my SON team members Dr. Stephen Mwanje, Nauman Zia, and Dr. Naseer Ul-Islam for sharing the ideas and the support they offered to me. Especially, many thanks for the numerous and very fruitful discussions with Stephen, where I particularly enjoyed his open mind and constructive proposals.

It was a pleasure to work with my colleagues from the International Graduate School of Mobile Communications. I like to thank all of them, but particularly Dr. Oleksandr Artemenko, for their support and suggestion, especially during the numerous presentations. A special thanks for proofreading parts or even my complete thesis: Andreas Mitschele-Thiel, Stephen Mwanje, Jens Mückenheim, Oleksandr Artemenko, Monika Blößl and my family. Last but not least, I would like to thank Nicole Sauer, Jennifer Unbehaun, Nadine Wolf, Dr. Mirko Kirschkowski, and Jürgen Schmidt from the TU Ilmenau for their friendly and engaged administrative and technical support.

I also would like to express my warmest thanks to my nice colleagues and friends from the TH Nürnberg Georg Simon Ohm. Especially many thanks to Prof. Patricia Brockmann, who encouraged me to start the PhD, for her friendly advices and support throughout this time. My thanks also go to Prof. Sibylle Kisro-Völker for her support on the scholarship, as well as my nice colleagues at the TH Nürnberg, especially Claudia Bär, Stephanie Schwertassek-Tieth and Lydia Krämer, who helped me to start and successfully perform my additional employment at the TH.

Most importantly, I thank my family, my parents, my husband Bernhard, and my children, Felix and Senta, for their immense confidence in my work and their unconditional support. Above all, Bernhard's support was fantastic, as he was always fully behind me and motivated me to keep going.

Contents

Abstract i

Zusammenfassung ii

Acknowledgement v

List of Figures ix

List of Tables xii

1 Introduction 1
- 1.1 Self-Organized Energy Saving . . . 2
- 1.2 Thesis Scope and Objectives . . . 3
- 1.3 Thesis Novelty and Contribution . . . 5
- 1.4 Terminology for Cell Identification . . . 6
- 1.5 Organization of Thesis . . . 6

2 Context and Related Work 8
- 2.1 Energy Saving in Radio Access Networks . . . 9
  - 2.1.1 Research Work on Sustainable RAN . . . 9
  - 2.1.2 Classification of Energy Saving Approaches . . . 10
  - 2.1.3 Load Aware Energy Saving Approaches . . . 12
  - 2.1.4 Assessment of Energy Saving Approaches . . . 14
- 2.2 Network Constraints and Organizational Aspects for Energy Saving . . . 15
  - 2.2.1 System Model: The LTE RAT . . . 15
  - 2.2.2 Base Station Power Consumption . . . 17
  - 2.2.3 Radio Network Layout . . . 20
  - 2.2.4 Energy Saving Use Case in Self-Organizing Networks . . . 23
  - 2.2.5 Energy Saving in 3GPP - Management Support for Potential Solutions . . . 25
  - 2.2.6 Architecture Solutions for Self-Organizing Approaches . . . 26

2.3 Temporary Cell Deactivation and its Energy Saving Potential in Operational Networks . . . 27
2.3.1 Cell Deactivation Strategies . . . 27
2.3.2 Spatial and Temporal Traffic Variation . . . 29
2.3.3 Energy Saving Potential based on Operational Network Data in Literature . . . 30
2.3.4 Side Effects of Temporary Cell Deactivation . . . 32
2.4 Strategies for Cell Activation and Identification . . . 33
2.4.1 Overview of the Fingerprinting Method in Wireless Communication 33
2.4.2 Fingerprinting Use for the Identification of Sleeping Cells . . . 34
2.4.3 Parameters for Cell Coverage Identification . . . 35
2.4.4 Sleeping Cell Identification Strategies . . . 36

3 Network Simulation 39
3.1 Evaluation Methods . . . 39
3.2 Simulated Network . . . 40
3.3 Mobile Users . . . 41
3.4 Radio Propagation Modeling . . . 42
3.4.1 BS Transmit Power and Antenna Configuration . . . 43
3.4.2 Pathloss . . . 43
3.4.3 Shadow Fading . . . 43
3.5 Simulation Model . . . 43
3.5.1 Generic Processing . . . 43
3.5.2 Cell Fingerprinting Application . . . 44

4 Cell Fingerprinting Approach - the Framework 46
4.1 Cell Fingerprint Overview - Data Processing . . . 47
4.2 Definition of RSS Metrics for Cell Identification . . . 48
4.2.1 Analysis of Neighbor Cell RSS Measurements . . . 48
4.2.2 Single Cell Fingerprint Metrics - Basic Set . . . 49
4.2.3 Outlier Definition . . . 51
4.2.4 Combined Cell Fingerprint Metric - Basic Sum . . . 52
4.3 Cell Fingerprint Generation . . . 54
4.4 Cell Fingerprint Processing During Cell Deactivation . . . 55
4.5 Cell Activation Using Cell Fingerprints . . . 56
4.5.1 Matching Procedure . . . 58
4.5.2 Cell Identification Based on Cell Fingerprints - Example . . . 60

5 Simulation Studies 62
5.1 Performance Indicators to Determine the Cell Fingerprint Accuracy . . . 63
5.1.1 Activation Set Size . . . 63
5.1.2 Energy Efficiency Index . . . 64
5.1.3 Accuracy Index . . . 65
5.2 Cell Fingerprinting Accuracy Using Basic CFP Metrics . . . 66
5.3 Averaged UE RSS Measurement Samples . . . 70
5.4 Reduction of Active Neighbor Cells . . . 73
5.4.1 Mapping Traffic Demand to Number of Active Cells . . . 73
5.4.2 Impact of Reduced Number of Active Neighbor Cells on Accuracy 74

5.5 Advanced Cell Fingerprint Metrics . . . 77
5.5.1 Difference to Median . . . 77
5.5.2 Additional Single Quantile CFP Metrics . . . 79
5.5.3 Advanced Set of Combined CFP Metrics . . . 81
5.5.4 Traffic Variation Impact on Advanced Single CFP Metrics . . . 83
5.5.5 Traffic Variation Impact on Combined CFP Metrics . . . 85
5.6 Summary . . . 86

6 Energy Savings Potential **88**
6.1 Energy Saving Model . . . 89
6.1.1 Daily Traffic Profile . . . 89
6.1.2 Network Layout . . . 90
6.1.3 Relative Power Saving Potential . . . 90
6.1.4 Assumptions for the Energy Saving Model . . . 91
6.2 Approaches for Cell Identification . . . 92
6.3 Results and Evaluation of the Energy Saving Potential . . . 96
6.4 Limits and Constraints of the Energy Saving Model . . . 98

7 Conclusion and Future Work **100**
7.1 Contributions and Constraints . . . 100
7.2 Energy Saving in Operational Networks . . . 102
7.3 Use of Cell Fingerprinting for Future Applications . . . 103

Glossary **106**

List of Acronyms **108**

Bibliography **111**

Erklärung **120**

List of Figures

1.1 Growth in Number of Mobile Subscribers . . . 2
1.2 Evolution of Mobile Data Traffic . . . 2
1.3 Energy Consumption of Cellular Network Components . . . 2
1.4 Energy Saving Self-Organized Network . . . 3
1.5 Cell Terminology: Target Cell, Best Matching Cell . . . 6

2.1 Global Carbon Footprint of Radio Access Networks . . . 10
2.2 Classification of Energy Saving Fields in Green Cellular Access Networks 11
2.3 Daily Traffic Profile for Cellular Networks in Europe . . . 13
2.4 Overview of LTE Network Components and Interfaces . . . 15
2.5 Generic Terms vs. LTE Terms for Cell Fingerprinting . . . 16
2.6 Main Power Consuming Components for Different Cell Types . . . 18
2.7 LTE Macro BS: Load Dependent Estimate of the Power Model . . . 19
2.8 Homogeneous vs. Heterogeneous Network . . . 21
2.9 Energy Saving States and Transitions in 3GPP . . . 26
2.10 UML Activity Diagram: Centralized Approach for Cell Deactivation . . . 29
2.11 Daily Traffic Profile of a Business Cell . . . 30
2.12 Daily Traffic Profile of a Residential Cell . . . 30
2.13 Phases of the Generic Fingerprinting Method . . . 34
2.14 Selected Measurements and Methods for Cell Identification in Cellular Networks . . . 35

3.1 Simulated Network Structure . . . 40
3.2 Mirrored Wrap-Around Network Structure . . . 40
3.3 Simulation Run for Cell Fingerprinting . . . 44

4.1 Overview of the Cell Fingerprint Approach . . . 47
4.2 RSS of Neighbor Cells Measured by UE . . . 48
4.3 Examples for Typical RSS Neighbor Cell Distributions . . . 49
4.4 RSS Distributions: Different Types of Neighbor Cells . . . 50
4.5 Example: Typical Neighbor Cell RSS Distribution with Fence Values for CFP Metrics . . . 50

4.6 Outlier Detection based on Interquartile Range: Upper and Lower Fence . 52
4.7 Weighting Factors for CFP Metrics 53
4.8 UML Activity Diagram: Cell Fingerprint Generation 54
4.9 Cell Fingerprint Structure 55
4.10 UML Activity Diagram: Cell Deactivation for Cell Fingerprinting Approach 56
4.11 UML Activity Diagram: Cell Activation Procedure for Cell Fingerprinting Approach 57
4.12 Data Flow of the Matching Procedure 58
4.13 Pseudo Code: Matching Algorithm 59
4.14 Example: Cell Identification Using CFP - Measurement Retrieval 60
4.15 Example: Cell Identification Using CFP - Processing 61

5.1 Calculation of the Activation Set Size (ASS) 64
5.2 Example: Use of the Activation Set Size (ASS) 64
5.3 Example: Use of the Energy Efficiency Index (EEI) 65
5.4 Example: Use of the Accuracy Index (AI) 66
5.5 Activation Set Size for Basic CFP Metrics 67
5.6 Energy Efficiency Index for Basic CFP Metrics 68
5.7 Accuracy Index for Basic CFP Metrics 68
5.8 Average of the Last 2 Received UE Measurement Samples 71
5.9 Activation Set Size: Single vs. Averaged User Equipment (UE) Samples . 71
5.10 Energy Efficiency Index: Single vs. Averaged UE Samples 72
5.11 Mapping of Network Traffic to Number of Active Cells 73
5.12 Basic CFP Metrics: Accuracy for Defined Number of Active Neighbors . . 74
5.13 Reduced Number of Active Neighbors: Accuracy Impact on Basic CFP Metrics 75
5.14 Energy Efficiency Index: Basic Sum CFP Metric 76
5.15 CFP Metric: Difference to Median 78
5.16 Activation Set Size: Difference to Median vs. Basic CFP Metrics 79
5.17 Example: RSS Distribution with New Percentile Metrics 80
5.18 Activation Set Size: Basic and Newly Defined Percentile Metrics 81
5.19 Activation Set Size: Basic and Newly Defined Combined CFP Metrics . . 82
5.20 Energy Efficiency Index: Comparison of Best Combined CFP Metrics . . 83
5.21 Activation Set Size for Varying Numbers of Active Neighbors: Single CFP Metrics 84
5.22 Activation Set Size for Varying Number of Active Neighbors: Combined CFP Metrics 85

6.1 European Average for a Dense Urban Area: Traffic Distribution on Hourly Basis 89
6.2 Daily Traffic Distribution Indicating the Period of Maximum Energy Wastage 89
6.3 Energy Saving Model: Network Layout 90
6.4 Energy Saving Model: Hourly Cell Activation Procedure 93
6.5 Reference Cell Identification Approaches: Relation to Traffic Demand . . 94
6.6 Cell Fingerprinting: Relation of Best Combined CFP Metrics to Number of Active Neighbors 95

6.7 Cell Fingerprinting: ASS of 2 Best CFP Metrics Mapped on Number of Cells to be Activated 95
6.8 Cell Fingerprinting: Daily Traffic Demand vs. Traffic Capacity 96
6.9 Number of Active Cells per Approach: Hourly from 6 am to 8 pm 97
6.10 Daily Average: Number of Activated Cells 98
6.11 Saving Percentage of the Total Power Consumption 98

List of Tables

2.1 Power Survey per Cell for BS Types in LTE 17
2.2 Energy Saving Potential for Traffic Profiles of Operational Networks . . . 31

3.1 Long Term Evolution (LTE) Simulator - BS Parameters and Values . . . 41
3.2 LTE Simulator - User Equipment (UE) 41
3.3 LTE Simulator - Radio Environment Parameters and Values 42
3.4 LTE Simulator - Cell Fingerprint Parameters and Values 45

5.1 Example Ranges from Simulation Studies for Basic CFP Metrics 69

CHAPTER 1

Introduction

Contents

1.1 Self-Organized Energy Saving 2
1.2 Thesis Scope and Objectives 3
1.3 Thesis Novelty and Contribution 5
1.4 Terminology for Cell Identification 6
1.5 Organization of Thesis 6

Worldwide the energy consumption keeps rising. As a result, climate change, nuclear waste and exploitation of non-renewable resources are putting a risk on the future of our planet [1]. One simple way to counteract is to save energy.

Also cellular networks contribute increasingly to the global power consumption, caused by the world-wide exponential mobile data growth. Globally, the number of mobile subscribers reached almost 7 billion by the end of 2014 (figure 1.1), which corresponds virtually to the number of people on earth. Consequentially, but also due to the continuous and extensive access to information, the data growth trend is expected to continue. Future services, such as the Internet of Things or Machine to Machine communication [2], [3] will accelerate the data growth. According to the Cisco Visual Networking Index [4] the data rate increases exponentially with an estimated 11-fold by 2018 over 2013, reaching 15.9 exabytes per month by 2018 as indicated in figure 1.2.

To compensate the dramatic growth in data volume, additionally to new Base Station (BS) generations supporting higher data rates, a high number of new BSs is installed. Future network deployments are therefore expected as heterogeneous networks composed of macrocells and small cells supporting multiple generations of radio access technologies. While the legacy networks provide the overall coverage, an increasing number of overlaying small cells are required to boost the capacity, [6], [7].

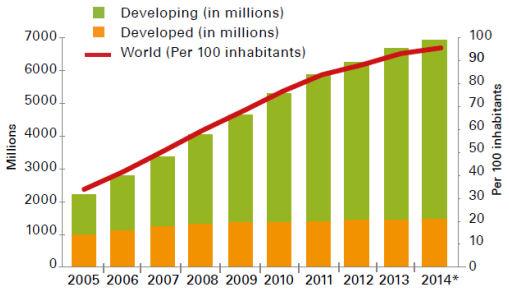

FIGURE 1.1: Growth in Number of Mobile Subscribers, [5]

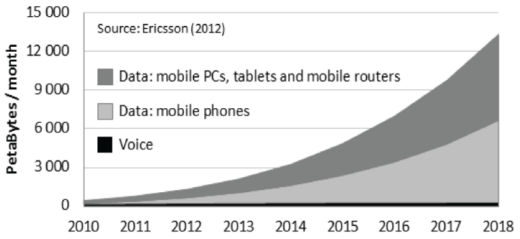

FIGURE 1.2: Evolution of Mobile Data Traffic up to 2018, [2]

As indicated in figure 1.3, the principle energy consumer in cellular networks is the BS, contributing between almost 60% [8], [9] and 80% [10] to the total network power consumption. Especially during low traffic periods, when the consumed energy per bit rate increases, BSs are found to be inherently energy inefficient [11]. Thus, the most promising energy saving candidate is the BS.

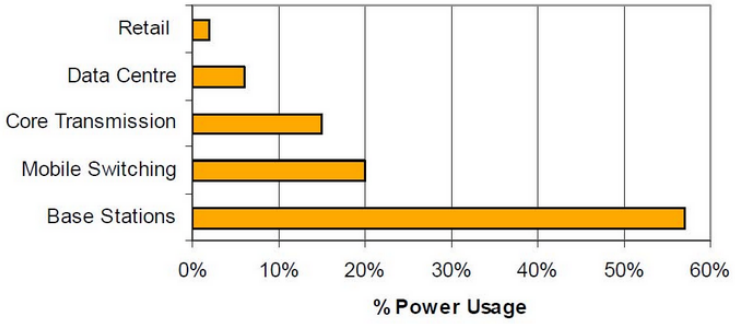

FIGURE 1.3: Energy Consumption of Components within a Cellular Network [8]

Although the increase in energy consumption is significantly lower than the corresponding data rate growth [12], the overall carbon footprint for mobile communication continues to rise. According to [13] the CO_2 equivalent emissions of mobile communication as a whole, including mobile devices increases almost linearly from 2007 to 2020 by a factor of 2.7 accounting for 0.6% of global direct CO_2 emissions.

Additionally, also caused by the shortage of non-renewable resources, the energy price continues to increase. Both, the increasing energy price and consumption contribute increasingly to the operational costs and are expected to reach 30% of the total Operational Expenditure (OPEX) with Long Term Evolution (LTE) [14]. Thus, energy saving is becoming a crucial factor for network operators in this highly competitive market.

1.1 Self-Organized Energy Saving

Not only the rising energy costs, but also the high complexity and huge number of network elements demand automated solutions to dynamically configure and optimize mobile networks. For energy consumption reduction, the Third Generation Partnership Project (3GPP) introduced the energy saving Self-Organizing Networks (SON) [15].

Considering the strong spatio-temporal traffic variation as well as the general dimensioning of cellular networks for peak traffic hours, cells may be deactivated during low traffic periods and reactivated on a need basis.

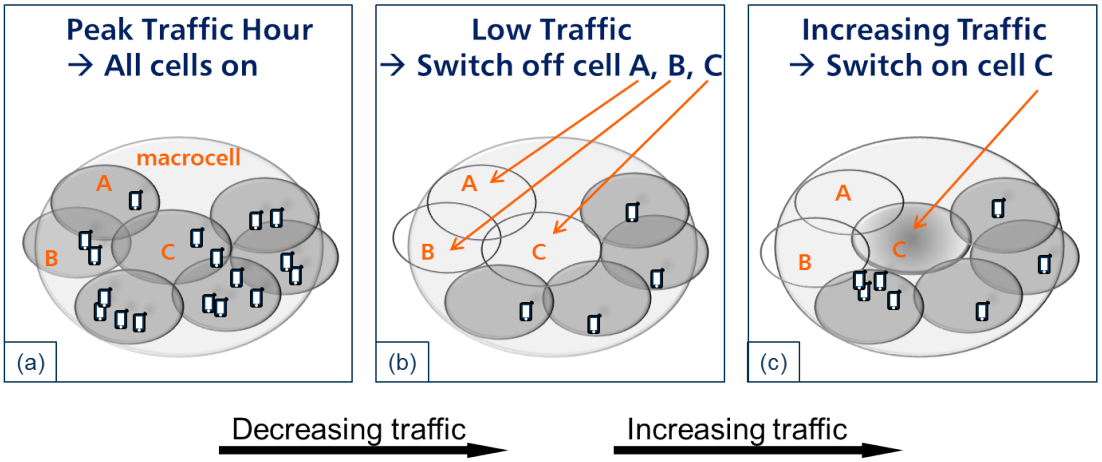

FIGURE 1.4: Energy Saving SON - Cell Deactivation and Activation based on Traffic Demand

Thus, the principle of the energy saving SON is to adjust the network capacity to the instantaneous traffic load. Figure 1.4 shows a small section of a network with 1 macrocell and an overlay of few small cells including cell A, B, and C. During peak hours all cells are activated, as indicated in figure 1.4(a). Then, cell A, B, and C are being deactivated during off-peak hours (figure 1.4(b)). All these 3 cells experienced either no or minor traffic. The cell deactivation procedure can be either performed autonomously by each cell or controlled by the umbrella cell. At periods of time, when the demanded resources exceed the currently provided resource volume, any operational neighbor cell may initiate the activation procedure (figure 1.4(c)). The cell to be activated should be the most appropriate to relieve the neighboring umbrella or small cell that is experiencing overload. Simultaneously, the Quality of Service (QoS) of the user is improved.

The identification of the most needed cell(s) at periods of time, when the demanded resources exceed the currently provided resource volume is not a trivial task requiring input from other network elements. If for a given area only 1 cell is inactive, the activation is obvious. This is not the case, however, where multiple cells are inactive.

In this thesis we present the fingerprinting method for the purpose of cell identification. Each unique fingerprint represents a cell, that is characterized by the signal strength of the neighbor cells as received by the User Equipment (UE). If additional capacity is needed, current UE measurements of the overloaded cell are matched with the fingerprints of the sleeping cells to determine the best fitting cell to be reactivated.

1.2 Thesis Scope and Objectives

The idea of energy saving by temporary deactivation of cells is part of the self-organized network procedures in 3GPP. Especially for cell activation up to now few basic methods are proposed, which mostly rely on constant spatial traffic variation over time, e.g., [15], [16].

Problem Statement

The core problem in this work is to find a reliable and robust method to accurately and timely identify the best sleeping cell to take over the traffic volume from highly loaded neighbor cells. The cell identification is expected to work, even if the traffic volume changes unexpectedly or in case only few cells are active.

The comprehensive problem is the increasingly high power consumption in cellular network, for which we propose the temporary deactivation of cells, demanding an accurate cell identification. Further challenges are the common use of multiple generations of network technologies and the wide variety of network deployments.

Proposed Solution

Fingerprinting requires the initial generation of fingerprints to uniquely identify each cell, the Cell Fingerprints (CFP)s. Input are the Received Signal Strength (RSS) values of each neighbor cell as measured by the UEs, while all cells are active. For each neighbor cell, the RSS distribution is deduced from a set of RSS measurements. As a next step, metrics modeling the characteristics of the RSS distributions are defined. One simple example of a Cell Fingerprint metric (CFP metric) is the minimum and maximum value of the RSS distribution. Correspondingly, the generated CFPs consist of the list of the neighbor cells and their associated CFP metrics.

In case of cell activation, one or multiple UEs served by the cell in overload retrieve a measurement sample consisting of the list of its active neighbor cells and their associated RSS. The retrieved sample is matched with all CFPs representing the sleeping cells. The most suitable cell is determined first, by the best matching neighbor cell list, and second, by matching each retrieved RSS with the CFP metrics of the identical neighbor cell. Thus, the cell providing the best radio condition for the capacity demanding UE is identified and subsequently activated. Details for the generic approach using the full set of measurements are provided in [17] and [18].

Even in case of limited measurements during low traffic periods, the best cell is determined, but with less accuracy. The accurate identification of the best cell allows the selective reactivation of cells based on load requirements. The proposed cell fingerprinting method is a probabilistic approach. In detail the solution consists of the following modules:

1. **Design of Cell Fingerprint:** Each cell has a unique Cell Fingerprint (CFP), characterized by the RSS of the neighbor cells. UEs resident in the cell retrieved the required RSS values. The CFP is then composed of the list of neighbor cells and their associated CFP metrics, which map the RSS distributions of the neighbor cells.

2. **Matching Method:** The possibly incomplete UE RSS measurements are matched with the CFPs representing the sleeping cells. Multiple single and combinations of CFP metrics are investigated in order to achieve the highest accuracy to determine the best match. The major challenge are incomplete RSS measurements. Then, the reduced number of cell comparisons can be partly compensated by increasing the number of CFP metrics for each active neighbor cell.

3. **Self-Organized Energy Saving:** Cells that are temporarily not required to provide the demanded capacity, are deactivated. In case of capacity shortages, the best

sleeping cell is identified by the cell fingerprinting method and subsequently reactivated. Prior to cell deactivation, each cell has to exchange its own CFP with the neighbor cells. Subsequently, each cell is able to deactivate itself, while the neighbor cells takes over the activation of the sleeping cells.

1.3 Thesis Novelty and Contribution

The 2 major contributions of this thesis are

1. to **characterize cells using their RSS values** as measured by the UE
2. to **apply the fingerprinting method towards energy saving** by being able to identify an appropriate cell (out of a set of inactive cell), that should be activated on a need basis, when the traffic demand increases.

The proposed approach is a major step forward to make the energy saving SON more reliable and thus, widely acceptable. The overriding goal of this work is, however, to reduce the energy consumption in cellular Radio Access Networks (RANs).

For completeness, a literature study provides a comprehensive survey of the state-of-the-art for energy saving techniques in cellular RANs followed by an insight into the control mechanisms for the energy saving SON. Besides the contributions, the following benefits can be deduced, although not all of them are evaluated in detail in this thesis:

- **Localization:** The cell fingerprinting approach is not restricted to the energy saving SON, but can be re-used for other RAN applications requiring cell identification, e.g. to identify the most appropriate small target cell during handover from a macrocell [19].
- **Cross Network Technologies Application:** The presented approach is evaluated for LTE. However, the framework is applicable for legacy networks as well as for future cellular network generations. The generated CFPs are solely based on standard measurements, commonly available in any cellular network.

The following papers and articles have been published based on this work.

1. Elke Roth-Mandutz, Andreas Mitschele-Thiel: "LTE energy saving SON using fingerprinting for identification of cells to be activated." Future Network and Mobile Summit (FutureNetworkSummit), pp. 1-8. IEEE, July 2013. [20]

2. Elke Roth-Mandutz, Stephen Mwanje, Andreas Mitschele-Thiel: "RSS based Cell Fingerprint Patterns and Algorithms for Cell Identification in the Context of Self-organized Energy Saving." Proceedings of the 11th International Conference on Mobile and Ubiquitous Systems: Computing, Networking and Services, pp. 397-400. ICST (Institute for Computer Sciences, Social-Informatics and Telecommunications Engineering), 2014. [17]

3. Elke Roth-Mandutz, Stephen Mwanje, Andreas Mitschele-Thiel: "Cell Identification based on Received Signal Strength Fingerprints: Concept and Application towards Energy Saving in Cellular Networks." EAI Endorsed Transactions on Mobile Communications and Applications, pp. 1-10, DOI: 10.4108/mca.1.4.e4, September 2014. [18]

1.4 Terminology for Cell Identification

To ensure the comprehensibility in this work, we define 2 terms to precisely distinguish between the cells involved in the cell identification procedure.

First the **target cell**: It is the objective of the cell identification procedure to uniquely identify the target cell. The measurement sample used as input for the matching originates from a UE resident in the target cell. Thus, the target cell is known from the outset to be the most suitable cell to serve this UE.

Second the **best matching cell**: It is the result of the matching algorithm of the cell identification procedure. In case the best matching cell corresponds to the target cell, the optimum result is achieved.

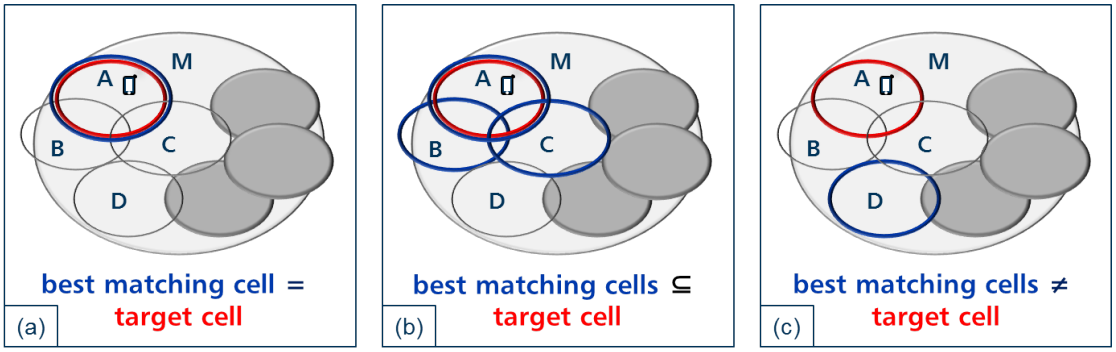

FIGURE 1.5: Cell Terminology: Target Cell, Best Matching Cell

The 3 scenarios in figure 1.5 illustrate the different cell terms, showing a small extract of a network with an active macrocell M, 4 sleeping small cells A, B, C, and D and 3 active small cells in dark gray. The target cell, which experiences overload is encircled in red, while the best matching cells are marked in green. The best result is achieved, if exactly one best matching cell is identified, which corresponds to the target cell as presented in figure 1.5(a). Also in figure 1.5(b) the target cell A is identified as part of a subset of the best matching cells A, B, and C. All 3 cells would be activated, although B and C are not required. Finally, figure 1.5(c) identifies and subsequently activates cell D as the best matching cell, while the target cell A remains sleeping. Thus, the resource demanding UE in cell A experiences no relieve, resulting in an expected negative Quality of Experience (QoE) impact on the users resident in cell A.

1.5 Organization of Thesis

In the previous sections we introduced the subject of the thesis, the problems involved as well as the proposed solution. To conclude this chapter, this section presents the summary of the remaining chapters.

Chapter 2 introduces the self-organized energy saving approach and assesses the related literature. It starts with a literature review of the state-of-the-art research on energy saving. Next, the network technology and layout applied in the rest of the thesis are introduced, followed by the network management for self-organized energy saving. The

rest of the chapter focuses on temporary cell deactivation to save energy, including a literature study of the energy saving potential using data from operational networks. The chapter ends with a brief review of fingerprinting and further approaches for cell identification.

Chapter 3 presents the simulation environment and the modeling required to simulate the typical Radio Frequency (RF) conditions expected in dense urban areas. I present the detailed parameter setting for the simulation studies carried out on an LTE system level simulator evaluated in chapter 5.

In **Chapter 4** the cell fingerprinting framework to identify the best matching cell is presented. As a prerequisite for the design of the CFP procedures, I detect characteristics in RSS distributions of the neighbor cell, which are mapped on CFP metrics. During fingerprint generation, these CFP metrics are calculated for each neighbor cell and stored in cell fingerprints. Subsequently, during cell identification, the metrics determine the individual matching degree for each neighbor cell.

The accuracy of cell fingerprinting is then determined in **Chapter 5**. For single and combined CFP metrics as wells as varying numbers of active cells, the accuracy is evaluated. It highlights the improved accuracy when multiple CFP metrics are combined. Interestingly, the highest accuracy is achieved using different combination of CFP metrics depending on the number of active cells.

Chapter 6 analyses and evaluates the energy saving potential of the Energy Saving Self-Organized Network (ES SON) for a small cell network overlay. The cell fingerprinting approach is compared to the theoretical optimum approach to validate the use of cell fingerprinting. The resulting energy saving potential using cell fingerprinting achieves more than 47%, only 0.8% less than the theoretical optimum.

Finally, **Chapter 7** summarizes the outcome of the thesis, where I highlight the major improvements regarding cell identification accuracy as well as the resulting effects on energy saving potential in cellular networks. Furthermore, I provide an outlook to possible future improvement directions as well as new opportunities for the cell fingerprinting technique in different applications.

CHAPTER 2

Context and Related Work

Contents

2.1 Energy Saving in Radio Access Networks 9
2.1.1 Research Work on Sustainable RAN 9
2.1.2 Classification of Energy Saving Approaches 10
2.1.3 Load Aware Energy Saving Approaches 12
2.1.4 Assessment of Energy Saving Approaches 14
2.2 Network Constraints and Organizational Aspects for Energy Saving 15
2.2.1 System Model: The LTE RAT 15
2.2.2 Base Station Power Consumption 17
2.2.3 Radio Network Layout 20
2.2.4 Energy Saving Use Case in Self-Organizing Networks 23
2.2.5 Energy Saving in 3GPP - Management Support for Potential Solutions 25
2.2.6 Architecture Solutions for Self-Organizing Approaches 26
2.3 Temporary Cell Deactivation and its Energy Saving Potential in Operational Networks 27
2.3.1 Cell Deactivation Strategies 27
2.3.2 Spatial and Temporal Traffic Variation 29
2.3.3 Energy Saving Potential based on Operational Network Data in Literature 30
2.3.4 Side Effects of Temporary Cell Deactivation 32
2.4 Strategies for Cell Activation and Identification 33
2.4.1 Overview of the Fingerprinting Method in Wireless Communication 33

2.4.2 Fingerprinting Use for the Identification of Sleeping Cells . . . 34
2.4.3 Parameters for Cell Coverage Identification 35
2.4.4 Sleeping Cell Identification Strategies 36

This chapter focuses on energy saving in RAN and its related research areas relevant for this work, which are all based on a comprehensive literature research.
Starting from a classification scheme for the different energy saving fields in radio access networks, multiple approaches are introduced and assessed.
Next, in the organizational subsection, we introduce network aspects, including LTE and multi-Radio Access Technology (RAT) support, followed by the impact of the BS power consumption and the network layout on energy saving. Furthermore, we describe self-organizing networks, including their use cases, architecture, and management.
In the third subsection, we focus on the temporary cell deactivation approach, its strategies for cell deactivation and its energy saving potential using data from operational networks, as derived from a comparative literature study.
The final part concludes with cell identification, which introduces and assesses the fingerprinting method, followed by various trigger conditions for sleeping cell identification.

2.1 Energy Saving in Radio Access Networks

In this section, we classify and introduce the key areas for energy saving in future cellular radio access networks. Besides the major research projects for energy saving, we provide a classification scheme for some most promising energy saving approaches, with focus on load-sensitive approaches.

2.1.1 Research Work on Sustainable RAN

From the very beginning of cellular networks, the reduction of power consumption was of major importance, but initially limited to the battery-operated mobile phones to extend the battery capacity. For the network, the reduction of power consumption is only addressed for a few years, but since then the interest is increasing steadily.

Several "green" research projects were setup in the last few years, to identify and investigate the most promising components and mechanisms to reduce the energy consumption. The Energy Aware Radio and NeTwork TecHnologies (EARTH) project (2010 - 2012) is further detailed below, as it serves as reference for multiple research works, including this thesis. Few further selected green projects are:

- **Green Touch Initiative** (2010 - 2015) addressing the improvement of energy efficiency of communication and data networks, including the Internet, [21].
- **5GrEEn - Towards green 5G mobile networks** (2013 - 2015) focusing on energy efficient 5G mobile networks, [22], [23].
- **TREND - Towards Real Energy-efficient Network Design** (2010 - 2013) aiming to assess the energy demand of current and future telecom infrastructures, and to design energy-efficient, scalable and sustainable future networks, [24].

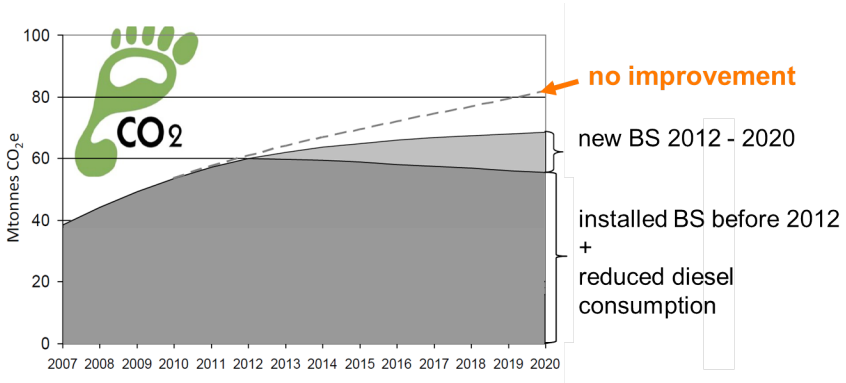

FIGURE 2.1: Carbon Footprint of Radio Access Networks [25]

The EARTH project investigated the energy efficiency of mobile networks, proposing mechanisms to reduce the energy wastage without compromising the users perceived QoS. The overall improvement that was planned to be achieved by EARTH is presented in figure 2.1. The gray dotted line indicates the course of carbon production by RANs in case of no improvement to the energy efficiency. The emission of carbon dioxide from BSs installed since 2012 is colored in light gray, while the BSs installed prior to 2012 is marked in dark gray. Diesel operated BS are deployed in case no power grid is available. A reduction of the diesel consumption due to modernizing the installed diesel sites with hybrid operation is assumed. Interestingly, even without any progress in energy efficiency, the energy consumption rise by approximately 40% from 2007 – 2020, is definitely less compared to the expected exponential traffic rise. One reason is the improved spectral efficiency of LTE compared to legacy systems.

The final EARTH project results are comprised in the chapter "Sustainable Wireless Broadband Access to the Future Internet – The EARTH Project" in [26]. One of the major sources for this thesis are the EARTH deliverables and research papers. For example, the EARTH reference traffic model is used as traffic profile for the evaluation of the power saving potential in chapter 5.

Besides the research projects, energy saving is becoming an increasingly significant topic in the cellular network standardization activities. Starting with LTE, 3GPP introduced an initial draft for self-organized energy saving, [27]. Meanwhile for LTE Advanced (LTE-A), 3GPP release 12 [28] summarizes several studies on system enhancements for energy efficiency such as energy saving management, solutions for BSs and operational aspects in radio networks.

2.1.2 Classification of Energy Saving Approaches

The proposed energy saving mechanisms for radio access networks vary widely. Energy saving fields range from sustainable energy resources, e.g. solar and wind energy, to less power consuming hardware components. Therefore, several publications classify the approaches according to different aspects. A detailed overview of the most current energy-aware management strategies is presented [29]. Other mostly high level classification schemes are provided in, e.g. [30], [31], [32], [33], and [34].

In figure 2.2 we present our condensed classification scheme, which is oriented towards the proposed solution of this work. At the highest level, we distinguish between the

following energy saving fields: hardware, architecture, deployment, energy sources, and finally the cell load awareness, used for the approach of this work. Subsequent, we describe one or more examples of energy saving mechanisms per field.

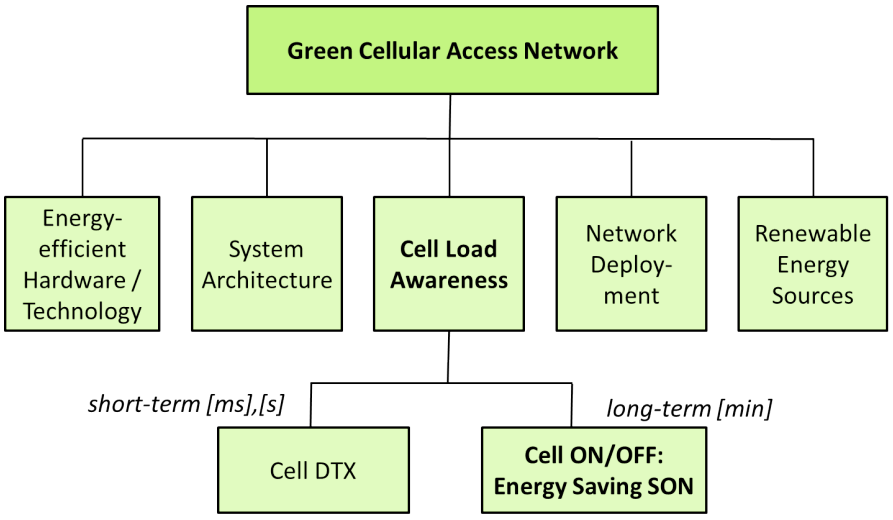

FIGURE 2.2: Classification of Energy Saving Fields in Green Cellular Access Networks

Energy-efficient Hardware / Technology

The design of network elements and BS components with lower power consumption is an ongoing activity, with a major focus on the high power consuming components, e.g. the power amplifier and cooling as illustrated in figure 2.6 of section 2.2.2. Cooling, for example, can be reduced due to hardware redesign, so that outdoor BS can operate within a wider range of temperature, but also by at least partially replacing the power consuming air conditioning with fresh air cooling, [35].

System Architecture

The BS is typically inherently energy inefficient, while in idle mode, i.e. without individual data and signaling transmission on the user plane. The signaling required in idle mode is limited to e.g., the distribution of access information, paging, and idle mode mobility. The complete idle mode signaling could be differently processed (e.g. bundled), compared to periods, when data is transmitted and received on the user plane. This way, the BS could implement an efficient Discontinuous Transmission (DTX)/Discontinuous Reception (DRX) functionality. This approach requires a logical separation of the transmission of system information during idle mode and during periods with data transmission on the user plane [2], [36].

Network Deployment

One possibly energy efficient approach is the deployment of Heterogeneous Networks (HetNets), as discussed in section 2.2.3. Due to several hierarchical layers with a mix of multiple types of base stations with different cell sizes, the propagation distance between the nodes is shortened, reducing the required transmission power. However, the additionally deployed small cells consume more power, although to a substantially lesser degree than macrocells. For example in [37], the power consumption of several HetNets and homogeneous network deployments are compared considering different inter site distances as well as load situations. In case the throughput is disregarded, the total

HetNets power consumption exceeds that of a macrocell only network. The decreased Transmit (Tx) power of small cell does not compensate for the increased power consumption of the small cells. However, in case the power consumption considers the energy consumed per bit, the increased throughput of a HetNet overcompensates the additional small cell power consumption, resulting in a power saving per bit especially for high load scenarios.

To improve the spectral efficiency, LTE and subsequent systems are typically equipped with multiple transmit and receive antennas, which require the transmission of auxiliary information to obtain the current radio channel conditions. Especially during low load periods, the signaling overhead negatively impacts the power consumption as the number of the transmitted auxiliary information remains the same, compared to full load. Only under full load, the increased spectral efficiency justifies the overhead [38]. Furthermore, also the additional signal processing power should be considered, which is caused by the increased computation complexity of the spectral efficient transmission.

Renewable Energy Sources

Renewable energy resources, such as wind and solar radiation, could replace fossil fuels to power a BS. "Green" BSs are urgently needed in areas without fixed power grid, e.g. deserts and remote areas, as alternative to the diesel-powered BS [14]. The diesel-powered BS is one of the current major carbon producers in cellular networks. To overcome the unpredictable power production of wind and solar energy, hybrid BSs are often seen as the inevitable alternative. For the hybrid BS, fuel cells are proposed, to convert fuel into electricity through a clean electro-chemical process [39]. According to [32], hybrid BS are already under development. Even more sophisticated, [6] investigated the optimal BS placement and power allocation scheme to reliably run "green" BSs.
The use of renewable energy sources will not reduce the power consumption, but is seen as a contribution to a more sustainable RAN. However, the successful operation of "green" BSs, typically demands low power consuming RANs, which requires the implementation of additional energy saving approaches, e.g. the temporary deactivation of cells.

2.1.3 Load Aware Energy Saving Approaches

Energy can be saved by reducing the network power consumption in line with the network traffic load. The power reduction is typically achieved by a sleep mode operation, which is regarded as especially promising in the highly under-utilized access network during low traffic periods. For the cell load aware energy saving, we further distinguish between short-term solutions that range from milliseconds to seconds, and long-term solutions in the minute range as illustrated in figure 2.2.

Short-term Approaches

Cell DTX is introduced as a prominent energy saving approach for the short-term intra BS energy saving. It is especially useful for underutilized radio links for very short time periods on a milliseconds or seconds basis. Subframes or parts of the subframes are configured to reduce the BS Tx power consumption, while neither signaling nor data is transmitted. Several publication discuss this idea, e.g. [40], [10], [15].

Opposite to Cell DTX, DTX is a long-proven power saving technique implemented in the UE, to switch off the radio transmission on the short-term, whenever neither voice nor data is transmitted. However, different to UEs, BSs have to transmit at least the pilot signal to provide global cellular basic functionality, such as synchronization and roaming. Therefore, Cell DTX is not possible for Wideband Code Division Multiple Access (WCDMA)/High Speed Packet Access (HSPA), which requires continuous pilot transmission. Different in LTE, the cell specific reference symbols are not continuously transmitted. However, the synchronization signal and broadcast channel require the transmission on short intervals [38]. Therefore, an immediate reaction on empty frames suspending transmission in the order of milliseconds is absolutely critical, but also vice versa to ensure an immediate re-activation.

Cell DTX could be applied by configuring sub-frames using the maximum allowed number (5 to 6) of Multicast-broadcast single-frequency network (MBSFN) sub-frames per radio frame. As MBSFN sub-frames have less common reference signals than normal sub-frames, the BS transmission time is reduced [15]. Alternatively, as proposed in [40] almost blank sub-frames could be configured.

Additional approaches on a short-time scale are listed in [29], including bandwidth and capacity adaptation and Multiple Input Multiple Output (MIMO) muting.

Finally, any kind of the listed short-term approaches can be combined with the following long-term approaches, as evaluated in [41].

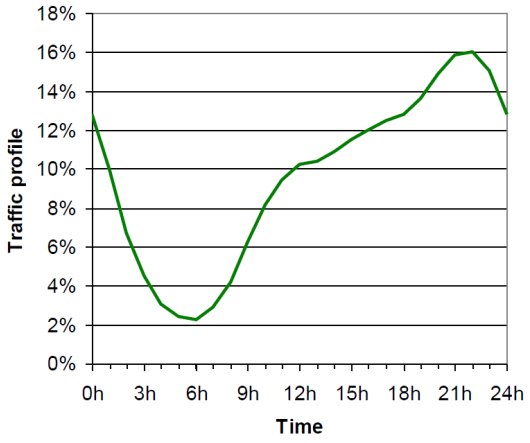

FIGURE 2.3: Daily Traffic Profile for Cellular Networks in Europe, EARTH-Project - Reference Model, [33]

Long-term Approach

The idea of the long-term load aware energy saving is to minimize the energy consumption by exploiting temporary unused resources of the RAT. The resources, e.g. BS or cells are deactivated in low traffic periods, if they are backed up by the network underlay or other RATs [15]. Contradicting the energy saving idea, mobile networks are first of all designed to provide a high throughput level at any time, and are therefore deployed to serve peak traffic hours. However, the generated traffic is subject to strong periodic variations as presented in figure 2.3. This figure illustrates the daily traffic profile based on the average data traffic volume in Europe. According to [42], the proportion of time when the traffic is below 10% of the peak during the day is about 30% on weekdays, and

45% on weekends. This behavior causes extremely underutilized BSs, which consume more than 90% of its peak energy, even when they are inactive.

Deactivation and reactivation of cells in line with the current traffic load is currently the most widely discussed long-term approach according to the recent publications, such as [29], [43], [44], [45]. Especially for homogeneous networks, **cell zooming** may be requested, if cells are switched off, as descried in [46], [47], [29]. Cell zooming expands the cell range by increasing the Tx power of the cells which stay active, to compensate the coverage losses, [29]. As a drawbacks, the user's QoS may be impacted by possible coverage holes e.g., due to the limited maximum BS power. Additionally, the battery life for the users may decrease due to the higher transmission power required to connect to a possibly remote active cell, [43].

Typically, load aware long-term approaches are implemented on the cell level. However, also **complete BSs** can be deactivated / reactivated in case of sectorized cells, to increase the energy saving by deactivation of central BS components. Finally, even **complete networks** could be shared between operators. Especially in rural areas, equipped with less cells, this is considered as an efficient approach, although legal reasons may restrict these approaches, [36]. As we pursue a long-term approach in this work, we will provide the details on procedures and trigger conditions in following sections.

2.1.4 Assessment of Energy Saving Approaches

Diverse fields and approaches for energy saving were introduced in the previous 2 sections. As the approaches are not mutually exclusive, a combined use is expected to further reduce the overall power consumption. For example, energy-efficient hardware, energy-optimized network deployment and the temporary deactivation of cell are not expected to directly interfere with each other. However, the implementation of one approach may reduce the saving potential of another approach. For example, if the hardware of the small cells is optimized to consume very low power, while active, the energy saving of a cell in the sleep mode or cell DTX will decrease.

Furthermore, a critical analysis of each approach regarding the use in an operational network is required. Often multiple conditions have to be met to achieve the anticipated reduction of the power consumption. One major condition is the traffic load, e.g. for the use of multiple transmit and receive antennas, but also for the deployment of HetNets and small cells. In case of multiple antennas, the achieved increase of throughput compensates the additional power consumed only in case of high load. For HetNets, the deployment of each new BSs initially increases the energy consumption. A holistic view is required, considering e.g. the network traffic load and the interference situation, to evaluate the impact on the network power consumption in relation to the achieved throughput.

One example is the deployment of HetNets, where the deployment of each new BSs initially increases the power consumption of the network. To evaluate the overall impact of the new cell, the geographical constraints, e.g. the traffic load and interference, as well as the BS placement and alternative deployment would need to be considered.

In summary, the introduced approaches and especially their combinations have a high potential to significantly reduce the power consumption in a radio access network, provided that the operator is able to control and adapt each approach according to the individual network behavior and customer needs.

2.2 Network Constraints and Organizational Aspects for Energy Saving

In this section, we introduce the radio network and management aspects to provide the context for the consecutive work.
The first 3 subsections describe the network aspects and constraints regarding the temporal deactivation of cells to save energy. This includes the support of cell fingerprinting for different RATs with focus on LTE, the power consumption behavior of the BS, and the role of HetNets and small cells.
Self-organized networks, introduced in the subsequent 3 subsections, are due to the high complexity and huge number of network elements an essential contribution to correctly and timely configure, optimize or heal current and future mobile networks. Here, we start with the introduction of use cases and their interaction with energy saving, followed by the architectural options and finalize the chapter with the management as defined in the 3GPP standards.

2.2.1 System Model: The LTE RAT

The load aware energy saving approach, we pursue in this work, is implemented and evaluated on LTE, the Fourth Generation (4G) cellular network technology. LTE [48], also referred to as Evolved Universal Terrestrial Radio Access Network (E-UTRAN), is the access part of the Evolved Packet System (EPS). Figure 2.4 presents an overview of the purely Internet Protocol (IP)-based network, which is restricted to the few details needed for this work.

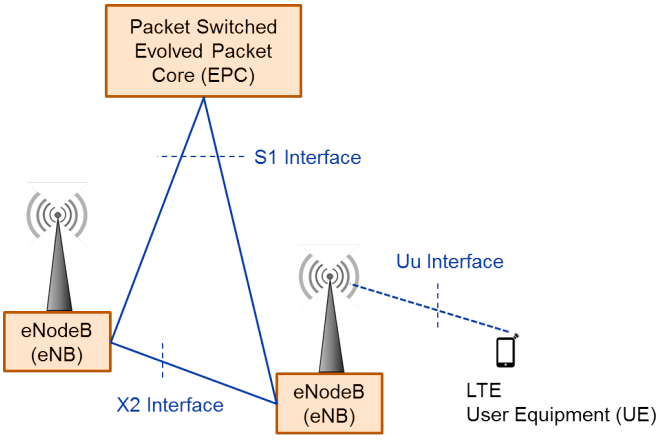

FIGURE 2.4: Overview of LTE Network Components and Interfaces

LTE was introduced in the 3GPP standard in release 8, targeting high peak data rates and improved QoS. It is based on high spectral efficiency as well as a short round trip time and implemented on a flexible system in terms of frequency and bandwidth. The

BS, named E-UTRAN NodeB (eNodeB) respectively eNB in LTE, is connected to the packet switched core via the S1-interface. The simple and flat RAT architecture consists of eNodeBs only, connected via a newly introduced interface, called X2 as presented in figure 2.4. The Uu interface is the radio interface between eNodeB and UE and uses Orthogonal Frequency Division Multiple Access (OFDMA) as digital multi-carrier modulation method.

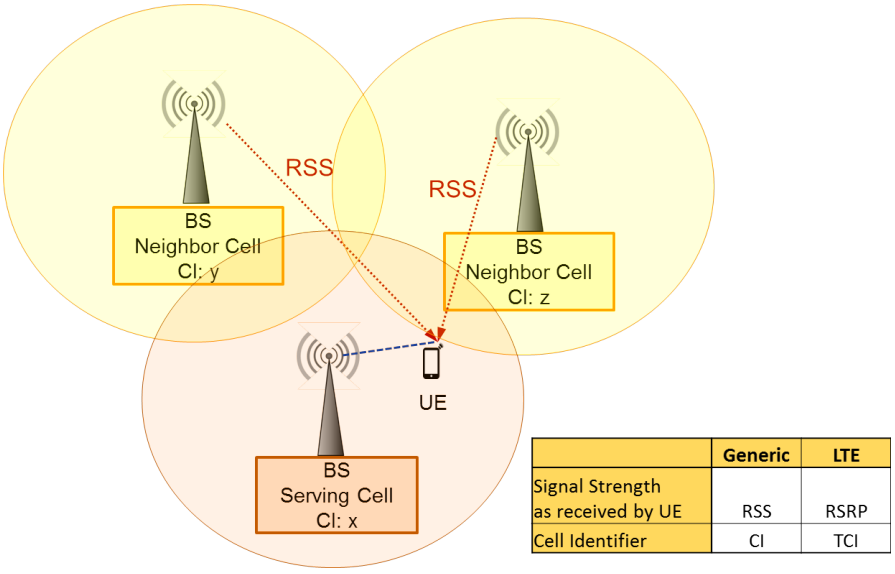

FIGURE 2.5: Generic Terms vs. LTE Terms for Cell Fingerprinting

The newly introduced cell fingerprinting method for cell identification and subsequent activation requires few basic radio link measurements and parameters, which are essential for any type of cellular radio network. To setup a new radio link or to maintain an existing radio link, the UEs need to measure the signal strength as received from the pilot channel of the surrounding cells, indicated by the red line in figure 2.5. The received signal strength is associated to the measured cell, uniquely identified by a cell identifier (CI).
Depending on the used RAT technology, solely the terms and ranges may vary for the RSS and Cell Identification (CI). Therefore, to emphasize the more general approach independent of the used RAT, we use in this work generic terms, although the simulation studies are based on LTE. For clarification and mapping reasons, the 2 frequently used terms and their LTE correspondence presented in figure 2.5 are shortly defined:

- **Received Signal Strength (RSS)** represents the received pilot signal strength of the associated neighbor cell as received by the UE. The LTE correspondence is the Reference Signal Received Power (RSRP), ranging from -44 to -140 dBm.

- **Cell Identifier (CI)** identifies a cell in the cellular network. Network-wide the Identifier (ID) may not be unique depending on the technology and the operator setting, but it identifies unambiguously the neighbor cell in the measurement report retrieved from the UE, called Target Cell Identifier (TCI) in LTE.

However, the overall concept of cell fingerprinting as proposed in this thesis is expected to apply not only for LTE. We assume that it can easily adjusted to the legacy RAT, i.e. Second Generation (2G) and Third Generation (3G), i.e. Universal Mobile Telecommunications System (UMTS) and HSPA as well as to the future cellular network generations, LTE-A and the Fifth Generation (5G).

2.2.2 Base Station Power Consumption

Base Stations are not only the major power consumer in the cellular network, but also the only network element affected by the proposed energy saving approach in this work. Therefore, this subsection provides an insight into the BS power consumption, also regarding the traffic load, the power consumption of individual BS components as well as the impact of the BS sleep mode.

Power Consumption of Different BS Types

As the major power consumer in a cellular network, the BS is clearly the most promising candidate to reduce the overall network power consumption.
However, base stations as well as their power consumption differ strongly, e.g. depending on the size of the cell and the application. Therefore, they are categorized by types. Basically, we distinguish between the 4 types of BS supporting different cell sizes as listed in table 2.1: the macrocell providing the coverage for extended areas on the one hand and the so-called small cells, i.e. the micro-, pico- and femtocells, which are further detailed in section 2.2.3. Macrocells typically provide the basic cell coverage, while the small cells are mostly used as capacity booster in a multilayer network or for indoor coverage.

Table 2.1 summarizes the BS power consumption for a LTE system at maximum load with a 2x2 MIMO configuration. It presents for the different cell types the power consumption considering one sector or cell as well as the maximum Tx power at the Power Amplifier (PA), [43].

TABLE 2.1: Power Survey per Cell for BS Types in LTE

Cell Type	Maximum Tx Power	Power Consumption
Femto	0.05 W	6.2 W
Pico	0.13 W	9 W
Micro	6.3 W	94 W
Macro	39.8 W	321.6 W

Small cells are typically deployed as omnicells, i.e. one cell corresponds to one BS. Conversely, a macrocell is mostly deployed as one out of multiple sectors installed at one BS site. The antennas of a BS site are arranged to support several (typically 3) sectors to minimize the number of BS sites and to increase the network capacity. In case a sector is deactivated, only the cell specific components of the BS are deactivated, e.g. the power amplifier, while central BS components, e.g. Media Access Control (MAC) and scheduler, are still operational, to run the still active cells.

Figure 2.6 illustrates the main power consuming components of a BS transceiver, separately for the different cell types, based on the EARTH-project, [49]. The RF transceiver and the baseband interface provide the transmission / reception capability of the radio signal, while the PA increases the transmitted radio signal.
For all cell types, the PA is a major power consumer, followed by the baseband interface with regard to small cells. As seen in the figure 2.6, the 3 radio interface components

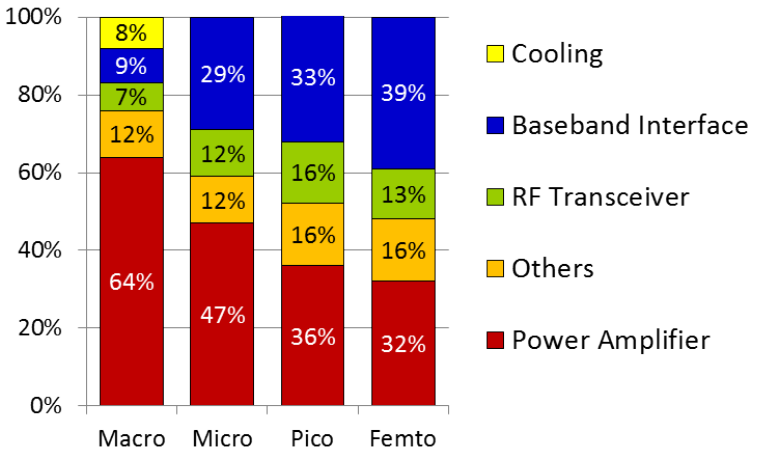

FIGURE 2.6: Main Power Consuming Components for Different Cell Types, [49]

offer a significant energy saving potential ranging from 80% for the macro to 88% for the microcell.

Impact of Traffic Load on Power Consumption

Besides the high power consumption of the BS, also the insensitivity of the BS to adapt the power consumption to the traffic load, anticipates a high energy saving potential, e.g. by temporary cell deactivation, [50]. This is especially true in low load periods, where transmissions of control signals dominate over data. Ideally, the consumption of the BS would decline linearly with the traffic load of the cell as shown by the black dotted line in figure 2.7. Then, cell deactivation would be obsolete. However, also regarding load sensitive power consumption, there is a major difference between the macrocell and the small cell behavior.

Figure 2.7 illustrates the ratio of the BS power consumed P_{in} to the RF output power P_{out}, for a typical characteristic power model of an LTE macro BS, [51]. The BS load, defining P_{out}, is proportional to the amount of utilized resources, consisting of data and control signals and depends, in addition, on the power control setting, [51]. The blue dashed line represents the power consumption. Power P_0 is consumed at the minimum non-zero RF output power, while P_1 is consumed at the maximum RF output power P_{max}. Obviously, there is a dependency of the BS power consumption to the load, although to a minor extent. Even at zero RF output power, the power consumption of a state-of-the-art macro BS is approaching the maximum power consumption.

An energy-efficient BS is expected to closely follow the black dotted line in figure 2.7, so that the consumed BS power corresponds to the load pattern, i.e. ideally, P_0 would reach the value zero. Although this can be considered as unrealistic due to the continuously required pilot signal, the input power of a BS optimized for low energy consumption should more closely follow the RF output power, especially for BSs frequently operating in low load.

In [52], the changing power consumption of different generations of macro BSs was measured during the course of the day. Resulting, the consumed power varies from (∼39%) for Global System for Mobile communication (GSM) 900 to (∼27%) for GSM 1800 and finally to (∼20%) for UMTS depending on the traffic load. The lower variation in daily

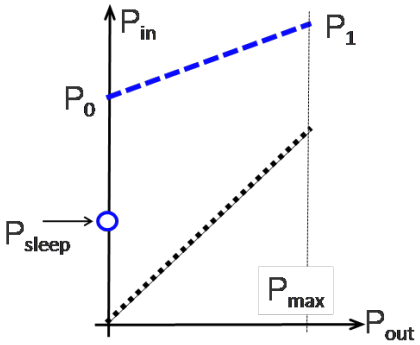

FIGURE 2.7: Load Dependent Estimate of the Power Model for a Typical LTE Macro BS [51]

power consumption for the newer technologies GSM 1800 and UMTS are assumed to results from hardware improvements, [52].

Different to the power consumption of macro BSs, the load dependent factor is limited to almost negligible for small cell BSs - especially pico and femto cells [51]. The reason is the major contribution of the PA to the power consumption (see figure 2.6), which scales for the macro BS and to some extend for micro BS and remain almost constant for pico and femto BS. Other BS components hardly scale with the load, [53].

Concluding, the macro BSs consumes by far the most power from all types of BSs. However, the risk to degrade the coverage in case of inactive macrocells and thus, the user's QoE is assumed to be much higher, than for small cells. The reason is the use of the small cells, which are usually set up as second tier, i.e. the capacity boosting network overlay. Consequently, addressing the user's experience with high priority, we consider small cells as more appropriate for temporary cell deactivation compared to macrocells.

BS Sleep Modes

The implementation of a low power sleep mode in the BS, is a prerequisite for the temporary deactivation of the cells. According to [30] and [16], this kind of sleep mode is currently designed for state-of-the-art BSs, whilst the hardware of present BS generations deployed today was designed for occasional switch on and off procedures. Currently only the use of modems managed by separate tools, can put BS in stand-by mode, [54].

In literature the following 2 major kinds of sleep mode are distinguished:

1. **"Deep" sleep mode:** In this mode the transmitting or receiving parts of the RF circuitry of the BS are entirely turned off. Thus, the BS processing is reduced to the very minimum, e.g. to the supervision of the X2 or S1 interface in LTE (see figure 2.4) for an incoming wake-up trigger.

   The "deep" sleep mode is usually intended for longer periods with low traffic with no need for fast wake-up time. However this implies, that the active cells have to provide the full radio coverage of the network at any time, to guarantee the QoE for the user, [16].

Additionally, this kind of sleep mode is more commonly assumed in literature. It is also referred to as dormant state (in 3GPP), off state, low power saving state, or often simply called sleep mode.

2. **"Light" sleep or stand-by mode**: In this mode the degree of deactivation is low with the intention that the transition of the BS from sleep state (or energy saving state) to active state is fast. Only select parts of the hardware and specifically those that take a short time to be activated, are deactivated, [10]. Such a mode can be implemented in two forms: either 1) by deactivating only a part of the RF circuitry or 2) deactivating the complete RF circuitry.

   Deactivating only components of the RF circuitry would, depending on the cell activation trigger condition, retain either the transmitting or receiving parts of the BS active. In case the receiving parts remain active, the BS would be able to monitor the received UE uplink power. Using this information, the BS would be able to detect nearby UEs and autonomously decide to transit to the active state.

   In the alternative implementation of light sleep, the complete set of RF components is switched off. The BS retains as active only the components that take non-negligible time to be reactivated, e.g. the baseband processing components [45]. This ensures that the BS wake-up time is significantly lowered, although with a higher energy consumption compared to deep sleep. However, the achieved reduction in power consumption is still significant. For example, solely deactivating the RF parts and PA results in reductions of up to 45% for pico cells and 51% for femto-cells as shown in figure 2.6.

Regarding the **wake-up time**, there is a trade off between the kind of the sleep modes: The deeper the sleep level, the more energy can be saved, while the transition time from sleep and active mode increases [16]. Resulting, the time to move from the "deep" sleep mode to active mode is non-negligible, and may require 10 to 20 seconds or even more, [10]. This delay may impact the QoE of the user, e.g. if the expected data rate can not be delivered in time.

On the other hand, the "deep" sleep mode is expected to achieve more energy saving. This is because if all major power consuming components are turned off, the amount of power consumed by a small cell BS is assumed to be negligible [45], i.e. close to zero Watt. As the deep sleep is the preferred mode, especially for multi layer networks, we refer in this work to "deep" sleep mode, which is also in line with the proposed solutions in 3GPP, in [15].

2.2.3 Radio Network Layout

In this section, we describe the impact of a homogeneous or a heterogeneous radio network on the energy saving potential of temporary deactivated cells. Additionally, the associated advantages and potential risks are discussed.

Homogeneous Networks

A homogeneous cellular network typically consists of one layer of macrocells with extended coverage radius using legacy macro BS [55]. Usually, it is deployed in rural and

sparsely populated regions. Figure 2.8 presents a small extract consisting of 4 macrocells.
In case of cell deactivation, we expect a significant risk on the network coverage. One approach to avoid the potential coverage holes is to increase the power of the still active neighbor cells as proposed e.g. in [16]. Alternatively, the antenna tilt setting and further user associated parameters for cell selection, cell re-selection and handover could be adjusted to compensate possible performance degradation, [12].

Additionally, the deactivation of macrocells poses a considerable risk to deteriorate the network quality. The reasons are e.g., the network parameter settings, which were usually optimized assuming, that all cells are constantly active. Additionally, the increased power of the still active macrocells to avoid coverage holes may result in an increased inter-cell interference. On the long term, however, considering the network data growth, homogeneous networks may increasingly be converted to HetNets, which are detailed in the following section.

Heterogeneous Networks

Heterogeneous networks (HetNets) are mostly deployed to deal with the growing number of mobile subscribers and data rate intensive services. Typically, HetNets consist of at least 2 network layers with small cells and macrocells and may support different radio access technologies, which are combined to operate seamlessly. A small extract of a HetNet showing a network underlay of one macrocell and a network overlay consisting of multiple small cells is presented in figure 2.8. According to [56], the heterogeneous deployment is a cost-efficient way to significantly enhance the network capacity. Thus, HetNets are expected to play a major role in dealing with the forecasted exponential growth in data traffic.

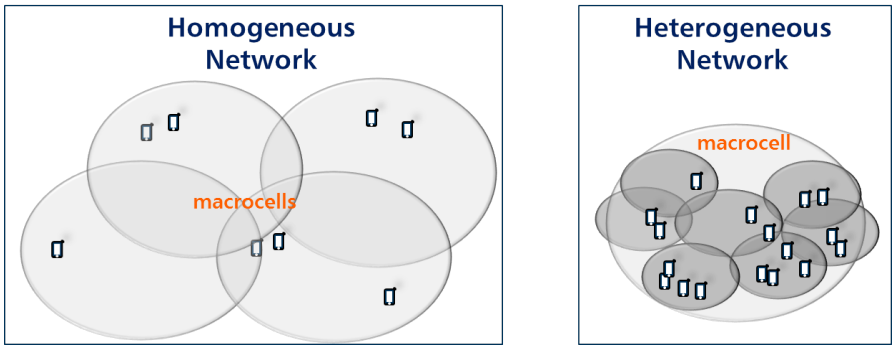

FIGURE 2.8: Homogeneous vs. Heterogeneous Network

In 3GPP standard, HetNets were introduced with LTE adding privately owned Home E-UTRAN NodeBs (eNBs) in release 9 [57]. The future relevance of HetNets may also be deduced from the latest 3GPP standardization work, listing HetNet topology enhancements as one of the key areas to be improved in 3GPP release 11 and 12, [58].

Although the temporary deactivation of cells is not limited to small cells, we assume that most future approaches considering cell deactivation will be implemented on the small cell overlay. The reason is that the macrocell underlay, acting as umbrella cells, provide the coverage and basic throughput. It is thus not surprising that multiple recent energy saving publications consider the small cell network overlay for cell deactivation, e.g. [59], [60], [6], [45], [61], [62].

Comparing the energy saving potential for a homogeneous and a heterogeneous network, cell deactivation in the homogeneous networks was found to outperform the HetNets in [16]. The reason is the increased energy saving due to the deactivation of the high power consuming macrocell, compared to small cells as presented in table 2.1.

Unless otherwise indicated, we assume in the energy saving approach of this work by temporary deactivation of cells a HetNet consisting of 2 layers: the first layer serves as the network underlay consisting of continuously active macrocells, while the second layer provides the capacity boosting small cells as the network overlay. Cell deactivation for energy saving is then restricted to the small cell network overlay. Additional configuration details will be provided in the respective sections.

Small Cells

Small cells have a small coverage radius of few meters to a maximum of 2 kilometers, in comparison to macrocells with a maximum range of several 10s of kilometers. Depending on the maximum Tx power, we distinguish between micro, femto and pico cells as listed in table 2.1. Besides the limited coverage radius, the major distinguishing features of small cells are the application, the management and the power consumption. The coverage area of a femto- and picocell is restricted to 10s of meters, while the microcell covers 100s of meters. The semi-autonomous femtocells are typically customer deployed nodes for indoor applications, but still remotely managed by the operator. The pico- and microcells on the other hand, require regular BS with lower transmit power compared to a macro-BS, which are completely manged by network operators.

The main purpose of small cells is to improve the capacity by increasing the radio spectrum efficiency. From 3G onwards, small cells were used to offload the mobile data from the macrocells. In dense urban areas as well indoor locations, e.g in homes and enterprises, small cells are particularly important, to enhance the data capacity and coverage. Additionally, the UEs save battery due to the mostly short distance to the BS. Differently to small cells, which are deployed as low-powered BS, also relay nodes and remote radio heads expand the network, but operate as extensions of fully operational BS [63].

Due to the promising coverage and capacity enhancement, but also due to the low cost and easy deployment, the number of installed small cells has kept rising in the recent years [62]. For the future, ultra dense small cell deployment are expected, to cope with the forecasted traffic growth in dense urban outdoor and indoor areas, e.g. for huge, multi-layer malls requiring 10s to 100s of small cell, [45], [7].
Besides the advantages of small cells, new challenges are expected in small cell HetNets. One major risk is the likely negative impact of the cross-tier interference, in addition to the intra-tier interference, caused by the significant difference of the maximum transmit power of macrocells and small cells. For example, a cell edge UE may be strongly interfered by the downlink transmission of a near-by small cell, [64], p. 18. During low traffic periods, however, the interference impact is expected to relieve, if small cells are deactivated to save energy [65].

2.2.4 Energy Saving Use Case in Self-Organizing Networks

In addition to the network aspects described in the previous sections, also the self organization has advantages and constraints for the proposed approach of this work, which are described in the following 3 sections.

Network configuration and optimization is a highly sophisticated task in the present mobile cellular networks. The high number of network elements, each equipped with thousands of parameters and, moreover, the mutual interference between parameters of the same as well as neighboring network elements require expert knowledge to guarantee efficient and reliable operation. All in all, the high complexity, the numerous users and network elements as well as the rapidly changing radio conditions urge for the implementation of a self-organized capability. Manual adaption is seen as a potentially error-prone, time-and cost-consuming task, [54].

Self-organizing networks are first of all intended to reduce the OPEX causing less human interaction due to the simplification of the network management tasks. However, also the overall network quality and thus, the user benefits from the fast and proper reaction to the changing traffic patterns and radio conditions by improved resource management and fast network response time.

The following 3 organizations and consortia respectively worked closely together and took a major step forward in the definition and implementation of the SON use cases:

- The **Next Generation Mobile Networks (NGMN) Alliance** [66] created by a group of operators, starting in 2006.
- The European funded **SOCRATES** (Self-Optimisation and self-ConfiguRATion in wirelEss networkS) project [67] with member from the mobile communication industry, network operators and research, running from 2008 to 2010.
- **3GPP** starting the standardizing work on SON with the first LTE version in release 8.

3GPP initiated its work on SON in release 8 and 9 for LTE with focus on QoS aspects, e.g. adapting the network to the varying radio channel conditions and thereby improving the network performance. The resulting definition of 9 high-priority **Use Cases (UCs)** in 3GPP 36.902 (release 9) [27], were enhanced and extended in 3GPP release 10, e.g. by inter-RAT operation [54]. A more recent study of next generation SONs in 3GPP 37.822 [68] for release 12 includes e.g. a SON to optimize the parameter settings for small cells. Future input is expected from the European FP7 SEMAFOUR project [69] aiming at a unified self-management system to holistically manage complex heterogeneous mobile networks.

The energy saving use case was introduced by 3GPP for LTE-A in release 10 as part of the Self-Organizing Networks [15]. Basically, it is intending to efficiently reduce the power consumption by temporary deactivation of unused resources (typically cells), especially for heterogeneous, high density networks. Since release 10 the standardization work for energy saving is steadily increasing, as indicated e.g. in the 3GPP release 12 overview [28] summarizing several studies on energy efficiency, including energy saving management as further detailed in section 2.2.5.

Opposite to most 3GPP defined use cases, targeting to enhance the network capacity and quality, the energy saving use case may even compromise the network. The reason is the clear objective to reduce the energy costs by the deactivation of resources.
The relation and interference of the energy saving use case with SON use cases specified in 3GPP [27], are summarized below:

- **Interference Reduction** has the objective to increase the capacity. Cells, which are not required at some point in time, e.g. home eNodeBs when the user is not at home, should be switched off to reduce the interference, expecting an increase in capacity.
  According to the high level description in 3GPP [27], the behavior matches with the Energy Saving Self-Organizing Networks (ES SON), but differs only for the purpose.

- **Automatic Neighbor Relation Function** is used to create and maintain neighbor cell relations. Therefore, the BS instructs the connected UEs to measure the signal strength of all neighbor cells.
  This set of UE measurements defined in [70] are also required as input for the fingerprinting approach of the ES SON as proposed in this thesis and may therefore be re-used. Additionally, temporary deactivated neighbor cells may need to be tagged appropriately, to ensure successful handovers to the currently active cells.

- **Mobility Load Balancing (MLB)** distribute the traffic load equally among cells by optimizing the setting of handover and cell re-selection parameters, while keeping the number of handover, respectively cell re-selections needed to reduce the cell load at the very minimum.
  In respect to improve the effectiveness of the ES SON, this SON could be adapted to empty lightly loaded cells, which could subsequently be deactivated in order to save energy, [54].

- **Coverage and Capacity Optimization (CCO)** aims to ensure the coverage without holes, while maximizing the capacity.
  Regarding the ES SON, coverage optimization is especially required in homogeneous networks to compensate possible coverage holes caused by deactivated cells, e.g. by expanding the cell radius or antenna tilting of the remaining active cells.
  Additionally, CCO and Energy Saving (ES) may conflict with each other. In case ES requests a cell deactivation, but CCO requires the cell to remain active, e.g. to compensate for a previously deactivated energy saving cell, a SON coordination function is required. Priorities may be introduced to resolve these conflicted, where the higher priority is expected for the coverage as detailed in [71].

- **Mobility Robustness Optimization (MRO)** optimizes the Handover (HO) parameter settings to avoid unnecessary handovers. The reduced number of handovers are expected to result in less HO-related radio link failures, ping-pong handovers and HO failures and consequently, in an improved user experience. Depending on the implemented solution, mobility parameters may be optimized. Either the handover execution may be delayed (using parameters such as Time to Trigger and HO Hysteresis) or, handovers to individual neighbor cells are preferred (using the Cell Individual Offset (CIO) parameter), [27].
  The handover setting and thus, the MRO are clearly impacted by the temporary cell deactivation to save energy. Handover parameter require adaptation to consider the restriction to the active cells at a given time. For example, in case of a HetNet with multiple deactivated small cells, handover to the macrocell may by the preferred by

the appropriate setting of its CIO of the HO hysteresis. This way, the number of handovers, but also possibly unsuccessful HOs within the partially inactive small cell network overlay, may be reduced.

- **Inter-Cell Interference Coordination (ICIC)** optimizes the resource coordination between the neighbor cells to reduce the inter cell interference. The idea of the ICIC SON is to tune ICIC configuration parameters, e.g. the reporting thresholds and periods as well as resource preference configuration settings, [27].
  Obviously, the temporary deactivation of cells is impacting the resource coordination between neighbor cells. Especially during periods of strongly changing traffic conditions, causing multiple cells to be switched on or off respectively, within a short period of time, a fast reaction to adapt the resource coordination for the current set of active cells may be required. Thus, ICIC parameter to accelerate the response to the network changes could be adapted, e.g. by reducing the measurement reporting thresholds and periods.

2.2.5 Energy Saving in 3GPP - Management Support for Potential Solutions

For energy saving, 3GPP specified a management concept to control the use case and potential solutions, [15]. In this section, we start with a summery of the potential approaches, followed by the introduction of the energy saving states and finalize with the supported steps of the cell deactivation and activation procedure in 3GPP.

The energy saving approaches in 3GPP include scenarios for deactivation of temporary unused cells, with one exception for the case of intra-BS energy saving [72]. For this case, Cell DTX solutions as described in the section 2.1.3 are proposed. In any other case energy saving refers to cell deactivation and activation on a cell level.

However, it is a prerequisite in 3GPP, that the coverage area is not compromised by a sleeping cell. For HetNets this condition can be easily fulfilled by restricting the cell deactivation to the capacity boosting small cell of the network overlay. Then, the underlaying umbrella cells proving the coverage are assumed to be always on. In homogeneous networks, cells are only deactivated, if neighboring cells are able to compensate the coverage area of the cell considered for deactivation. Additionally, inter-RAT HetNets and HetNets for the same RAT at the different layers are foreseen.

Energy Saving States

The energy saving SON management concept defines a set of energy saving policies, which were introduced in the 3GPP release 10 3GPP 32.551 [72]. Starting, we introduce the 2 energy saving states are introduced, which are supported on a per cell level. These states, referred to as *notEnergySaving* and *energySaving* state [72], and the transitions are presented in figure 2.9.

In case a cell is in *notEnergySaving* state, it is active and provides full service to UEs in the coverage area, while a cell in *energySaving* state is deactivated providing no service. From network management point-of-view, the *energySaving* state is neither seen as an outage nor a fault condition. The definition of the ES states in 3GPP implicitly requests the BS manufacturers to implement an sleep mode for energy saving in the BS.

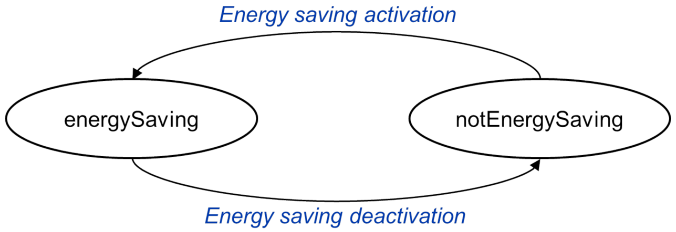

FIGURE 2.9: Energy Saving States and Transitions in 3GPP 32.551

Cell Deactivation and Activation

Both procedures are meanwhile supported by messages on the X2 interface for LTE and the S1 interface in case of inter-RAT ES SON [73]. The latest enhancement of the ES SON management added inter-RAT energy saving management to allow cell deactivation and activation for inter-RAT cells in release 11 [74].

For **cell deactivation** the following significant steps are supported [73], [54]:

1. Any cell in the network overlay can autonomously decide to deactivate its radio transmissions and change into sleep mode based on low / no load in the cell.
2. In case of low load, the cell may initiate handovers in order to off-load the cell.
3. To avoid frequent changes between active and sleep mode, the cell may wait for a defined guard period before that cell changes to sleep mode. During this time, the cell in transition to sleep mode may prevent idle mode UEs from camping in the cell and incoming handovers.
4. Prior to entering the sleep mode, all neighbor cells are informed by the concerned cell either via the X2 Configuration Update [75] for LTE or in case of inter-RAT cells via the S1-interface.
5. All informed cells maintain the cell configuration data e.g., neighbor relationship configuration, even when the concerned cell is sleeping.

Once a cell is in sleep mode, it cannot determine, when it should be reactivated. Therefore, it is up to the neighbor cells to observe the traffic load. If any neighbor cell needs capacity, it initiates the **cell activation** procedure as supported by 3GPP [73]:

1. The sleeping cell is activated by the capacity demanding cell either via the S1 interface or the X2 Cell Action Request message [75].
2. In addition, the cell initiating the cell activation will inform all neighbor cells about the reactivation of the previously sleeping cell via the X2 or S1 interface.

2.2.6 Architecture Solutions for Self-Organizing Approaches

Subsequent to the management capabilities, this section presents the potential architecture solutions for SON approaches. For the implementation of individual use cases, including self-organized energy-saving, 3 architectural solutions are proposed: the centralized, the distributed, and the hybrid architecture, [76].

The **centralized approach** executes functions, e.g. measurement and data collection and processing on the central network management node and may be more appropriate, if a huge number of cells is involved. Advantages of the centralized processing are besides the possible implementation of any kind of multi-vendor or multi-RAT solution, also the easy access to detailed and long-term statistics.
In contrast, the **distributed approach** restricts the SON implementation to the network element i.e. the BS only. This is seen as the preferred approach, if the use case is restricted to few cells. Then, for the communication between the cells, the X2-interface should be used, which allows also multi-vendor solutions. A possible advantage is the more timely reaction for time critical applications, if executing the function reside within the network element.
Finally, for the **hybrid approach** the functions are partly implemented on the network management level and partly on the network element level.

The architecture decision for self-organized energy saving, strongly depends on the implemented approach, e.g. the processing and the kind and number of parameters involved. Additionally, cell deactivation (see section 2.3.1), and cell activation needs to be considered separately.

Regarding the proposed cell activation approach of this work, the distributed architecture is proposed. The entire processing for cell identification using fingerprinting is performed at the cell level. The signaling exchange with the neighbor cells is limited to a wake-up trigger for cell activation and the distribution of the cell fingerprint. This spatial scope, limiting the approach to the neighbor cells as well as the limited signaling exchange are further reasons advocating the distributed approach.

2.3 Temporary Cell Deactivation and its Energy Saving Potential in Operational Networks

In this section, we focus on the temporary cell deactivation approach, its potential to save energy and its possible side effects. We start with strategies for cell deactivation described in literature, in order to optimize the number of deactivated cells. Next, we present the typical traffic variation and distribution for different types of area, followed by a literature study of the energy saving potential, if data from operational networks is used. Concluding, we consider possible side effects of temporary cell deactivation.

2.3.1 Cell Deactivation Strategies

With the aim of minimizing the energy consumption by temporary cell deactivation, several cell deactivation strategies are proposed in literature. The intention of these strategies is to maximize the number of sleeping cells, as well as to extend the period of time a cell remains in sleep mode.

Basically, we distinguish between a centralized and distributed deactivation approach as defined in section 2.2.6. In case of a distributed deactivation, the cell decides itself to initiated and perform its own deactivation, while a centralized node, e.g. in the core network, controls the centralized deactivation.

Decentralized Cell Deactivation: Idle Cell

This very basic approach assumes, that no UEs are connected to the cell, i.e. there is zero traffic load in this cell. In case the situation remains unchanged for a predefined period of time and parameter settings allow the cell to move to sleep mode, the cell autonomously decides to deactivate itself.

Decentralized or Centralized Cell Deactivation: Underutilized Cell

A more efficient approach for HetNets in [77] considers all underutilized small cells, especially during off-peak hours, for deactivation. UEs connected to these cells are forced to find a new connection on the macrocell. The forced handover is applicable, if the concerned macrocell cell is not in overload and the cell intended for deactivation is underutilized for a predefined period of time.

A more general approach, not limited to macrocell HO, distributes the UEs to any type of neighbor cell. This may require a centralized load balancing function to distribute the UEs, forced to leave the cells to be deactivated, between the a active neighbors.

Centralized Cell Deactivation Strategies

The centralized approach requires a central Operation, Administration and Maintenance (OAM) node to determines the most appropriate cell(s) to be deactivated.

Most publications studying cell deactivation to save energy assume multiple underutilized cell as a prerequisite. The problem to be solved is mostly reduced to find the optimum order of underutilized cell to be deactivated. Prior to deactivation, the central node verifies, that no UEs are resident in the selected cell. Resident UEs would be forced to perform a HO, as presented in figure 2.10. To determine the optimum order of the cells to be deactivated, one or multiple criteria are used in the publications listed below:

1. In [78], the energy saving potential for different network deployments in off-peak hours is evaluated. Sequentially cells are deactivated, which have the **minimum distance to its closest active neighbor cell**. Cell deactivation is continued as long as the coverage of the study area exceeds 95%.

2. [16] uses **periodic traffic patterns** to initiate cell deactivation and activation. Based on historic traffic patters indicating low traffic, cells start the deactivation according to their current load, starting with the minimum loaded cell first.

3. In [42], neighbor cell based parameters are used as input, including **the number, the distance, and the utilization of the neighbor cells**, in addition to the **cell utilization of the candidate cell to be deactivated**.

4. A pricing based algorithm considers the utility, i.e. **the number of UEs** and the **power expenditure of the cell** [79].

5. [47] uses the **achieved data rate** as indicator for the QoS in relation to the **BS transmission power** to sort the cells to be deactivated.

6. A **reinforcement learning based scheme** is presented in [44], which is re-used for cell activation in the same publication. Further details are provided in subsection 2.4.4.

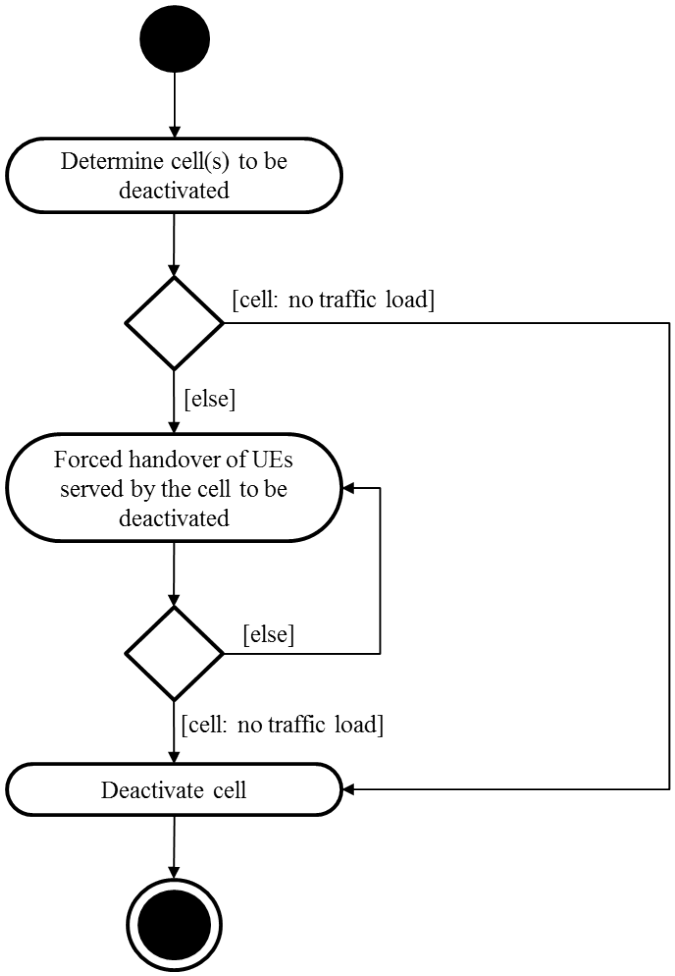

FIGURE 2.10: UML Activity Diagram: Centralized Approach for Cell Deactivation

It applies to all centralized approaches described before, that the central OAM node requires additional data from all involved cells to optimized the order of the cells to be deactivated. As a drawback, this is expected to result in an increase of the processing and signaling overhead.

2.3.2 Spatial and Temporal Traffic Variation

Multiple factors strongly influence the energy saving potential of temporary deactivated cells in operational networks. Among them are the network layout and configuration, as well as the deployed types of BSs.

A further crucial impact is expected from the spatial and temporal traffic distribution. Obviously, the potential reduction on power consumption depends on the intensity and periodicity of the traffic variation. The stronger the variation and the longer the times with very low traffic, the more cells can be switched off, resulting in an increased saving potential. Examples of the traffic variation in operational networks are provided in figures 2.11 and 2.12. They present the daily traffic profile from the network of an anonymized cellular operator. Each figure illustrates the traffic of an urban cell, one located in a business and one in a residential area. Both figures include 2 traffic profiles: the first represents a weekday averaging the traffic profile of all weekdays of a week, and

the second a weekend traffic profile averaging the profiles of the 2 weekend days. It is evident, that the profiles of both figures differ completely.

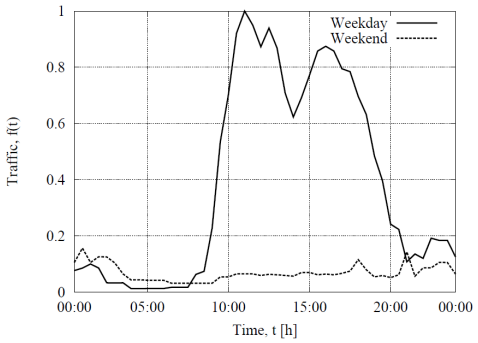

FIGURE 2.11: Daily Traffic Profile of a Business Cell: Weekday and Weekend Traffic Variation, [16]

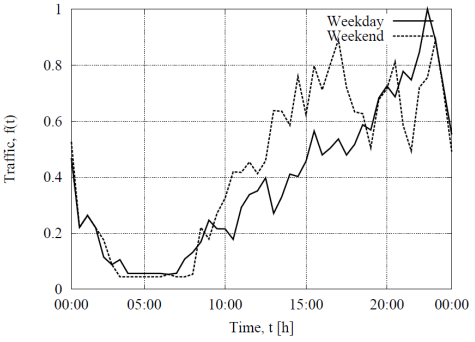

FIGURE 2.12: Daily Traffic Profile of a Residential Cell: Weekday and Weekend Traffic Variation, [16]

The business cell in figure 2.11 experiences a sharp rise in the morning, and a similar sharp drop in the evening of weekdays, while we observe almost no traffic during night hours and weekend. We expect a similar traffic profile also for differently used areas pursuing a specific purpose for a predetermined periodicity, e.g. shopping areas, school areas and industrial zones. Although the periodicity and the duration may vary, all these areas are characterized by a rather constant periodicity of high traffic peaks followed by very low traffic periods. In contrast, residential areas (see 2.12) experience almost identical profile during weekday and weekend and a rather moderate traffic rise and drop. From a more overall perspective, the geographic traffic distribution is proportional to the population density, ranging from dense urban to rural areas [80].

2.3.3 Energy Saving Potential based on Operational Network Data in Literature

In literature, few studies assess the energy saving potential of the temporary cell deactivation application. To compensate possible limitations of simulated data models, we restrict the studies to those, using data and network configurations from operational networks.

Table 2.2 summarizes the results of 4 papers, evaluating 4 homogeneous and 1 heterogeneous 3G networks. Besides the average and maximum saving potential, the activation trigger is provided, which is a major concern in this thesis.

The first table entry [78] merges 2 different data sets: the data traces of voice calls from 5 UMTS BS in a metropolitan area are mapped on the deployed UMTS network in Manchester, UK with 139 BS at 128 locations. The overlapping cells are deployed as a homogeneous network, which are considered for deactivation in case of little to no traffic. The BSs are sequentially deactivated keeping a minimum distance to the nearest active BS to meet the coverage conditions. Activation details are not provided. The resulting averaged energy saving ranges from 8 to 22%.

TABLE 2.2: Energy Saving Potential for Traffic Profiles of Operational Networks

Average Saving	**Maximum Saving**	**Network Type**	**Cell Activation Trigger**	**Source**
8-22%	35% during off-peak hour	HomoNet	-	[78]
30-40%	90% weekend, business area	HomoNet	periodic traffic patterns	[16]
14-39%	only weekday evaluated	HetNet	periodic traffic patterns	[16]
23-53%	urban area, low traffic	HomoNet	traffic increase	[77]
4-72%	72% low traffic, urban area	HomoNet	neighbor cells: number, distance, utilization	[42]

The second paper [16] evaluated both, a homogeneous and a heterogeneous 3G network. For the homogeneous network the coverage holes of the deactivated cells are compensated by the power increase of the active neighbor cells. Based on the traffic profiles presented in figures 2.11 and 2.12, corresponding low-power network configurations for the business and residential area are derived. The activation and deactivation follows then a predefined schedule derived from historic daily traffic patterns. The resulting average energy saving for the homogeneous network achieves 30-40%, while the HetNet achieves lower 14-39%. The different energy saving potential is mainly caused by the assumptions, that in homogeneous network all BS can be deactivated, while in HetNets the macrocell remains always active. Additionally, the macrocell power consumption is assumed to be 7 times higher compared to the small cell.

The third paper [77] is based on 3G traffic data, measured in 4 areas served by 45 to 177 BSs. Each area represents a different density level from very dense to medium dense. The user density corresponds closely to the BS density in the homogeneous networks, providing strongly or partially overlapping coverage. In case of low traffic, preselected underutilized BS within a grid are switched-off, assuming that the coverage is still provided by the close-by active BS within the same grid. Depending on the area density, the energy consumption is reduced by 52.7% to 23.4%. The best results are achieved in dense networks during weekend and night periods.

Finally, the last paper [42] maps a traffic profile, originally derived from a wired network, on an operational homogeneous 3G network. Three types of areas are evaluated: an urban, a suburban, and a rural area. The switch on / off algorithm is based on the energy saving potential as well as the individual cell load. Input for the algorithm include the number, distance and utilization of neighbor cells. Then, the load level of the serving cell is correlated with the load level of neighbor cells, similar to a load balancing approach. The achieved energy saving varies strongly for the different area types. For the rural area a maximum saving potential of 4% was achieved, while the urban area during low traffic periods achieved up to 72%.

Summarizing the evaluation from literature, we can draw several conclusions.

1. **Rural areas** are still mostly covered by few macrocells, achieving poor energy saving results [42]. Otherwise, rural area is rarely considered for cell temporary

deactivation in literature. However, we expect a change of the network density in the future e.g., due to the economic need to increase the coverage in rural area with access to high speed broadband networks and the public promotion to close the gap between urban and rural areas [81].

2. While the simulation studies based on **homogeneous networks** consider macrocells for deactivation, which exceed the power consumption of small cells multiple times, HetNets studies consider small cell deactivation only. Thus, the energy saving potential for homogeneous network seems to be more promising, often disregarding possible coverage issues and the future trend towards HetNets.

3. Responding to the traffic density, **HetNets** are the preferred solution to deal with the rapidly varying and periodically huge demand of traffic data [45], [60], [6]. Here, numerous variations of the network layers, cell types and the relation of small cells to macrocells will further impact the reduction of the power consumption.

4. The saving potential of temporary deactivated cells can be deduced from the characteristics of the area, which comprise the traffic volume, the related BS density, the variation of the traffic profile as well as the length of the periods with extremely low traffic. Additional major impact is expected from the network configuration and the deployed types of BSs.

5. The major insight from this literature study, however is **extreme range of the saving potential** from 4% to 90%, making it impossible to generalize the energy saving potential of temporary deactivated cells.

2.3.4 Side Effects of Temporary Cell Deactivation

Temporary deactivation of cells contain risks and uncertainties, but also positive side effects for the network, which are summarized below.

The implementation of self-organized energy saving procedure consumes **extra power**, although typically to a minor extent. For homogeneous networks, this applies for the enlarged coverage areas of the active cells (cell zooming). Additionally, in HetNets the macrocell power consumption may increase, when UEs are moved to macrocell to switch off small cells. The reason is, that macrocells partially scale the power consumption with the load.

Besides the network power, also the **UE power** may be impacted. For example, if UEs are forced to handover from a small cell to a macrocell in order to deactivate this small cell, the radio links to the mostly further distant macrocell require a higher power level compared to the typically nearby small cells, [59].

Deactivated cells may also **compromise the QoE** of the users, in terms of coverage and throughput. Especially for homogeneous networks, deactivating cells impose an obvious risk on the network coverage. Additionally, if the required cells are not activated in time, the demanded data rates may not be achieved. For example, if the cell activation triggers use static periodic traffic patterns, even urgently needed cells may not be activated in case of an unexpected event. Even if the cell activation trigger identifies the most needed cell in time, there is a considerable delay expected, until a cell moving from sleep to active mode is able to transmit and receives radio signals.

However, besides energy saving, switching off small cells in the network overlay **reduces the inter-cell interference**, as studied in [65], [29], [45]. The increased Signal to Interference and Noise Ratio (SINR) of the UEs may result in a better modulation and coding scheme for the data transmission, resulting in a throughput gains of up to 25% for low traffic scenarios [45].

2.4 Strategies for Cell Activation and Identification

In this section, we introduce strategies for cell activation, with focus on cell identification of a sleeping cell and the use of fingerprinting method. In the first 3 sections, we introduce the fingerprinting method, starting with the generic fingerprinting approach. Next, the fingerprinting use for the identification of a sleeping cell is described, followed by the comparison of fingerprinting with alternative methods for the purpose of cell identification. In the last section, we focus on the cell activation strategies and discuss the alternative approaches to cell fingerprinting to identify the best matching cell.

2.4.1 Overview of the Fingerprinting Method in Wireless Communication

Fingerprinting is an increasingly popular localization method in wireless communication networks. In literature, fingerprinting is also referred to as "database correlation" and "pattern matching". In contrast to the more common fingerprint applications used to determine the position of a UE, we use the fingerprinting method in this thesis to identify a deactivated cell.

Initially, fingerprinting was especially popular in **Wireless Local Area Networks (WLANs)** as an alternative or complementary solution for indoor environments, where Global Positioning System (GPS) did not work [82]. Typically, a fingerprint database of WLAN based positioning systems stores for each predetermined geographical location a data set consisting of a list of access points identified by the MAC addresses and per MAC address the associated signal strength. Examples for fingerprinting using the RSS measurements to determine the characteristics of a position can be found in [83], [84], [85], [86], and [87].

For **cellular networks**, RF fingerprinting to determine the UE position was initially described in the patent [88] and studied in a basic localization work [89], both published in 2001. Using similar measurements and parameter sets as in this thesis, in [90] and in [91] a median accuracy of the UE position of approximately 30 meters has been achieved in GSM networks. Both sources used RSS measurements of multiple neighbor cells in an urban environment as an input for the fingerprinting procedure.

In general, a fingerprint in a wireless environment maps a physical location on a list of uniquely identified nodes and their associated measurement values. However, the measurements required for the fingerprint need to be collected in advance and stored in a database, as a prerequisite for the subsequent localization procedure. Thus, all fingerprinting systems consist of 2 phases: The initial preparation phase, also referred to as learning or offline phase and the operational phase as illustrated in figure 2.13.

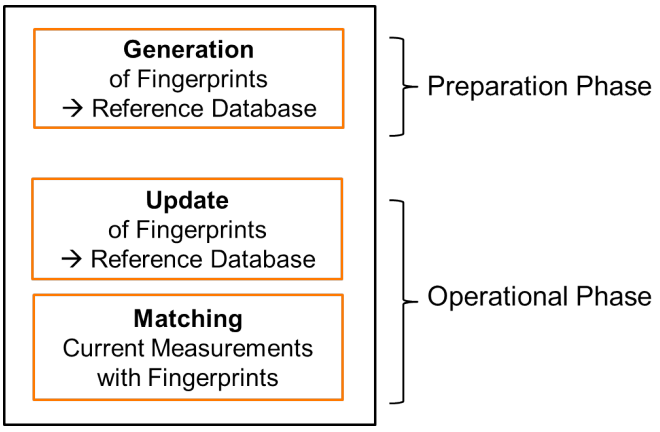

FIGURE 2.13: Phases of the Generic Fingerprinting Method

The phases are explained as follows:

1. During the **preparation phase** the characteristic measurements for each predefined geographic location are collected, e.g. the signal strength or signal travel time, to generate the reference database. The resolution of the physical location corresponds to a certain extent to the localization accuracy.

2. The **operational phase** starts as soon as stable fingerprints are available. Then, in case a UE requests its position, a measurement sample of this UE is matched with each fingerprint representing a geographical position. The best matching fingerprint(s) is used to estimate the current UE position. In addition, the fingerprints are continuously updated to accurately reflect the latest radio conditions.

2.4.2 Fingerprinting Use for the Identification of Sleeping Cells

Cell identification is a trivial task, if all cells are active, since each cell typically broadcasts periodically its cell identifier to enable UEs to uniquely identify their surrounding cells. A sleeping cell, however, with deactivated Tx and Rx components, demands new approaches. This section introduces fingerprinting as a method to identify a sleeping cell, which, if activated, is assumed to provide the best radio conditions for UEs in an overloaded cell.

First, just like generic fingerprinting, cell identification requires a preparation phase as presented in figure 2.13. In this phase, each cell generates its fingerprint using the RSS of each neighbor cell as measured by its connected UEs. The operational phase starts as soon as stable cell fingerprints are available. In case a cell in overload condition has multiple sleeping neighbor cells, the overloaded cell requests current measurements from its connected UEs. Then, the retrieved UE measurements are matched with the cell fingerprints of the sleeping cells to identify the most appropriate cell to be activated. Details and algorithms for the fingerprinting approach, proposed in this thesis, are provided in sections 4.3 to 4.5.

In this thesis, a fingerprint characterizes a cell based on the radio conditions in the neighbor cells as seen from the measuring UEs served by this cell. Consequently, we refer to this specific approach as **cell fingerprinting**.

However, we see 2 challenges for the fingerprinting approach typically used for localization to identify temporary deactivated cells:

1. We do not determine a geographical position, but a cell.
2. The cell to be identified is deactivated, i.e. neither transmitting nor receiving any radio signal. Thus, the current input for the localization procedure is limited to signals from surrounding active BSs, presumably neighbor cells.

To meet the first challenge, each fingerprint needs to uniquely characterize the coverage area of a cell. The retrieved measurements for each cell ID need to map the radio conditions of the entire cell area. Thus, the range and distribution of the RSS values measured in the entire cell need to be taken into account.

The second challenge is caused by the inability of the sleeping cell to contribute to its identification. However, the cell fingerprints were generated in advance, while all cell were active. Thus, the signal strength of any currently active neighbor cells can be matched with fingerprints of the deactivated cells. The impact of the limited number of active neighbor cells is then evaluated in chapter 5.

2.4.3 Parameters for Cell Coverage Identification

In this section, parameters are proposed, that could be used to identify the cell or its coverage, respectively.

Figure 2.14 presents few examples of commonly used location dependent parameters, i.e. the signal delay-based absolute time Time of Arrival (ToA), the Time Difference of Arrival (TDoA) as well as the RSS. These parameters are functions of the distance between the BS and the device, evaluated for an individual and combined use to identify a position, e.g. in [92].

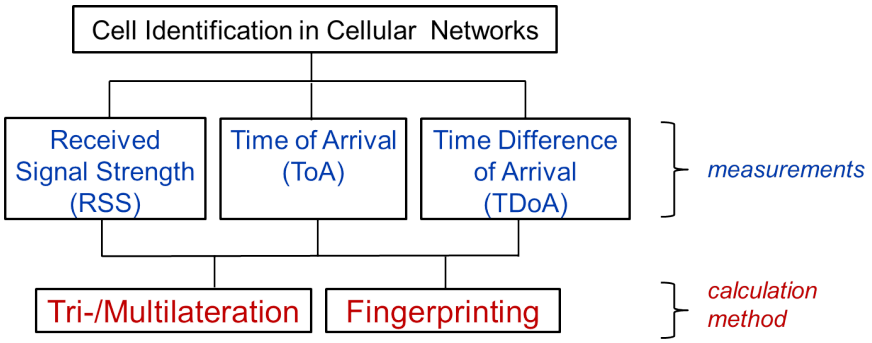

FIGURE 2.14: Selected Measurements and Methods for Cell Identification in Cellular Networks

These distance-related parameters serve as input for the localization methods, e.g. tri-/multilateration and fingerprinting respectively, presented in figure 2.14. Trilateration estimates the UE position from distance related measurements using the intersection point of at least 3 circles around the BSs. Additionally, the coordinates of the BSs are required as input for trilateration, as well as the synchronization of the BSs in case of TDoA measurements, [93]. Conversely, the RSS is a basic parameter, required to maintain and optimize the radio link, which may be re-used for cell identification.

A major important impact of all localization approaches considered for cell identification, is that the result is a geographical position. Thus, an extra step is required to map the geographical coordinates to the deactivated cell.

Summarizing, we see several advantages of the RSS-based cell fingerprinting.
Firstly, the cell identification can easily be implemented by using the cell ID instead of the geographical coordinates in the reference database.
Secondly, fingerprints of the deactivated cells are generated in advance, while being active. During cell identification, the signal strength received from the still active neighbor cells may partly compensate the missing measurements of currently deactivated cells.
Thirdly, fingerprinting is assumed to be rather robust against noise, as both, the measurements in the database as well as the currently retrieved measurement set used for the matching were at least partially impacted by the same radio disturbances. Thus, in [94] the RSS based fingerprints were found to experience low degradation in environment even with significant multipath.
In contrast, for ToA and TDoA the achieved accuracy depends to some extent on the line-of-sight between the nodes, which is hardly achievable in dense urban areas. For example, cell fingerprinting is expected to partially reflect the true radio conditions of the real network, providing a stable basis for identifying cells. Thus, we assume that RSS-based cell fingerprinting is an appropriate approach to identify a sleeping cell, even in a noisy environment.

2.4.4 Sleeping Cell Identification Strategies

In this section, we introduce alternative approaches to cell fingerprinting to identify a sleeping cell. The objective of the identification of a sleeping cell is to assure the QoE of the users by activation of the most needed cell.

We distinguish between 2 scenario: In the first, the cell is continuously sleeping, once deactivated. The reactivation is exclusively carried out by an active node via S1 or X2 interface. The second scenario demands radio signaling, however limited to the pilot signal and Interference over Thermal (IoT) measurements respectively, of selected cells in "light" sleep mode. These scenarios are also distinguished in the 3GPP technical report 36.927 "Potential solutions for energy saving for E-UTRAN" [15]. Selected approaches to determine the most needed cell to be activated from [15] and recent publications are introduced below.

Approaches for cell identification - without radio support of the sleeping cell

1. **No Cell Identification Information - Random Cell Section**

In this case, no information is available, how to identify the best matching cell. If the traffic increases in the area with multiple sleeping cells, one or multiple cell(s) are randomly selected and activated, [95], [96], [15], [77].

This solution may fit for scenarios with very few sleeping cells, increasing the chance to select a feasible one, while load balancing provides some support to distribute the traffic load. However, there is a considerable chance to activate a cell, which is not able to take over the traffic load. Thus, users may not achieve the demanded data rate. Alternatively, to avoid the negative impact on the QoE, all sleeping neighbor cells could be activated at once, resulting in an obvious increase of the power consumption.

2. **Periodic Traffic Patterns**

Based on historic daily traffic pattern, a characteristic daily periodicity is assumed, [16], [97], [15], [98]. The prerequisite is the strict periodicity of the traffic profile. This approach makes use of a cell based time schedule. Historical statistics of the traffic load in the cell are used to generate reliable traffic patterns. This approach requires some lead time to collect and condense the traffic pattern as well as continuous updates.

This approach is not feasible for any area with irregular or event-oriented traffic, e.g. cell locations near concert halls or football stadiums. Additionally, the QoE is impacted in case of any non-predictable event impacting the traffic load, e.g. special holidays. Consequently, as there will be no reaction on spontaneous traffic peaks, e.g. in case of an emergency, this further risk has to be considered.

3. **Time-Referenced Surrounding Cell Load for Reinforcement Learning**

This approach [44] uses a combination of fuzzy logic and Q-learning technique based on the number of active users, the average throughput as well as the time of day and the aggregated load of the whole day. Prior to cell activation the neighbor cells of each sleeping cell are monitoring (using the listed parameters), to determine the load in the surrounding area. The learning strategy implies, that the predicted times for cell activation improves over time.

Although several network informations are required, all parameters are easily accessible in operational networks. Further improvements are planned, including the reduction of the high effort to tune the algorithm as well as to avoid the possible service degradation for the users during the initial learning phase. Combing the load for specific periods of time with learning seems to be a promising approach, although it could be compromised by any non-predictable traffic demand.

4. **Optimum Power Usage / BS Distance**

More sophisticated approaches require multiple network information to determine accurately the best matching cell. In [42], 2 approaches with different grade of complexity are proposed. The more complex algorithms selects the BS with the optimum power usage in comparison to all other deactivated BSs, requiring the spatial system-load density as input. The second algorithm selects the BS according to geometric mean of the distance to neighbor BSs. The sleeping BS with the most distant neighbor BSs is activated.

According to the authors, the second approach was proposed, to overcome the high complexity as well as to avoid the signaling and measurement overhead required for the spatial system-load density of the first approach. The second approach, however, does not consider the traffic distribution or the positions of UEs demanding higher data rate. Thus, the selected BS may not be able to meet the local demand for higher data rates.

5. **Highest Load / Maximum Number of UEs**

Another approach [99] minimizes the number of active cells to save energy assuming a set cover problem. To maximize the energy saving, 3 sorting criteria for cells to be activated are studied. The cells are sorted according to: 1. the highest load, which could be provided, 2. the maximum number of UEs, which could be served (best

results), and 3. the maximum number of UEs, which are close to the BS center, i.e. achieving good channel quality.

To determine the cells to be switched on, the approach assumes, that all cells are initially switched-off. Next, the UEs are associated to the cells according to the 3 criteria. The association of UEs to the cells assumes the knowledge of e.g. the cell load and number of connected UEs prior to cell activation. Thus, this approach may be seen as a more theoretical approach,

6. **Positioning Information**

For this approach, each macrocell is equipped with a database to store the channel quality (Signal to Noise Ratio (SNR)) in relation to its geographical location. The SNR is stored for all small cells controlled by the macrocell, [45], [61]. A geographic location report from the UE is used to select the best matching small cell.

For the generation of the database, the UEs have to transmit the requested data to the macrocell, which demands the introduction of a new message type. Furthermore, the required SNR measure is hard to obtain in a real network. Finally, there is significant effort involved to train the database. This highly complex procedure may be regarded as an interesting idea, but may result in a high processing and implementation effort.

This localization based approach demands positioning information of a significant number of UEs, which consumes extra power, e.g. in case GPS is used. Even more critical may be the impact of shadowing, typically experienced in urban areas, which may strongly impact the accuracy to map the UE position to the most appropriate cell.

Approaches for best matching cell identification - with partial radio support of the sleeping cell

Both of the following 2 approaches request the activation of some sleeping BS to allow partial radio signaling. This requires the introduction of a third cell mode, in between sleep and active mode, referred to as "light" sleep mode in section 2.2.2.

1. **IoT Measurements**

In case of high load, sleeping cells activate their radio interface to a degree to be able to perform and report IoT measurements, [98], [15].

2. **Pilot Signal**

In case of high load, sleeping cells transmit the pilot signal for a short time interval. The UEs in the coverage area of these cells are configured to measure and report the reference signal measurements retrieved during the time period from the pilot signal. Based on the evaluation, the most suitable cell(s) will be activated, [15], [70].

Both approaches use the "light" sleep mode for the partial transmission of selected data and additionally in the first case for the reception og IoT measurements. This requires the activation of radio components as described in 2.2.2, resulting in a significant reduction of energy saving.

CHAPTER 3

Network Simulation

Contents

3.1 Evaluation Methods 39
3.2 Simulated Network 40
3.3 Mobile Users 41
3.4 Radio Propagation Modeling 42
3.4.1 BS Transmit Power and Antenna Configuration 43
3.4.2 Pathloss 43
3.4.3 Shadow Fading 43
3.5 Simulation Model 43
3.5.1 Generic Processing 43
3.5.2 Cell Fingerprinting Application 44

In this chapter we describe the implemented simulations for the evaluation of the cell fingerprinting procedures using an LTE network simulator. First the network structure and radio environment relevant for cell fingerprinting are introduced, followed by the simulation model with focus on the particularities of cell fingerprinting.

3.1 Evaluation Methods

For the evaluation of the accuracy of cell fingerprints in this thesis, we use for the most part simulation studies. An LTE system simulator is used for the implementation of the cell fingerprint procedures as well as for the evaluation of the cell fingerprinting results. The simulator is a C++ event-driven LTE system level simulator based on software

libraries provided by Alcatel-Lucent Bell Labs Germany and the Institute of Communication Networks and Computer Engineering at the University of Stuttgart, Germany (IKR) [100]. The simulations consider a 3GPP compliant LTE downlink network.

The simulation environment is expected to model an operational network in the field, to validate the results achieved in the simulation studies. Therefore, the simulated procedures and parameter settings should closely approximate the behavior of an operational network in the field.

To compensate the unavailability of data from operational networks, the experience with "real" network data and their evaluation in literature are summarized and assessed in section 2.3. Additionally, for the final study of the energy saving, a simplified network model was developed (see chapter 6) to evaluate the saving potential for the achieved cell fingerprinting accuracy.

In the following sections we concentrate on those procedures and parameters of the LTE system simulator with relevance for cell fingerprinting. More details on the generic design, the structure and procedures of the simulator are provided in [101] and [102].

3.2 Simulated Network

The basic simulated network consists of 7 LTE BSs, each placed in the center of a hexagonal grid with a inter-site distance of 500 m (see figure 3.1). One BS consists of 3 transceivers, each of which represent the coverage area of a cell. The total of 21 cells constitute the basic network, with cell IDs ranging from 3 to 23 as indicated in table 3.1.

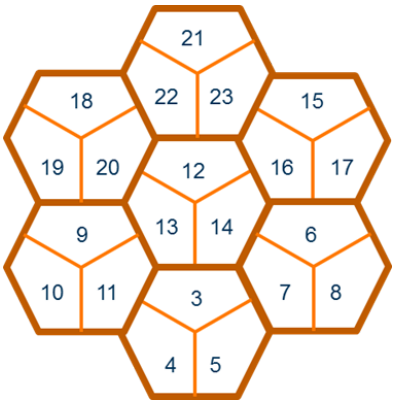

FIGURE 3.1: Simulated Network Structure

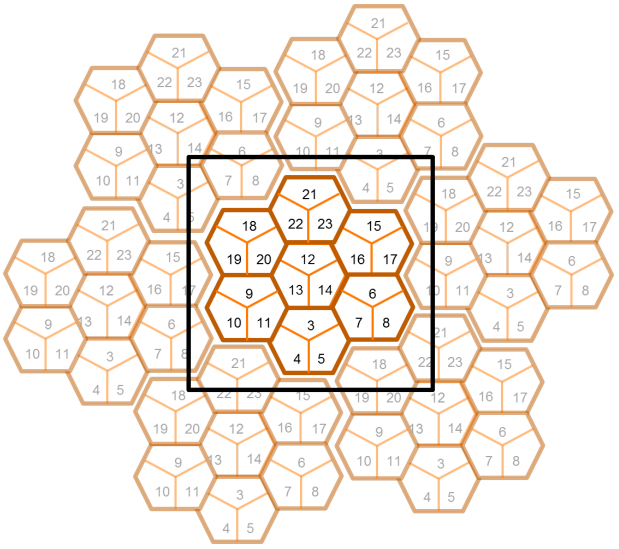

FIGURE 3.2: Mirrored Wrap-Around Network Structure

A wraparound mechanism is implemented by surrounding the basic network with 6 of its identical replicates as shown in figure 3.2. The purpose of the outer replicates is to avoid border effects caused by missing coverage, especially concerning the interference calculation.

Table 3.1: LTE Simulator - BS Parameters and Values

Parameter	**Value**
Number of Base Station Sites	7
Number of Sectors / Cells per BS	3
Cell IDs	3 to 23
Inter-site Distance	500 m

3.3 Mobile Users

Besides the fixed network elements, also mobile users with a realistic moving behavior are essential to generate accurate results, close to real operational networks. Therefore, the random-walk mobility model is implemented in the simulator, defining a set of movement parameters for UEs or alternatively, a group of UEs. The movement parameters consist of the speed, randomly selected from a defined speed range (see table 3.2) and the direction. Realistically, a constant speed can not be assumed over time. Therefore, whenever a snapshot of the measurements is taken, the UE speed may increase or decrease by a maximum of 5%.

Table 3.2: LTE Simulator - User Equipment (UE)

Parameter	**Value**
Receive Antennas Type	1 Omni
Antenna Height	1.5 m
Antenna Gain	2 dBi
Mobility Model	Random Walk
Number of Mobile Groups with 20 UEs each	3 Mobile Groups
UE Speed per Mobile Group (Variation of 40% within each Group)	- Pedestrian: 2.4 - 3.6 km/h - Bicycle: 12 - 18 km/h - Car: 24 - 36 km/h

In addition, the direction will change over time, as all UEs are restricted to stay in a rectangular area surrounding the inner central network, marked in black in figure 3.2. Whenever a UE reaches the border of the central network, it initiates a handover to any cell providing the best radio conditions. Even if the new cell is located in one of the outer, replicate networks, the UE maintains the direction of travel. Only in case a UE reaches the border of the rectangle, it changes the direction and will eventually travels back to the central network.

During the simulation, a UE is instantaneously handed over to that neighbor cell, whose RSS exceeds the RSS of the serving cell. A handover offset is not implemented, which could avoid e.g. UEs to switch back and forth between the cells. Resulting, the UE is continuously connected to the cell providing the strongest signal.

Finally, the UE movements and distribution over the complete network is a prerequisite for the generation of reliable cell fingerprints. It is essential to record the UE RSS measurements from different positions within each cell area. Therefore, 60 mobile users

are initially placed randomly in the coverage area. For modeling the mobility in an urban area, 3 mobile user groups are configured. The 3 mobile user groups consist of 20 users each. Each group represents a typical speed group in an urban area, i.e. pedestrians, bicycles, and cars. For the periodically retrieved UE measurements to generate the cell fingerprints, the distance between the previous and next UE position to provide the next measurement sample will vary in line with the UE speed. With different velocities, the measurements of very fast UEs will provide an rough picture of the UE course from a wide view of the network. The slower UEs will have a smaller, but a more detailed view, measuring points very close to each other to provide details about the RSS conditions at that point. For example, for a given period, many more samples with a finer granularity will be retrieved for the slow moving pedestrians compared to the fast moving cars.

Each mobile user group uses a defined speed as shown in table 3.2, which varies by 40%.

3.4 Radio Propagation Modeling

The cell fingerprints used in the application of this work are derived from the received signal strength of the neighbor cell pilot channel as received by the UE. Reliable RSS measurements based on an accurate radio propagation model are therefore another prerequisite for valid simulation results. The propagation of the radio signal in wireless communication depends on several radio and equipment characteristics as well as environmental factors. Any of these characteristics and factors impacting the relation between the transmitted power and the received power are summarized in table 3.3.

Table 3.3: LTE Simulator - Radio Environment Parameters and Values

Parameter	**Value**
Channel Bandwidth	10 MHz
eNodeB Tx Power	46 dBm
eNodeB Tx Antennas	1 per sector
Height of eNB Tx Antennas	32 m
eNB max. Antenna Gain	15 dBi
Pathloss	128.1 + 37.6 $\log_{10}$ (max (dKm, 0.035))
Shadow Fading Decorrelation Distance	50 m
Shadow Fading Standard Deviation	6 dB

The following equation expresses the received power in relation to the transmitted power and the major factors for the radio propagation:

$$P_{Rx} = P_{Tx} - PL - SF + G_{Ant}, \tag{3.1}$$

where P_{Rx} is the received power in dBm. The transmitted power, P_{Tx}, is reduced by the pathloss (PL in dB) and the slow fading (SF, in dB), also referred to as shadow fading, whereas fast fading is ignored. G_{Ant} (in dB) summarizes the antenna gain obtained for all simulated BSs.

3.4.1 BS Transmit Power and Antenna Configuration

All 7 BS in the LTE network are configured identically with a transmit power of 46 dBm. In LTE, Base Stations are referred to as eNodeB or eNB representing the complete RAN. Just as the Tx power, the antenna gain is identical for all cells. The gain is based on the use of directional antennas as detailed in table 3.3.

3.4.2 Pathloss

Pathloss (PL) defines the reduction of the signal power in relation to the distance between the transmitter and the receiver. 3GPP [103] defines the PL used in the simulator for a distance of d meters between the transmitter and receiver as:

$$PL = 128.1 + 37.6 \ \log_{10}(d), \tag{3.2}$$

with a BS height of 15 meters and an assumed carrier frequency of 2 GHz.

3.4.3 Shadow Fading

Fading is the variation of the attenuation of the radio signal strength, caused by e.g. interference or shadowing. The major impact on the RSS is expected from slow fading obscuring the line-of-sight caused by e.g. shadowing due to large obstacles, such as building and hills. This is a common phenomenon, especially experienced in urban areas, where the energy saving application by temporary deactivation of cell is most relevant. The impact on the signal strength varies slowly, resulting in a correlation of consecutive fading values of a moving UE. Between two consecutive values the normalized autocorrelation results in [104]:

$$R(\Delta d) = e^{-\frac{\Delta d}{d_{cor}} \ln 2}, \tag{3.3}$$

where Δd is the distance (in m) between the two UEs and d_{cor} is the environment dependent decorrelation distance (in m). Further details regarding fading and antenna gain are described in [101] and [102].

3.5 Simulation Model

The introduction of the simulation model starts with the generic part, followed by its particular adaptation for cell fingerprinting.

3.5.1 Generic Processing

At the start, each simulation deploys the cells as presented in figure 3.1, followed by the deployment of the UEs. The total number UEs as defined in table 3.2 are randomly deployed in the network and initially, evenly distributed between the deployed cells.

After the initialization, each of the simulation runs executes sequentially a configurable number of batches. Each batch runs for a configurable period of time, the "Batch Runtime" set to 100 s in our application as shown in table 3.4.

A batch is a job with predefined set of parameters, running for a fixed batch time, as illustrated for the cell fingerprinting application in table 3.4. At the start of each batch the UEs are randomly redeployed in the network. For each batch, the UEs are placed at different locations in the network, using a different path. In this way, it should be guaranteed to receive simulation results covering a wide range of radio conditions experienced for multiple independent scenarios. Within the runtime of a batch, periodic snapshots of the entire network are taken. Figure 3.3 illustrates the batches and snapshot periods used for the cell fingerprinting application.

3.5.2 Cell Fingerprinting Application

For cell fingerprinting, we demand relatively evenly distributed and robust statistics for the generation of the cell fingerprints.

Initial test studies with different numbers of batches proved, that we achieved consistent cell fingerprints, if the generated fingerprints were based on more than 50 measurements for each cell. Each batch obtains in average 14.14 RSS measurements for each cell. Consequently, for a given number of 100 simulation runs the computed cell fingerprints were based on an average of 1414 RSS measurements per cell, exceeding by far the required minimum of 50 measures.

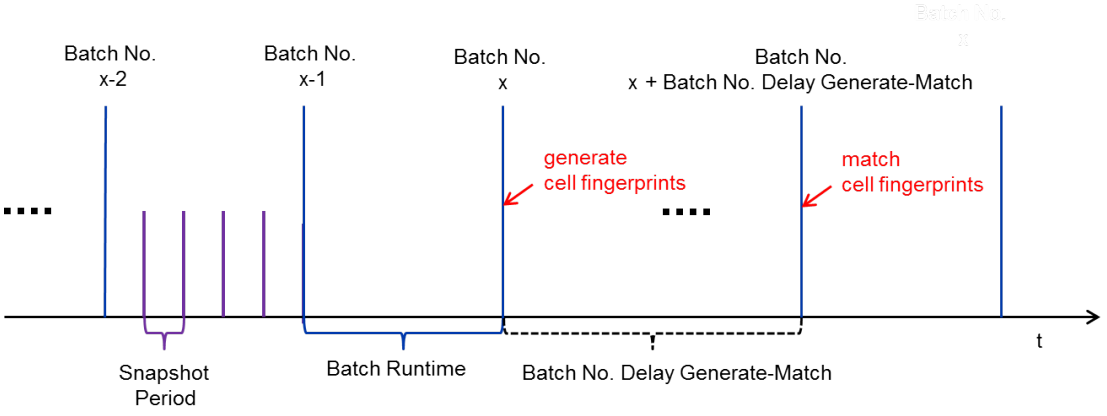

FIGURE 3.3: Simulation Run for Cell Fingerprinting: Batches Including Periodic Snapshots

In figure 3.3 we present the simulation run including the particularities for cell fingerprinting, explained step by step as listed below:

1. Each simulation run is initialized to run a predefined number of batches with a fixed runtime, presented in table 3.4. Each simulation run is split into 3 phases:

   (a) Fingerprint generation using the RSS measurements of either 100, 150, or 200 batches to generate the cell fingerprint databases.

(b) Delay period: The number of batches to delay the fingerprint matching after the fingerprint generation. The "Batch Number - Delay Generate-Match" as illustrated in figure 3.3 is set to 2 batches for the studies of this work.

(c) The matching is executed in the first batch after the delay period. To evaluate cell matching, 1 UE measurement sample per cell is taken from a consecutive simulation run and matched against all cell fingerprints. Details on the simulation parameters are given in table 3.4.

2. Within each batch runtime of 100 s, a snapshot is taken every 20 s.

3. At each snapshot, the UEs update their position and measure the signal strength on the pilot signal of their serving and of all neighbor cells. Due to the new UE position, a different cell compared to the previous snapshot may provide a stronger signal. Then, the UE is immediately connected to the new cell providing the stronger power. Consequently, all UEs are always connected to the cell providing the strongest signal during the entire simulation.

The evaluation of each simulation study is based on the averaged results of the 3 simulation runs to mitigate possible fluctuations. All studies in chapter 5 use the identical simulation settings as shown in table 3.4.

TABLE 3.4: LTE Simulator - Cell Fingerprint Parameters and Values

Parameter	**Value**
Batch Runtime	100 s
Snapshot Period	20 s
Batch Number - Fingerprint Generation	<100>/<150>/<200>
Batch Number - Delay Generate-Match	2
Number of UE Measures	<1>/<2>
Switch Off Cells	<TRUE>/<FALSE>
Switched Off Cell - Lower ID	<6>/<10>/<14>/<18>
Switched Off Cell - Upper ID	23

In addition to the batch and snapshot related parameters, table 3.4 introduces few major parameters to configure cell fingerprinting. "Number of UE Measures" indicates, whether 1 single or 2 averaged UE measures are used as input for the matching (see section 5.3). The remaining 3 cell deactivation parameters provide the flexibility to switch on or off different numbers of cells indicating the values we used in the studies of this work in section 5.4. In case "Switch Off Cells" is set to FALSE, all cells remain active. Otherwise, the parameters "Switched Off Cell - Lower / Upper ID" provide the range of the cell IDs to be deactivated.

While we present simulation results for 1 carrier, it is assumed, that fingerprinting works in a similar way on multiple carrier frequencies as detailed in [19].

CHAPTER 4

Cell Fingerprinting Approach - the Framework

Contents

4.1 Cell Fingerprint Overview - Data Processing 47
4.2 Definition of RSS Metrics for Cell Identification 48
4.2.1 Analysis of Neighbor Cell RSS Measurements 48
4.2.2 Single Cell Fingerprint Metrics - Basic Set 49
4.2.3 Outlier Definition 51
4.2.4 Combined Cell Fingerprint Metric - Basic Sum 52
4.3 Cell Fingerprint Generation 54
4.4 Cell Fingerprint Processing During Cell Deactivation . . . 55
4.5 Cell Activation Using Cell Fingerprints 56
4.5.1 Matching Procedure 58
4.5.2 Cell Identification Based on Cell Fingerprints - Example 60

This chapter introduces the framework of the cell fingerprinting approach to identify the best matching cell for activation, as an integrated part of temporary cell deactivation approach to save energy. The framework forms the basis for the simulation studies presented in the subsequent chapter.

Starting with an overview of the complete cell fingerprinting procedure, we continue in the second section to define the structure and content of the cell fingerprints. Analyzing the RSS values as measured by the UEs, results in the definition of single and combined RSS-metrics for cell identification. These metrics model the RSS range and distribution of the neighbor cells and are stored in the cell fingerprint. Next, the sections 4.3 to 4.5 detail the procedures for temporary cell deactivation as proposed in this thesis, consisting of cell fingerprint generation, cell deactivation and activation. Here we focus

on the matching procedure and introduce the scoring required for the cell fingerprinting approach during the cell activation procedure.

4.1 Cell Fingerprint Overview - Data Processing

Since the generic fingerprint procedure, for cell activation and deactivation were already introduced in the sections 2.3 and 2.4, the overview in this section focuses on the data processing.
Figure 4.1 demonstrates the central role of the RSS retrieved from the UEs as the only measurement required for fingerprint generation and matching.

The **RSS measurement sample** corresponds to a measurement report, sent periodically or on request from the UE to the BS. This report consists of a list of neighbor cells and their associated signal strength as measured by the UE.

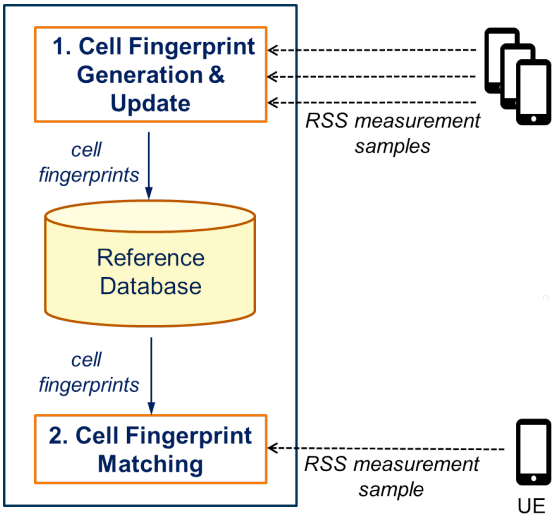

FIGURE 4.1: Overview of the Cell Fingerprint Approach

Basically, processing of cell fingerprint is split into 2 parts (see figure 4.1):

1. Cell Fingerprint Generation & Update: The RSS of the neighbor cell included in measurement samples sent by UEs are used to generate / update the cell fingerprints, which are stored in the reference database. The initial cell fingerprints are generated prior to the operational phase, while all cells are active (see section 2.4.2).

2. Cell Fingerprint Matching: For the matching as part of the cell activation procedure, a UE resident in an overloaded cell is requested to sent a measurement sample, which is matched with the cell fingerprints of the reference database representing the currently sleeping cells. The matching is performed for each RSS of the sample and compared against the cell fingerprint of each neighbor cell. The cell corresponding to the best matching CFP is assumed to provide the best radio conditions for the measuring UE. Consequently, this cell is activated to relieve the overloaded cell.

4.2 Definition of RSS Metrics for Cell Identification

Prerequisite for the fingerprint generation is the definition of RSS-metrics, which map the radio conditions of the neighbor cells. The determined metrics are used in the cell fingerprint to identify the cell. As a first step to identify potential metrics, the RSS values of the neighbor cells are analyzed, followed by the definition of RSS-based metrics in the subsequent sections.

4.2.1 Analysis of Neighbor Cell RSS Measurements

Analyzing the retrieved RSS of the neighbor cells, we intend to identify cell characteristics to determine a cell. As a prerequisite for the analysis of the distributions and ranges of the RSS values, RSS measurement samples of all active neighbors are captured from the UE at various positions within each cell as presented in figure 4.2 for the serving cell 12.

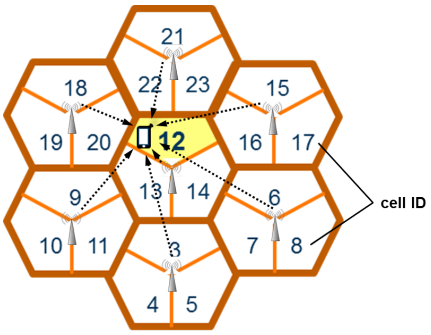

FIGURE 4.2: RSS of Neighbor Cells Measured by UE

Examples of resulting RSS distributions using in average 670 UE measurement samples per neighbor cell are presented in figure 4.3. The distributions illustrate the RSS measurements as retrieved by UEs connected to the same serving cell "12" for 4 instances, representing 3 different types of neighbor cells:

- intra BS adjacent cell: 2 neighbor cells "13" and "14" of the same BS
- inter BS adjacent cell: the adjacent neighbor cell "23" of a different BS
- the non-adjacent cell 3

All distributions are presented in RSS samples of 5 dB.

Based on the analysis of multiple RSS distributions, the following characteristics were derived:

1. Obviously, caused e.g. by distance from serving cell to neighbor cell, and environmental conditions, the neighbor cell distributions have different minimum and maximum RSS values, which largely overlap between the different neighbor cells.

2. Due to the common radio effects, such as shadowing and reflection, the measurement distributions for neighbor cells do not completely correspond to normal distributions. As the RSS distributions are unevenly distributed with varying ranges, quantiles are considered as a valid approach for modeling the RSS distributions.

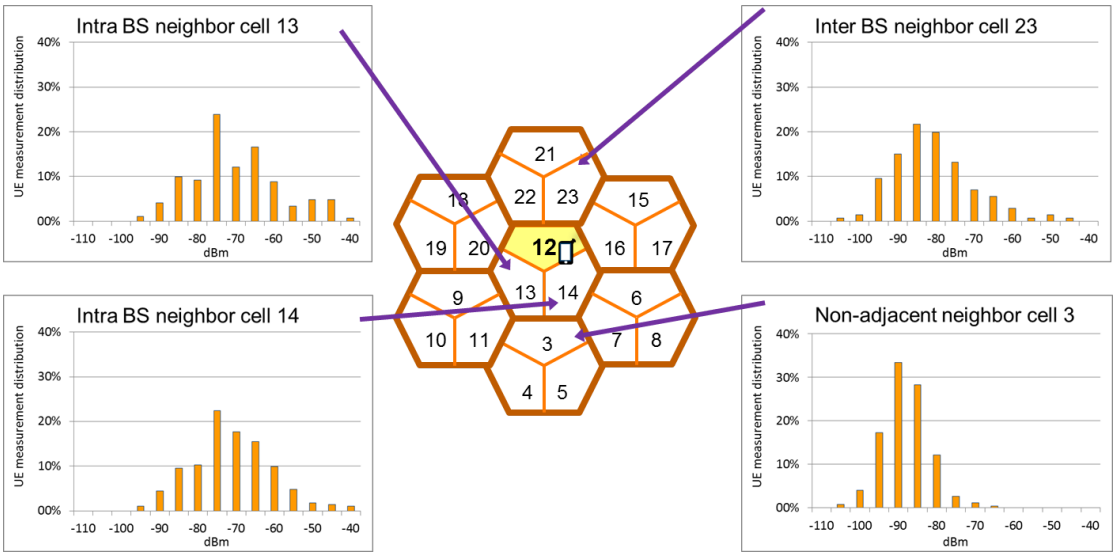

FIGURE 4.3: Examples for Typical RSS Neighbor Cell Distributions Measured by UEs Served by Cell 12

3. Outliers, i.e. RSS measures distinctly separate from the rest of the RSS measures, are observed.

These observations are used to derive metrics, which model the RSS distributions of the neighbor cells.

4.2.2 Single Cell Fingerprint Metrics - Basic Set

The initial 3 basic metrics, introduced in this section, are derived from the analysis of the RSS distributions in the previous chapter.

The following CFP metrics are derived:

1. **minMax**: the range between the minimum and maximum RSS.

2. **exclOut**: RSS range excluding the outlier as explained in section 4.2.3.

3. **Range between 10th and 90th Percentile (Q10)**, also referred to as $Q_{0.1}$ / $Q_{0.9}$ or decile: valid RSS range between 10th ($Q_{0.1}$) and the 90th percentile ($Q_{0.9}$).

Each of the 3 metrics, minMax, exclOut, and, Q10, is referred to as a **basic single CFP metric** within the scope of this work.

The first CFP metric, minMax, provides the minimum and the maximum signal strength for each neighbor cell. Figure 4.4 illustrates the different minimum / maximum RSS values depending on the types of cells. As expected, the close intra BS adjacent cell (in pink) provides the strongest signal strength and the more distant non-adjacent cell (in blue) provides the weakest signal. Restricting the matching to the minimum / maximum range only, may result in considering multiple or even all neighbor cells as valid due to the huge overlap of the RSS range.

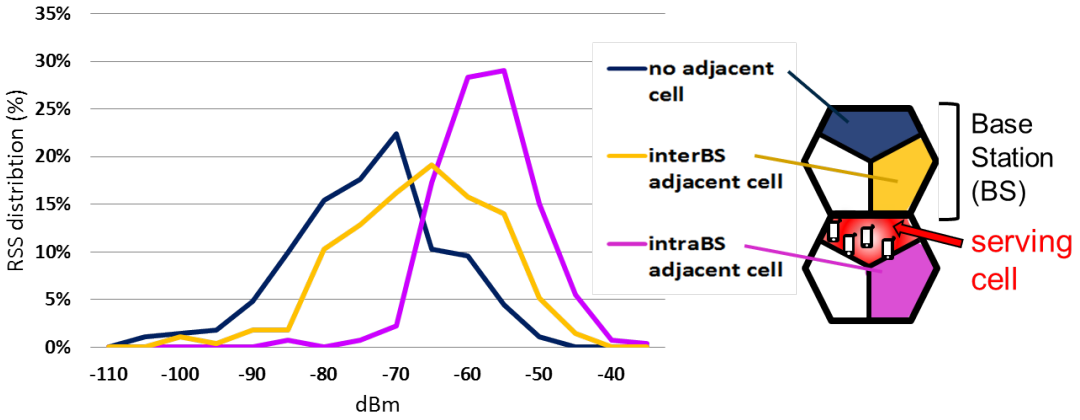

FIGURE 4.4: RSS Distributions: Different Types of Neighbor Cells

Thus, the CFP metric Q10 with limited RSS range is introduced. As illustrated in figure 4.3 and figure 4.4 the huge number of valid RSS values are concentrated towards the median. Excluding the RSS values at the edge, limits the range, but still regards the largest share of the RSS values as valid. Quantiles are typically used to extract a defined percentage of values, especially for unevenly distributed probability distributions. Using the upper and lower decile excludes 10% of the lowest and highest signal strength measures. The impact on the valid RSS range can be derived from figure 4.5. It presents a typical RSS distribution for an intra BS neighbor cell for the network constellation given in figure 4.2. The upper decile fence corresponds to a reduction of -20 dB compared to the maximum of -40 dBm, whereas the lower decile corresponds to an increase of 10 dB in relation to the minimum RSS value of -97 dBm.

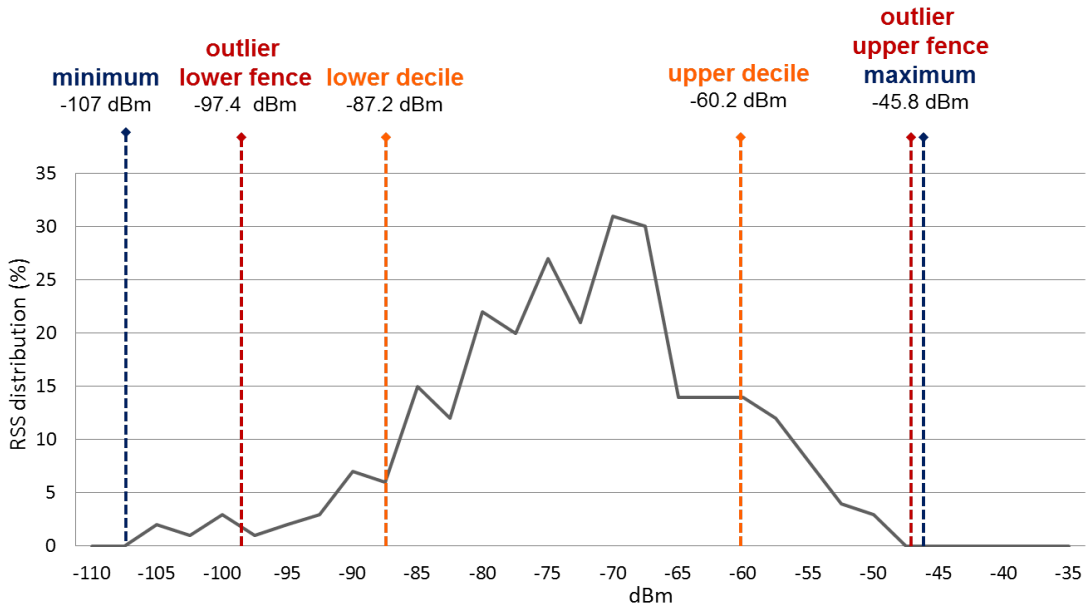

FIGURE 4.5: Example: Typical Neighbor Cell RSS Distribution of an Intra BS Neighbor with Fence Values for Basic Single CFP Metrics

Furthermore, figure 4.5 highlights the exemplary fence values of the other 2 basic single CFP metrics, the minimum / maximum fences and the fences of the third basic CFP metric exclOut to exclude outliers. In case of the outlier upper fence, no outliers

were detected, thus the outlier upper fence corresponds here to the maximum. How to calculate the outlier fences is detailed in the next section.

By definition, a **CFP metric** maps the retrieved RSS values, e.g. the RSS range or distribution of neighbor cells as retrieved by the UE, to identify a cell. The upper and lower RSS value of each metric are attributes of the cell fingerprint and associated to each neighbor cell.

Consequently, a cell fingerprint of a cell x consists of the list of its neighbor cells, where each neighbor cell includes the results of the CFP metrics to model its associated RSS distribution.

4.2.3 Outlier Definition

An outlier is a measure that is numerically distant from the rest of the measures. In practice, outliers are unavoidable mainly due to hardware malfunction or failure, environmental factors or adversary attacks [105]. Especially, the radio environment is vulnerable to outlier. For example, the received strength of a radio signal may vary strongly as they are very sensitive to the typical radio effects, such as fading caused by multipath propagation. Outliers may distort the RSS measurements and endanger the validity of the cell fingerprints. Therefore, to preserve robust fingerprints, outliers could be discarded or treated differently during the matching process.

One widely spread approach to calculate outliers is a method defined by Tukey [106], which uses the interquartile range to calculate the outlier fences. An outlier is defined as any measurement, which deviates more than one and a half times from the box of the interquartile range, as presented in figure 4.6. Then, the measurement is assumed to be too far off from the median to be reasonable. For the calculation, the interquartile range (IQR) is defined as the range between the first quartile Q1 and the third quartile Q3 as illustrated in Eq. (4.1a). The Interquartile Range (IQR) corresponds to 50% of the measurements around the median. The calculation of the fences are shown in Eq. (4.1b) and Eq. (4.1c).

$$IQR = Q_3 - Q_1 \tag{4.1a}$$

$$upperFenceOutlier = Q_1 - 1.5 \times IQR \tag{4.1b}$$

$$lowerFenceOutlier = Q_3 + 1.5 \times IQR \tag{4.1c}$$

Figure 4.6 shows an example for the upper and lower outlier fences using a box plot for graphical presentation. In case of a high IQR, the fence may exceed the minimum and/or maximum RSS value. If so, the concerned outlier fence is replaced by the appropriate minimum and/or maximum RSS sample. An example is demonstrated in figure 4.5, where the outlier lower fence is replaced by the minimum RSS.

Any RSS measurement received above the upper or below the lower outlier fences are considered as less reliable.

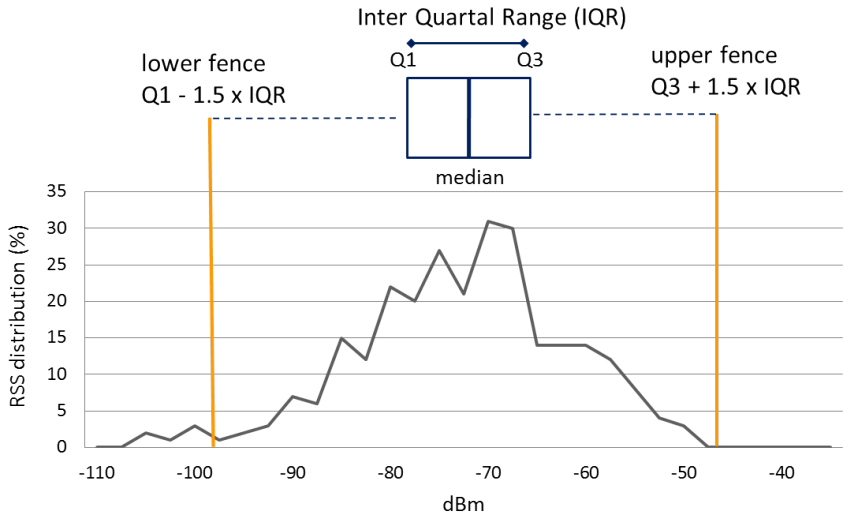

FIGURE 4.6: Outlier Detection based on Interquartile Range (IQR): Upper and Lower Fence of an Inter BS Neighbor Cell

4.2.4 Combined Cell Fingerprint Metric - Basic Sum

Until now the 3 basic single CFP metrics defined in section 4.2.2 were processed separately. A better modeling of the RSS distributions for a cell may be achieved, if the 3 single CFP metrics are combined in one metric. Thus, an additional basic sum metric is proposed, combining the results of the basic single metrics, i.e. minMax, exclOut and Q10. The idea is that the combined metric may compensate for possible limitations of the individual CFP metrics.

To explain the processing of the combined basic sum metric, we anticipate few basics of the matching procedure, which is described in section 4.5.1.

Any RSS included in a current UE sample is determined as a match, if it lies within the range of the corresponding CFP metric for a given neighbor cell. For each matching event a score is incremented, which corresponds to one of the single basic metrics, i.e. minMax, exclOut, and Q10. As a result the following 3 scores determine the grade of the matching for each single CFP metric: sMinMax, sExclOut, and sQ10 ("s": score).

Thus, the basic sum metric consists of the summands of the 3 scores, representing the single metrics minMax, exclOut, and Q10, as presented in Eq. (4.2).

$$basicSum = sMinMax + sExclOut + sQ10 \tag{4.2}$$

In this work this sum metric is referenced as the **basic sum** (variable name: basicSum) as it combines the 3 basic single metrics, or alternatively, in figures as sum(minMax; exclOut; Q10).

As a consequence of the summation, an implicit weighting for any combined metric is achieved. Measures closer to the median are weighted higher than those at the very edge of the RSS distribution. The weighting factor introduced by summing up the 3 single

CFP metrics depends on the given RSS value, whether it meets the conditions of each single CFP metric, as presented in Eq. (4.3a) to Eq. (4.3c).

Selected weighting factors are:

$$weightFactor = 1 : ((RSS \in minMax) \wedge (RSS \notin exclOut) \wedge (RSS \notin \text{Q10})) \quad (4.3a)$$

$$weightFactor = 2 : ((RSS \in exclOut) \wedge (RSS \notin \text{Q10})) \quad (4.3b)$$

$$weightFactor = 3 : (RSS \in \text{Q10}) \quad (4.3c)$$

where the weighting factor

- of **1** applies, if the RSS value is identified as a possible outlier, i.e it is within the minimum/maximum RSS range, but outside the outliers and decile ranges, see Eq. (4.3a).
- of **2** results from RSS values not considered as outlier, but outside the decile range, see Eq. (4.3b).
- of **3** applies for RSS values within the decile range, accepting it at the same time as valid for exclOut and Q10, see Eq. (4.3c).

As an example, figure 4.7 presents the weighting factor for an RSS cell distribution. For example, if an RSS value of -65 dBm is received, it lies within the range of all 3 CFP metrics, i.e. achieving a weighting factor of 3. In contrast, if an RSS of -100 dBm is received, only the minMax metric is true, resulting in a weighting factor of 1.

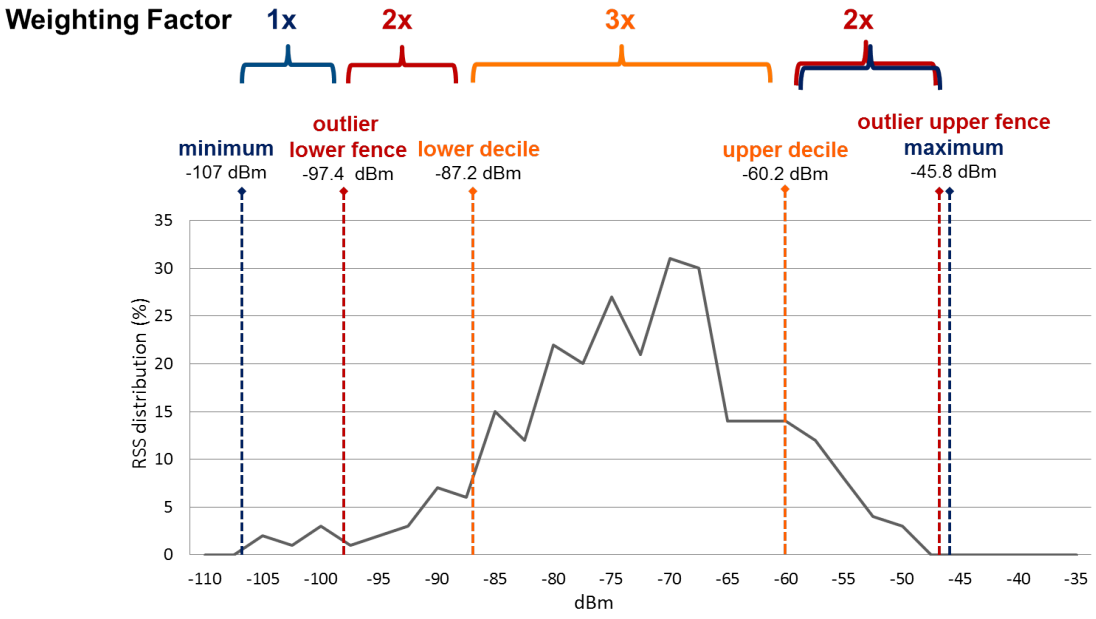

FIGURE 4.7: Weighting Factors for CFP Metrics

The expected advantages of the basic sum metric is first, the extended range of the scores providing a finer gradation of the basic sum score compared to the basic single scores. The expected results are a more exact selection of the best matching cell due to less duplicate high scores. Second, a higher weight for the assumed more reliable UE measures closer to median is achieved.

Further details and the evaluation of the summation effect are provided in section 5.2.

4.3 Cell Fingerprint Generation

Once the CFP metrics are defined, the generation of the cell fingerprints may start with the retrieval of measurement samples from the UE. It should be noted, that UE measurement samples, used for cell fingerprinting, are part of mobility procedures, e.g. handover. Therefore, no new measurement or additional signaling exchange is required.

Each cell has to perform the fingerprint generation by itself. The sequence of the cell fingerprinting generation is presented in the Universal Modeling Language (UML) activity diagram shown in figure 4.8.

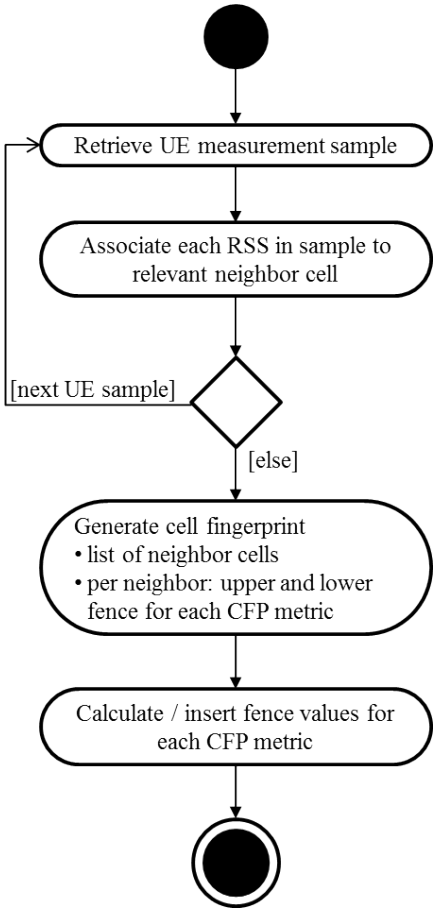

FIGURE 4.8: UML Activity Diagram: Cell Fingerprint Generation

Initially, the UE measurement samples are retrieved by the BS. Each sample consists of a list of neighbor cell IDs with the associated RSS, representing the received pilot signal strengths as measured by the UE. The RSS values are buffered separately for each neighbor cell, until the defined (configurable) number of RSS values is retrieved.

Next, the cell fingerprint is created, structured as shown in figure 4.9. Finally, for each neighbor cell, the upper and lower fence for each CFP metric is calculated and stored in the cell fingerprint.

The structure of a cell fingerprint, presented in figure 4.9, consists of:

1. the list of neighbor cells using the cell IDs as identifier. The cell ID provides the unique identification of the neighbor cell. One data record is generated per neighbor cell .

2. the list of CFP metrics. In figure 4.9 the basic single CFP metrics minMax, exclOut and Q10 as defined in section 4.2.2 are presented. It should be noted, that combined metrics are not stored in the cell fingerprint, as they are processed during the matching procedure.

3. the upper and lower fence for each CFP metric. The RSS of the UE sample is considered as valid for the CFP metric, if it lies in the range between the upper and the lower fence for that metric.

cell fingerprint						
cell pattern →	minMax		exclOut		Q10	
neighbor cell ID ↓	upper fence	lower fence	upper fence	lower fence	upper fence	lower fence
3	...	...	...	...	...	...
...	...	...	...	...	...	...
...	...	...	...	...	...	...
...	...	...	...	...	...	...
...	...	...	...	...	...	...
23	...	...	...	...	...	...

RSS

FIGURE 4.9: Cell Fingerprint Structure

4.4 Cell Fingerprint Processing During Cell Deactivation

After the successful generation of the cell fingerprints, the fingerprinting system is operational, i.e. cells may be deactivated and reactivated in line with the temporary traffic demand. As the generic cell deactivation procedure is already covered in section 2.2.5, this section concentrates on the particularities of the cell fingerprints during the deactivation procedure.

The diagram in figure 4.10 provides a simplified sequence of the cell deactivation procedure. Initially, 2 requirements have to be met by the cell to enter the sleep mode: first, the traffic volume of the cell has dropped below a pre-defined threshold to initiate deactivation, and second, the parameter setting allows the cell to enter the sleep state, as explained in 2.2.5. Before deactivating itself, the cell has to inform all active neighbor cells about the anticipated change to sleep mode. The message to the neighbors includes also the current cell fingerprint of the cell transitioning to sleep mode.

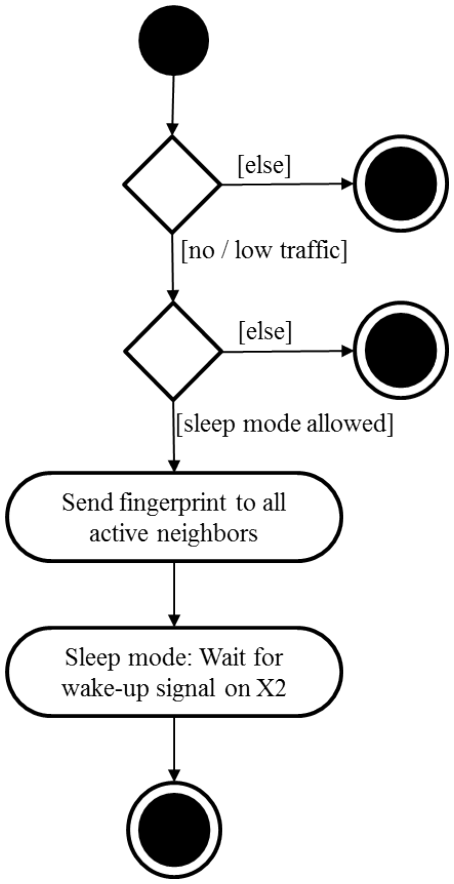

FIGURE 4.10: UML Activity Diagram: Cell Deactivation for Cell Fingerprinting Approach

Upon receipt of this message, the neighbor cells will:

1. store the received cell fingerprints in the list of sleeping neighbors considered for activation

2. exclude the cell from any mobility procedures, e.g. to prevent any future handover to this cell or interrupt any ongoing handovers

The inclusion of the current cell fingerprint guarantees the availability of the most up-to-date cell fingerprint, required for accurate results of the cell identification. Finally, the cell will enter the sleep mode, reducing the activity to the monitoring of the reception of a wake-up signal from any neighbor via the X2-interface.

4.5 Cell Activation Using Cell Fingerprints

Cell activation is performed to reactivate one or multiple sleeping cell(s), identified by the best matching cell fingerprints, to take over the increasing traffic demand. Any macrocell or small cell, that is a neighbor cell to the sleeping cell, may trigger the cell activation procedure. The complete procedure is split into 3 major activities, i.e. retrieval of a sample measurement, fingerprint matching and cell selection.

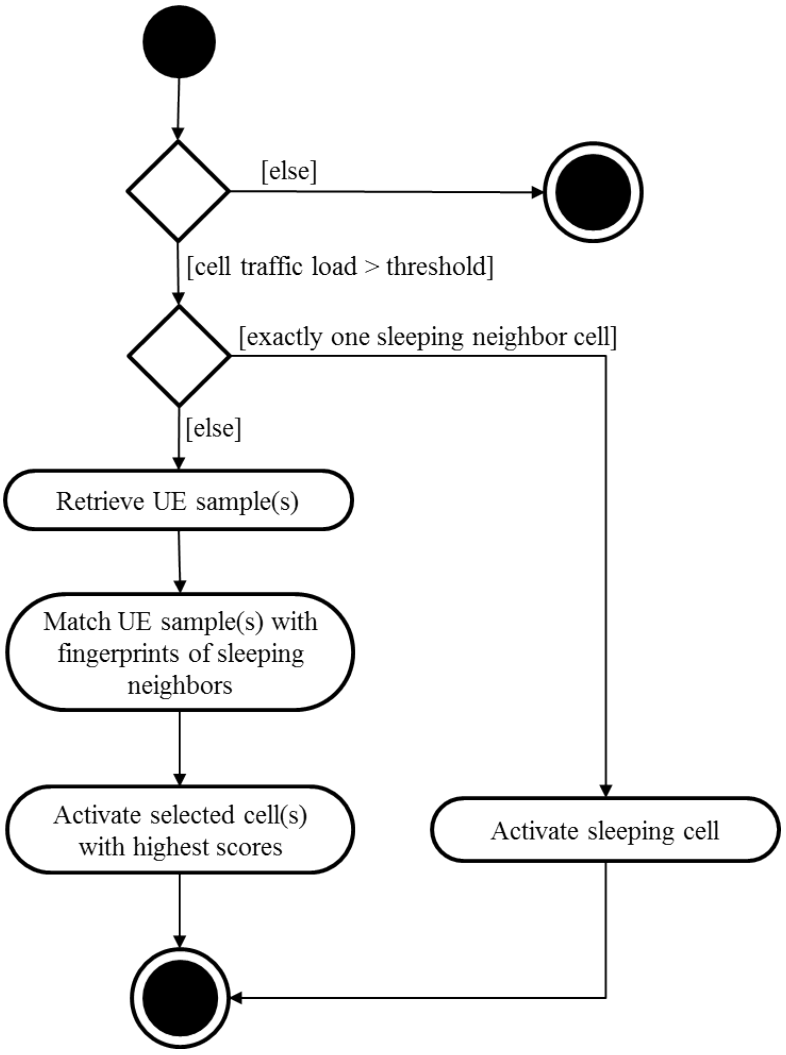

FIGURE 4.11: UML Activity Diagram: Cell Activation Procedure for Cell Fingerprinting Approach

In figure 4.11 we present the major steps for cell activation. It is initiated by a cell experiencing high load, and proceeds as explained below:

1. Two preconditions must be fulfilled to initiate the cell activation procedure. First, the traffic load in a cell must exceed a predefined load threshold indicating the need for additional capacity. Second, there has to be more than one sleeping neighbor cell. In case of only one sleeping neighbor cell, this cell is activated immediately.

2. If both conditions are met, the cell in overload requests one or multiple measurement samples, to initiate the matching procedure. Samples from high-data-rate demanding UEs are preferred, raising the probability of moving that UE to the cell to be activated.

3. For the cell identification, the retrieved sample is then matched with each stored cell fingerprint, where each cell fingerprint represents a sleeping neighbor cell. The RSS of each neighbor included in the UE sample, is matched with each CFP metric of

the corresponding neighbor stored in the cell fingerprint. The matching procedure is explained in more detail in figures 4.12 and 4.14.

4. The sleeping cell(s) with the highest scores are determined as the most appropriate cell(s) and are therefore selected for activation. Consequently, the activation of the selected cell(s) is triggered via the X2 interface by the overloaded cell executing the matching. The number of cells to be concurrently activated is controlled by the policy set by the operator.

4.5.1 Matching Procedure

The matching procedure determines a cell based on the degree of the matching between a currently measured sample of a UE and the cell fingerprints of the sleeping cells.

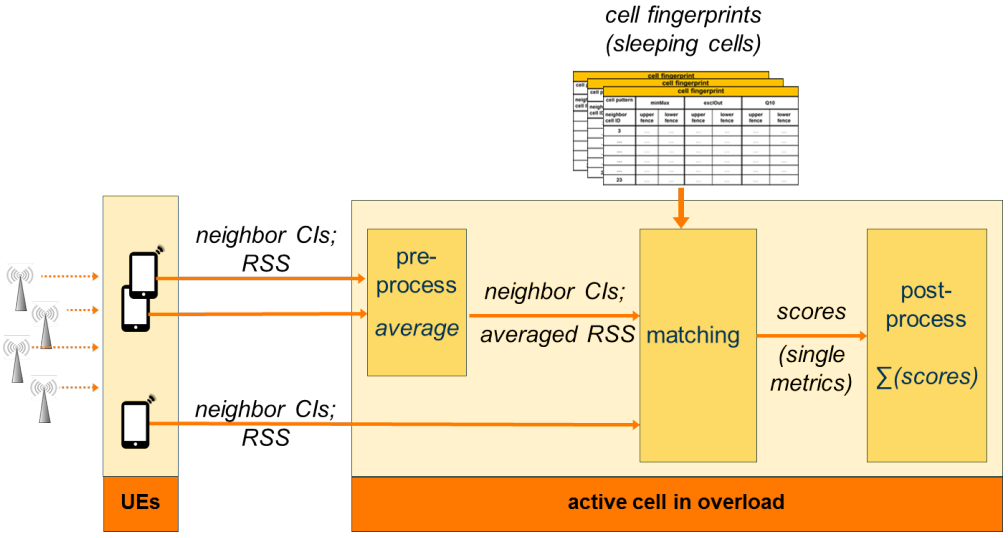

FIGURE 4.12: Data Flow of the Matching Procedure

Figure 4.12 presents the data flow of the cell identification procedure, including pre- and post-processing. Initially, we differentiate between the number of samples sent by the UEs, which include the list of neighbor CI and RSS.

- In case more than 1 UE sample is retrieved as input for the matching, the RSS values of the samples for the same neighbor cell are averaged.
- Otherwise, in the case of only 1 UE sample, no preprocessing is required.

The next step is the matching, where each (averaged) RSS of the UE sample is matched against the CFP metrics of the corresponding neighbor cell for each fingerprint. Separate scores for each basic single CFP metric are implemented as detailed in the algorithm 4.13.

Finally, during post-processing the combined metrics are calculated, i.e. the scores of single CFP metrics are added up to calculate the scores of the combined metrics as detailed in the section 4.2.4.

Depending on the network traffic load, the number of active neighbor cells may vary significantly, impacting on the one hand, the number of cell fingerprints (sleeping cells) and on the other hand the active neighbors contained in the measurements sample. In other words, for very low traffic situation, the number of sleeping cells is high, while the number of RSS values representing the active cells in the UE sample is low. This may put a risk on the matching accuracy as further detailed in section 5.4.

```
IF (traffic load > cell overload threshold)
  retrieve measurement sample from UE in overloaded cell;
  FOR each cell fingerprint                  // representing sleeping neighbor cells
    FOR each cell Id in UE measurement sample
      IF  (cell Id (sample) == cell Id (cell fingerprint)
        IF ((RSS(sample) ≥ lower fence minMax) AND (RSS(sample) ≤ upper fence minMax))
          sMinMax ++;                        // minMax score
        ENDIF
        IF ((RSS(sample) ≥ lower fence exclOut) AND (RSS(sample) ≤ upper fence exclOut))
          sExclOut ++;                       // exclude outlier score
        ENDIF
        IF ((RSS(sample) ≥ lower fence Q10) AND (RSS(sample) ≤ upper fence Q10))
          sQ10 ++;                           // decile  score
        ENDIF
      ENDIF
    ENDFOR
  basicSum = sMinMax + sExclOut + sQ10;
  ENDFOR
ENDIF
```

FIGURE 4.13: Pseudo Code: Matching Algorithm

The detailed matching procedure is represented by the pseudo code of the scoring algorithm in figure 4.13. For each cell fingerprint (sleeping cell) a separate set of scores exits. For the 3 basic single CFP metrics the corresponding score is incremented by "1", whenever the matching conditions are fulfilled. In each case, the cell is considered to match the fingerprint, if 2 conditions are fulfilled:

1. the cell ID of the UE measurement sample matches the cell ID in the fingerprint and

2. the RSS of the UE measurement sample falls within the fingerprint RSS range defined by upper and lower fence of the CFP metric.

As the UE measurement samples do not contain values for sleeping cells, the corresponding cells included in the cell fingerprints are ignored.

The following scores associated to each CFP metric are presented in figure 4.13:

- sMinMax is incremented, if the received RSS lies within the minimum to maximum RSS (minMax) range for the given neighbor cell.

- sExclOut and sQ10 are incremented respectively, if the RSS lies within the range of the corresponding CFP metric.

- basicSum: the sum of the scores of the 3 basic single CFP metrics: sMinMax, sExclOut and sQ10, representing the basic combined sum metric.

For each CFP metric the cell(s) with the highest number of scores are determined as the best fitting cell(s) to be activated. Parameters control the number of cells to be activated at the same time.

4.5.2 Cell Identification Based on Cell Fingerprints - Example

As a summary, figure 4.14 and figure 4.14 present an example of the complete cell identification procedure. The gray cells represent the active cells, while the white cells indicate sleeping cells. Due to the presence of a high data rate user at the edge, cell "12" experiences high load, while the cells "3" to "5", "13" and "14" are sleeping. Thus, cell "12" triggers cell activation, requesting the high data rate user to send a measurement sample including the retrieved signal strength of all active neighbors (all 15 active neighbors in gray of the serving cell 12). The UE sample is matched against each of the 5 cell fingerprints representing the sleeping cells.

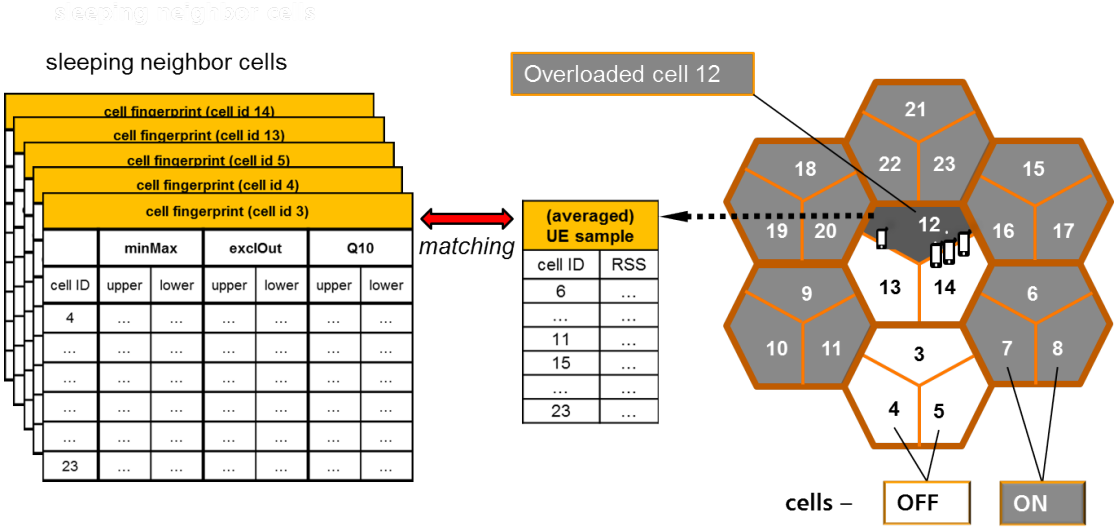

FIGURE 4.14: Example: Cell Identification Using CFP - Measurement Retrieval

Next, figure 4.15 presents the matching procedure as performed by the overloaded cell "12": each of the 3 single basic CFP metrics is scored separately for each CFP, in case the sample RSS matches with the CFP RSS range. A maximum score of 15 may be reached for a basic single CFP metric, if the RSS of all 15 active neighbors matches the individual CFP metric range. Consequently, the basic sum metric, which is the combination of the 3 single metrics, may reach the total high score of 45.

In case only one cell should be activated, cell "12" selects the sleeping cell reaching the highest score. In figure 4.15, cell "13" is assumed to reach the high score and is activated as the most appropriate cell to unload cell "12".

In summary, we have described cell fingerprinting, which is implemented as a distributed approach, requiring a limited amount of extra data and a limited number of involved

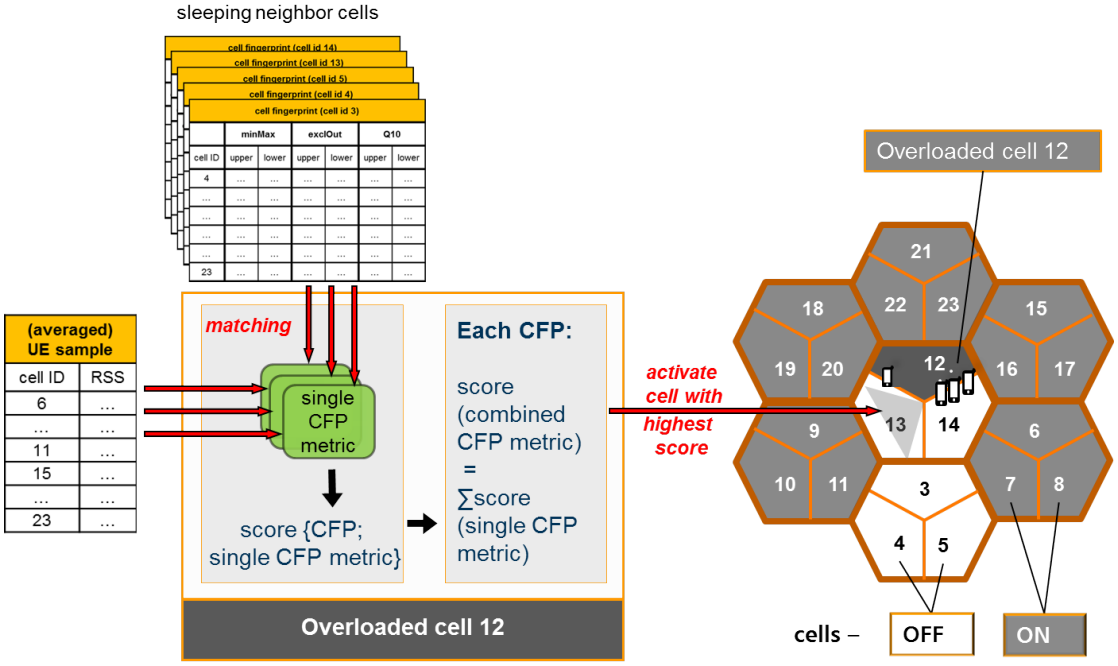

FIGURE 4.15: Example: Cell Identification Using CFP - Processing

cells. Thus, we assume that the required signaling exchange and additional processing cost are kept at a very low level. Applying self-organized procedures and the re-use of existing interfaces and hardware, we expect cell fingerprint as a low cost approach.

CHAPTER 5

Simulation Studies

nc

Contents

5.1 Performance Indicators to Determine the Cell Fingerprint Accuracy 63
5.1.1 Activation Set Size 63
5.1.2 Energy Efficiency Index 64
5.1.3 Accuracy Index 65
5.2 Cell Fingerprinting Accuracy Using Basic CFP Metrics . . 66
5.3 Averaged UE RSS Measurement Samples 70
5.4 Reduction of Active Neighbor Cells 73
5.4.1 Mapping Traffic Demand to Number of Active Cells 73
5.4.2 Impact of Reduced Number of Active Neighbor Cells on Accuracy 74
5.5 Advanced Cell Fingerprint Metrics 77
5.5.1 Difference to Median 77
5.5.2 Additional Single Quantile CFP Metrics 79
5.5.3 Advanced Set of Combined CFP Metrics 81
5.5.4 Traffic Variation Impact on Advanced Single CFP Metrics . . . 83
5.5.5 Traffic Variation Impact on Combined CFP Metrics 85
5.6 Summary 86

In this chapter we evaluate the accuracy of the cell fingerprinting approach in respect to cell identification. The goal is to determine the most appropriate parameter settings and CFP metrics to achieve the highest accuracy. In the first section, performance indicators that characterize the cell identification accuracy are defined. In the remaining 4 sections, cell fingerprinting is evaluated. Section 5.2 starts with the basic metrics, followed by a comparison of single vs. averaged UE sample as input for the matching procedure in section 5.3. Next, section 5.4 evaluates the impact of low numbers of active neighbor cells on the accuracy and the subsequent final studies in section 5.5 introducing an additional set of single and combined CFP metrics.

For all simulations studies presented in this chapter, the following conditions apply:

1. the number of simulation runs and corresponding number of measurements used for the generation of the cell fingerprints are as defined in section 3.5, which also describes the possible configuration settings.

2. the target cell is known from the outset to be the most suitable cell, as described in the terminology in section 1.4.

5.1 Performance Indicators to Determine the Cell Fingerprint Accuracy

In this section we define the performance indicators that are used to analyze and interpret the achieved results of the subsequent simulation studies. The performance indicators are used to assess how good the different settings are able to identify the target cell, i.e. the most suitable sleeping cell to take over the traffic from the overloaded cell.

5.1.1 Activation Set Size

The ASS provides an accuracy indication of the best matching cells for a given set of CFP metric and parameter settings.

Definition: The Activation Set Size is defined as the minimum number of cells that must be activated, if the target cell is to be activated. In other words, it is the smallest number of the best matching cells that includes the target cell, regardless whether the target cell achieved the highest score or not.

The Activation Set Size (ASS) result corresponds to the number of cells with a score greater than or equal to the score of the target cell, as presented in figure 5.1.

Example: A simple example of a scoring table in figure 5.2 is presented, to demonstrate how to interpret the results. The very small network consists of the 4 cells with the cell IDs ”3” to ”6”, in which cell ID ”5” is the target cell. For the case A, the target cell reaches the high score and so do 2 other cells. As a result, 3 cells need to be activated

```
FOR any CFP metric
  FOR each cell ID
    IF (score(cell ID) >= score (target cell ID))
      ASS = ASS + 1;          // Activation Set Size
    ENDIF
  ENDFOR
ENDFOR
```

FIGURE 5.1: Calculation of the Activation Set Size (ASS)

to ensure the activation of the target cell. Similarly, ASS=3 is true for case C. The target cell is 1 of the 3 best cells, although it does not reach the highest score. Case B represents the optimum ASS of 1; solely the target cell is identified as the best matching cell.

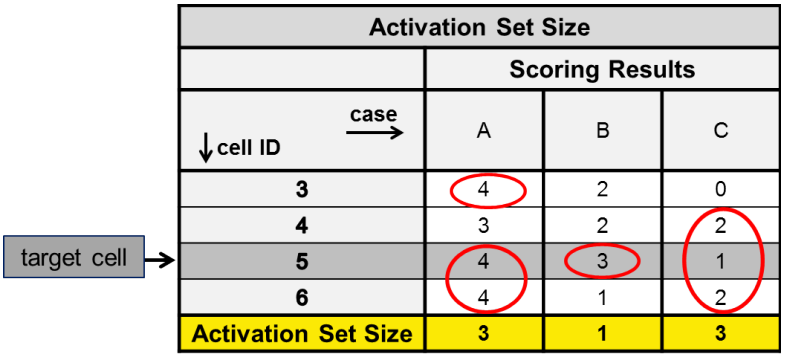

FIGURE 5.2: Example: Use of the Activation Set Size (ASS)

5.1.2 Energy Efficiency Index

The Energy Efficiency Index (EEI) indicates to which extent the target cell is one of the cells to be activated, in case only a limited number of cells will to activated. It is the probability (in %) that the target cell is activated for a given Number of Cells to be Activated (NoCA). Increasing the NoCA, increases also the probability of activating the target cell, but impacts the energy consumption. The cells to be activated strictly follow the achieved scores, i.e. cells with highest scores are activated first. For example, allowing 3 cells to be activated at once, increases the probability of activating the target cell, whilst impacting the energy consumption as 2 of the 3 cells may not be required at that time.

In Eq. (5.1), EEI is the probability P, that the target cell is included in the set of cells to be activated (SetCA), given that NoCA neighbor cells are activated. If True Positive (TP) = 1.0, NoCA corresponds to the ASS.

$$EEI = P((target\ cell \in SetCA) \mid NoCA) \tag{5.1}$$

where:

– P is the probability

– SetCA is the set of cells to be activated

– NoCA is the number of cells to be activated

Example: The example in figure 5.3 presents the EEI for the results/scores in table 5.2. It shows the probability in percent to activate the target cell for NoCA= 1 to 3. For case A, the NoCA of 3 includes the target cell. If 1 of the 3 cells is activated (Nc=1), the probability to activate the target cell is 33%, in case of Nc=2 it is 66% and in case of Nc>=3 it is 100%. For case B, when only the target cell achieves the highest score, the probability to activate the target cell is obviously always 100%. Different to A and B, the target cell in case C does not give the highest score. Since the 2 cells with highest score are activated first, the probability to activate the target cell for Nc=1 or Nc=2 is 0%.

Energy Efficiency Index			
Nc: No. of cells to be activated → / ↓ case	1	2	3
A	33%	66%	100%
B	100%	100%	100%
C	0%	0%	100%

FIGURE 5.3: Example: Use of the Energy Efficiency Index (EEI)

5.1.3 Accuracy Index

The Accuracy Index (AI) indicates how often the target cell is among the cells reaching the highest score. Its intention is to supports operators to better differentiate between the energy saving potential and the risk impacting the user's QoE. In case operators are most concerned about their customers experience and reputation in quality, the simultaneous activation of all cells reaching the highest score without restriction to the number is expected to be most beneficial; whilst operators focusing on OPEX minimization may prefer the restriction to activate just 1 cell at a time.

The AI is the probability that the target cell is activated, given only the highest scoring cells are activated, regardless of the number of those cells. In Eq. (5.2), the AI is the probability (in %) that the target cell achieves the score of the best matching cell, i.e. the highest score during the matching procedure.

$$AI = P(score(target\ cell) == score(best\ matching\ cell)) \tag{5.2}$$

Example: Reusing figure 5.2, we present in figure 5.4 the AI. As long as the target cell achieves the highest score (case A and B), the target cell is activated, if all cells,

achieving the highest scores, are activated. Case C illustrates the case the target cell does not achieve the highest score, which results in no activation of the target cell.

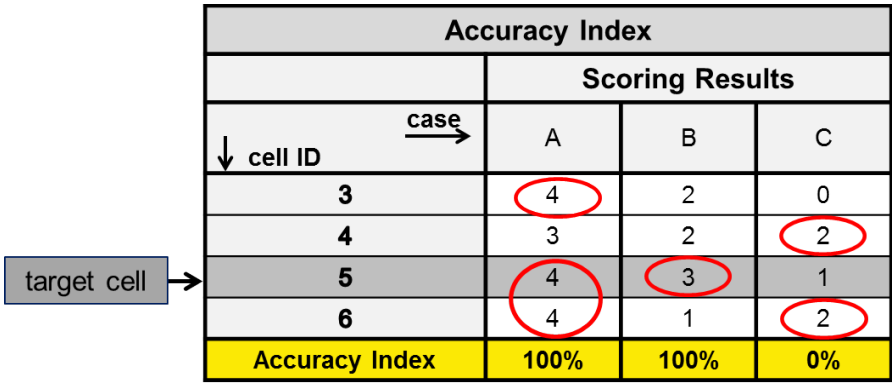

FIGURE 5.4: Example: Use of the Accuracy Index (AI)

The results restricted to 0% and 100% in figure 5.4 are caused by the restriction to 1 matching event. Typically the AI is calculated for a complete simulation run, i.e. matching the UE sample with all neighbor cells included in any CFP representing a sleeping cell.

5.2 Cell Fingerprinting Accuracy Using Basic CFP Metrics

In this section, we start with the evaluation of the cell fingerprinting approach using simulation studies. First, we presents the fingerprint results of the single and combined basic CFP metrics defined in sections 4.2.2 and 4.2.4, followed by a comprehensive assessment of the results.

The simulation studies for the basic CFP metrics in this section are based on the initial simulation setting, assuming 20 active neighbor cells and 1 single UE RSS sample as input for the matching procedure. More details regarding the simulation setup and number of measurements are presented in section 3.5. This initial scenario, assuming all cells to be active, is performed to assess the basic method of cell identification using the proposed CFP fingerprints, i.e. to which extent it delivers the expected accuracy, but also to estimate the extent to which the performance of the 4 proposed CFP metrics diverge.

Activation Set Size

As the matching is restricted to 1 single UE, we expect to identify the sleeping cell(s) to which the selected UE would be connected at the time the UE measurement sample was sent, if all cells had been active.
The corresponding performance measured in terms of ASS is presented in figure 5.5.

We observed that from the results of the 3 single CFP metrics, minMax, exclOut, and Q10, as well as the combined sum of the 3 CFP metrics, the sum achieves the best result. With an average of 1.4 cells, the sum CFP metric ensures the activation of the

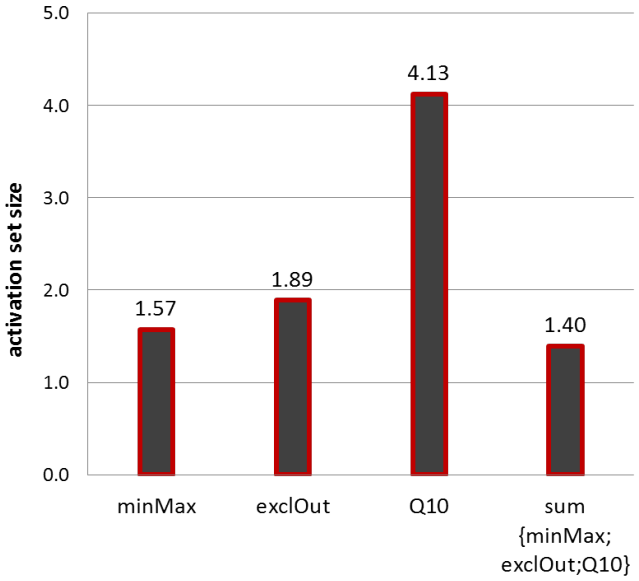

FIGURE 5.5: Activation Set Size for Basic CFP Metrics (Single UE Sample, 20 Active Neighbors)

target cell. The minMax CFP metric reaches with an ASS around 1.6 cells almost the same good results as the sum CFP metric. Excluding the outliers (exclOut) leads to an increase of the ASS by approximately 0.3 cells compared to minMax. Finally, by far the worst accuracy results are achieved by the 10th quantile Q10 CFP metric.

Thus, the best results of the **basic sum** CFP metric with an ASS of 1.4 cells are contrasted by Q10 that required more than 4 cells in order to ensure inclusion of the target cell. One reason for the good results of the basic sum metric is the extended range of the scores. With 20 active neighbors, any single CFP metric may by scored up to 20 times, while the maximum score for a sum with 3 summands triples. The resulting finer gradation in turn, allows to differentiate more precisely between the high score neighbor cells.

Energy Efficiency Index

For a more detailed evaluation, figure 5.6 presents the EEI performance indicator for the basic CFP metrics. Two cells must be activated using minMax or the basic sum CFP metric, while more than 10 cells must be activated using the Q10 CFP metric, to ensure with a probability of 90% the activating of the target cell. On the contrary, it shows that the activation of at least 2 cell (NoCA), minMax performs better or at least equal to the sum CFP metric as indicated by the red circles. However, for exclusive detection of the target cell, the **basic sum** CFP metric achieves with 76%, the best result for single target cell identification. Accepting the activation of 2 cells improved the successful inclusion of the target cell significantly to 92%.

Accuracy Index

The third performance indicator Accuracy Index (AI) presented in figure 5.7 indicates for each of the CFP metrics the proportion of target cell reaching the highest score (light

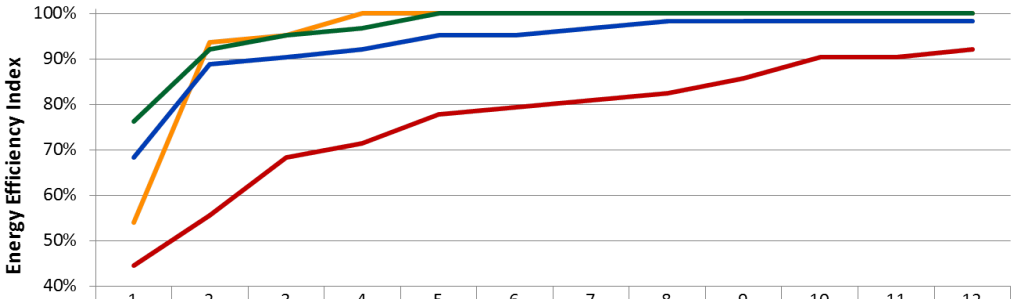

	1	2	3	4	5	6	7	8	9	10	11	12
minMax	54%	94%	95%	100%	100%	100%	100%	100%	100%	100%	100%	100%
exclOut	68%	89%	90%	92%	95%	95%	97%	98%	98%	98%	98%	98%
Q10	44%	56%	68%	71%	78%	79%	81%	83%	86%	90%	90%	92%
sum {minMax; exclOut;Q10}	76%	92%	95%	97%	100%	100%	100%	100%	100%	100%	100%	100%

NoCA (number of cell to be activated)

FIGURE 5.6: Energy Efficiency Index for Basic CFP Metrics: Relation of Target Cell to Number of Cells to be Activated

gray bars). For comparison reason, we add the figure with exclusive identification of the target cell based on the highest scores in dark gray.

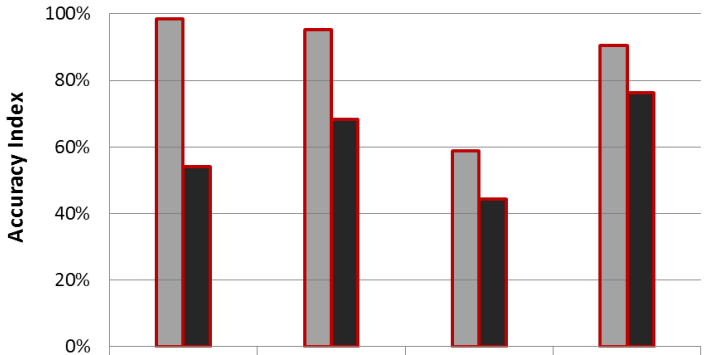

	minMax	exclOut	Q10	sum {minMax; exclOut;Q10}
Accuracy Index: target cell included	98%	95%	59%	90%
Accuracy Index: target cell exclusive	54%	68%	44%	76%

FIGURE 5.7: Accuracy Index for Basic CFP Metrics: Target Cell Included in Set vs. Target Cell Exclusive

Interestingly, the difference between the 2 performance indicators in figure 5.7 varies strongly. While minMax reaches the best 98% to identify the target cell in a set of cells, only rather poor 54% percent identify the single best cell. For the rather stable sum CFP metric, the difference between single and one out of many target cell detection is only 14%. In line with the performance indicators ASS and EEI, (exclOut) provides results nearly as good as minMax.Q10, however, consistently provides the worst results.

Comprehensive Assessment of Basic CFP Metrics

The reason why the basic sum outperformed the single CFP metric was not only the extended range of the scores, but also the implicit weighting factor for combined CFP metrics, see section 4.2.3. Since the sum adds up the scores of the 3 single CFP metrics, possible limitations of the individual CFP metrics are compensated. That way, values within the decile range are scored 3 times, i.e., for the minMax, the exclOut and the Q10 CFP metric resulting in a weighting factor of 3 for the more reliable values closer to the median.

Out of the 3 single CFP metrics, the **minMax** CFP metric achieved with an ASS of 1.6 the best results (figure 5.5). Also, minMax had a very wide RSS range, which may exceed 70 dB as presented in table 5.1. Obviously, considering all RSS values without any restriction as valid, was beneficial for achieving the good results. Consequently, using minMax the target cell will almost always (98%) achieved the highest score, as presented in figure 5.7. Only in case the ASS was restricted to 1, minMax achieved poor results: only in 54% of the cases the target cell was identified (see figure 5.6). The reason is the very wide range, which assume many cells as valid, which results in rarely reaching the high score just for the one target cell.

TABLE 5.1: Example Ranges from Simulation Studies for Basic CFP Metrics

Example RSS Ranges for Basic CFP Metrics		
	Upper Fence (dB)	**Lower Fence (dB)**
minMax	-35.2	-105.4
exclOut	-55.7	-103.1
Q10	-66.8	-88.9

On the other hand, the wide RSS range provides equal weight even for values at the very edge of the RSS range, resulting in a major difference between minimum and maximum RSS values. This may result in false positives, where non neighbor cells are assessed as valid neighbors, especially in case of few active neighbor cells. Therefore, for the interpretation of the results, the context and parameter setting has to be noted. With 20 active neighbors, and thus a maximum score of 20, single CFP metrics still have a good chance to distinguish between different scoring levels. With less active neighbors and thus, correspondingly shrinking range of the scores, a major impact on the accuracy is expected.

A behavior similar to minMax was observed for the **exclOut** CFP metric, improving the isolation of the target cell from 54% for minMax to 68%, but with slightly worse general results, see figure 5.7. However, only the single cell activation benefit from the removal of outlier, while multiple cell activation achieved continuously worse results than minMax. The reduced RSS span of the exclOut metric (see table 5.1) increased the ASS compared to minMax a by 0.3 cells. The more restricted range based on the removal of outliers did not hold, what was expected in chapter 4.2.2. At least for the used configuration

with a single UE measure and many active neighbors, ignoring RSS values assumed as outliers, negatively impacted the accuracy result.

Finally, by far the worst accuracy results were achieved for the 10th quantile **Q10** metric. Owing the strongly restricted range of 22.3 dB in table 5.1, Q10 was only scored for RSS value within the limited RSS range towards the median. Ignoring far too many valid RSS values impacted the ASS substantially, resulting in an average of 4.1 cells, i.e. almost 3 times more cells would need to be activated compared to the basic sum CFP metric to guarantee the activation of the best cell. Even the restriction to 1 cell activation achieved with only 44% target cell activation the worst results in figure 5.6. Obviously, the exclusion of the upper and lower decile at the edges of the RSS range eliminated by far too many valid RSS values. Consequently, the exclusive use of Q10 is not acceptable as much more cells would be activated than needed resulting in a negative impact on the energy consumption. However, used as summand within the basic sum CFP metric, Q10 may contribute to the constantly best results of the sum due to the higher weight to the more reliable RSS values closer to the median.

Overall, it became evident that the sum of the 3 single CFP metrics achieved the most promising results to reduce the energy consumption.

5.3 Averaged UE RSS Measurement Samples

In the previous section 5.2 a single UE measurement sample is used as input for the matching with the neighbor cell fingerprints. Owing the quickly changing radio conditions, caused by impairments such as shadowing, multi-path propagation and interference, a single sample per cell may not always provide reliable measurements. An average of more than 1 UE measurement samples is therefore expected to stabilize the RSS measures.

Furthermore, we expect an impact on the fingerprinting result not only regarding the sample number, but also the position of the UE providing the signal strength of the neighbor cells. If a single sample is taken from a UE at the very cell edge, the closely adjacent neighbor cells are expected to match better than the neighbor cells significantly further away. Therefore, the position of the UE within the cell area is expected to impact significantly the fingerprinting results, if a single UE sample is used. Using averaged RSS from different UEs in a cell, this effect is partly compensated as long as the UEs are located further apart. Thus, averaged results have a higher probability to identify the best fitting neighbor cell for more UEs of the overloaded cell, while single UE results will favor neighbor cells closer to the current UE position.

Thus, we use in this study the average of the latest 2 measurement samples received from 2 different UEs as indicated in figure 5.8.

The simulation studies are based on the initial standard configuration with 20 active neighbor cells using the basic set of CFP metrics as defined in section 4.2.1. Input for the matching is the average of the 2 last measurement samples received from different

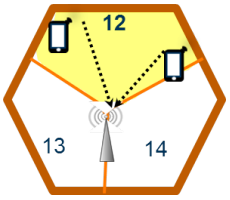

FIGURE 5.8: Average of the Last 2 Received UE Measurement Samples

UEs served by cell in overload. Figure 5.9 shows the resulting bar charts for the 4 basic CFP metrics separately for single and averaged UE samples. The single UEs sample results in dark gray correspond to the results in figure 5.5.

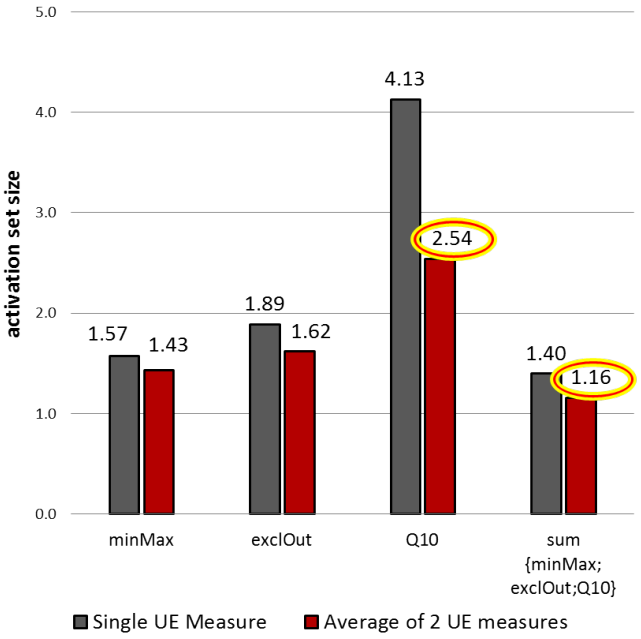

FIGURE 5.9: Activation Set Size: Single vs. Averaged UE Samples

The major finding in figure 5.9 is that the accuracy improves for all 4 basic CFP metrics. With approximately 40%, the Q10 metric improves the most. However, with an averaged ASS of 2.5, it delivers still the least accuracy. Also the CFP metric minMax and exclOut improve, whereas minMax with the widest RSS range benefits least from the averaged sample. The accuracy of the sum of the 3 single CFP metrics, however, improved remarkably. With an averaged ASS of 1.16, it is getting close to the very optimum of 1.0, if exclusively the target cell is activated. Thus, the basic sum continues to provide the most accurate result compared to the single CFP metrics.

Additional details can be observed from figure 5.10, providing the Energy Efficiency Index for the simultaneous activation of 1 to 6 cells. For better readability, it is restricted to the 3 CFP metrics delivering more interesting results. Again, any of the averaged UE samples exceeds its single pedant. While the basic sum is significantly better for 1 cell activation (89% versa 76%), the improvement is mino, if 2 cells are activated simultaneously. Then, if 3 cells are activated, both minMax and the sum can guarantee the

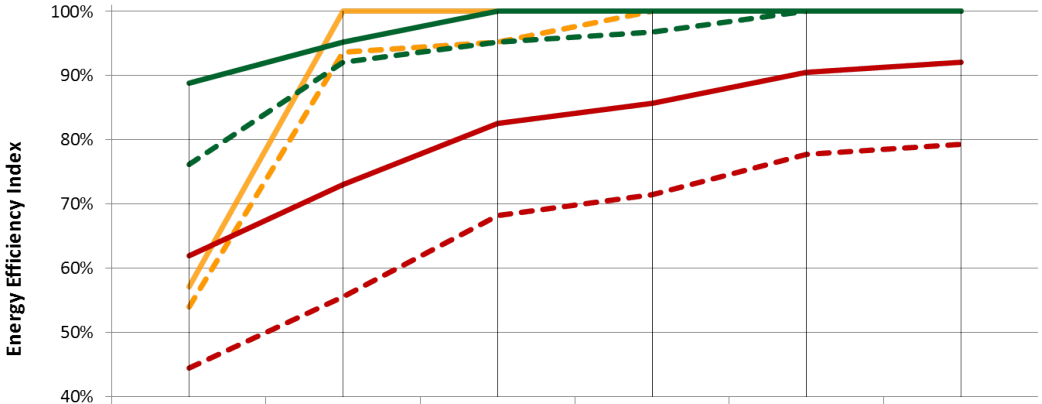

	1	2	3	4	5	6
SI minMax	54%	94%	95%	100%	100%	100%
AV minMax	57%	100%	100%	100%	100%	100%
SI Q10	44%	56%	68%	71%	78%	79%
AV Q10	62%	73%	83%	86%	90%	92%
SI sum{minMax; exclOut;Q10}	76%	92%	95%	97%	100%	100%
AV sum{minMax; exclOut;Q10}	89%	95%	100%	100%	100%	100%

NcCA (number of cells to be activated)

FIGURE 5.10: Energy Efficiency Index: Single vs. Averaged UE Samples

inclusion of the target cell - using an averaged UE sample. For the CFP metric excluding the upper and lower decile (Q10) the major improvement from singe to averaged UE sample of approximately 15% is almost independent from the number of cells being activated.

Analyzing these results, it can be deduced for all CFP metrics, but mostly from the strong improvement of Q10, that the averaged RSS measures were closer to median. Obviously, single UE RSS measures at the cell edge may not fit within the restricted decile range. As the averaged UE measure partly extinguish the characteristics of the single UE measure, even more cells seemed to fit into the wide range of the minMax and exclOut CFP metric. Especially, the basic sum profited from the improvement of all its summands, reaching a close to the optimum result. As a consequence of this study, any subsequent simulation studies are based on averaged UE samples.

It should be noted, that this study is just an initial step for enhancing the UE measurement sample. However, involving more samples means also more delay and additional processing. Especially, the delay should be seen as critical factor during overload situations, since it causes even more delay until the sleeping cell is up and running.

5.4 Reduction of Active Neighbor Cells

In this chapter, we study the impact of reduced number of active cells, expected during off-peak hours, on the accuracy of cell fingerprinting. Instead of the fixed number of 20 active neighbor cells, used in the preceding studies, we introduce first a mapping of the traffic to the number of active neighbors. The subsequent evaluation for reduced active neighbor cells is performed on the previously introduced set of CFP metrics.

5.4.1 Mapping Traffic Demand to Number of Active Cells

Peak hour requires all cells to be activated. For the network model of this work, this results in the activation of 21 cells, which were applied so far, to validate the generic method of cell fingerprinting, i.e. assuming 20 neighbor cells for the matching. To prove that cell fingerprinting is reliably delivering accurate results under all conditions, the number of active cells needs to be reduced, following the current traffic demand. For cell fingerprinting, the reduction of active cells impacts the matching procedure. The number of active neighbors corresponds to the number of matching events per fingerprint and to the same extent to the maximum attainable value of the score. Low numbers of active neighbor cells limit therefore the gradation to identify the best cell based on the highest score. For example, considering a business area during off peak-hours, as illustrated in figure 5.11, most neighbor cell will be sleeping. Assuming 4 active neighbors, the maximum score will be 4, restricting the gradation to the 5 values from 0 to 4.

Figure 5.11 presents the daily traffic profile of an operational network in Italy for one cell in a business and another cell in a consumer area, each for a week-day and a week-end traffic scenario. The measured traffic is based on averaged and normalized measurements received on a 15-minute basis. The traffic conditions, subdivided in 5 sectors, are indicated in color.

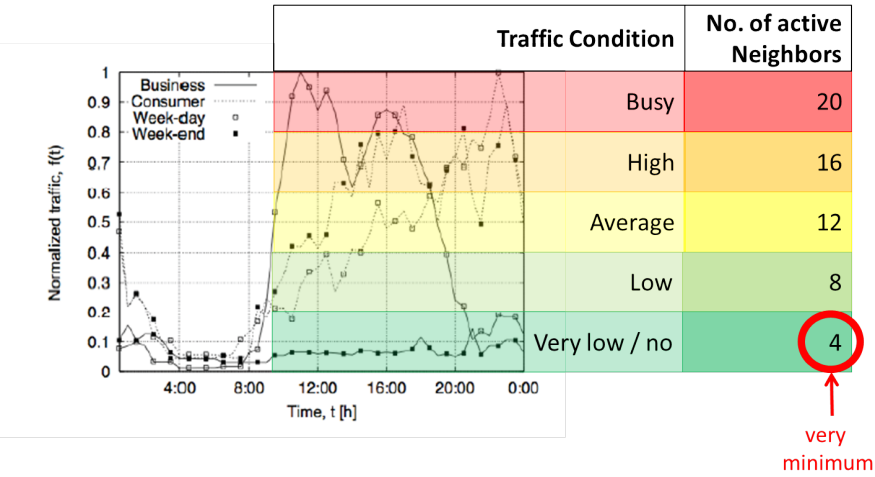

FIGURE 5.11: Mapping of Network Traffic to Number of Active Cells, see [30]

More important, figure 5.11 presents the mapping of the traffic condition to the number of active neighbor cells. The maximum of 20 neighbor cells correspond then to the

network setup of the LTE system simulator of 21 cells as described in chapter 3.5.2. Even with very low or no traffic, 4 active neighbor cells are assumed as the very minimum for a functional network, e.g. to ensure the mobility in the network and to guarantee the user expected QoE. With a step size of 4 cells the traffic condition is mapped to the number of active neighbor cells.

5.4.2 Impact of Reduced Number of Active Neighbor Cells on Accuracy

In line with the preceding simulation studies, this study reuses the basic set of CFP metrics and the average of the last 2 UE samples received from different UEs served by the overloaded cell as input for the matching. New to this study is the changing number of active neighbor cells. Based on the mapping of traffic conditions to the number of cells presented in figure 5.11, we use a step size of 4 cells. Then, the studies are performed for 4, 8, 12, 16, and 20 neighbor cells, whereby 20 neighbor cells correspond to the initial configuration used in previous sections.

The simulation results for reduced number of active cells are presented in the figures 5.12 and 5.13. Both figures provide the cell identification accuracy as ASS for the 4 basic CFP metrics highlighting:

- the impact of the reduced number of active neighbors on each single metric in figure 5.12
- the overall effect of the reduced active neighbor cells on all CFP metrics in figure 5.13

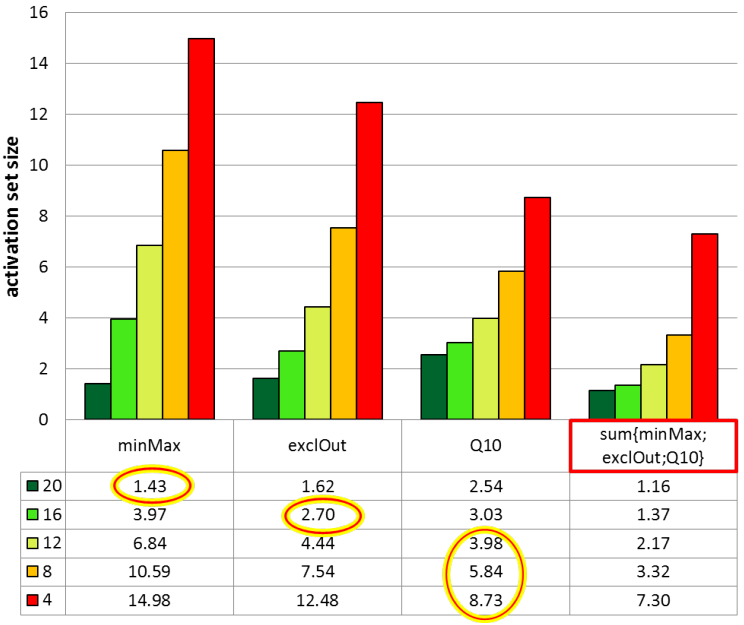

	minMax	exclOut	Q10	sum{minMax; exclOut;Q10}
20	1.43	1.62	2.54	1.16
16	3.97	2.70	3.03	1.37
12	6.84	4.44	3.98	2.17
8	10.59	7.54	5.84	3.32
4	14.98	12.48	8.73	7.30

FIGURE 5.12: Basic CFP Metrics: Accuracy for Defined Number of Active Neighbors

The major observations in both figures are the steady increase of the averaged ASS for each CFP metric with decreasing number of active cells, i.e. the accuracy of cell identification and thus, the potential energy saving decreases.

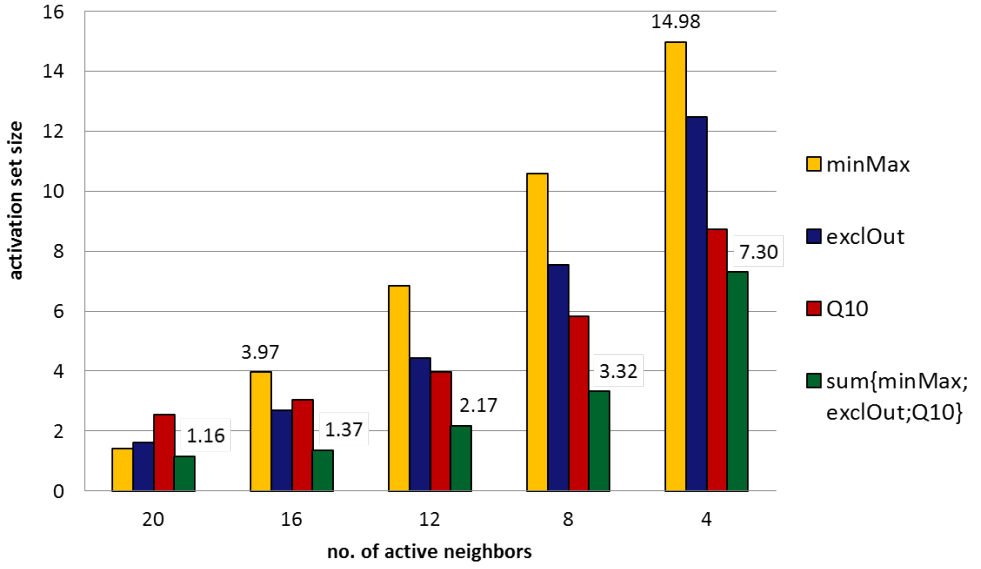

FIGURE 5.13: Reduced Number of Active Neighbors: Accuracy Impact on Basic CFP Metrics

One possible reason is, that the reduced number of matching events, which corresponds to the number of active neighbor cells. Less matching events result in a reduced gradation of the scores, i.e. an increasing number of sleeping cells may reach the high score.
A second reason, we assume for the accuracy degradation is the dependency on the number of neighbors to precisely map the sleeping cell: each neighbor cell distribution contributes to more precisely map the sleeping cell.

Going into more details of figures 5.12, the declining number of active cells impacts each CFP metric in a different degree. Furthermore, the fewer active neighbors are available, the stronger is the negative impact on the accuracy.
For the **sum** CFP metric the accuracy decrease is minor, compared to the single CFP metrics, until the number of active neighbors reaches 8. Then, reducing the active neighbors from 8 to 4, a major impact on the accuracy is observed, more than doubling the ASS to 7.3 cells.
Also **Q10** is affected, however to a much lesser extent than minMax and exclOut. Already with the still rather high number of 16 active neighbors, Q10 outperforms minMax. With 12 neighbors, also **exclOut** is outperformed by Q10 marked with a circle in figure 5.12. Finally, **minMax** is most significantly impacted by the reduction of active neighbors, receiving continuously the worst results of all CFP metrics for 16 to 4 active neighbors.

So far the **basic sum metric** consistently outperformed all other CFP metrics by a significant degree. Therefore, figures 5.14 presents with the Energy Efficiency Index a more detailed view of the sum metric to determine the impact of a specific NoCA on networks with increasing numbers of sleeping cells.

Interestingly, with 8 or more active neighbors, the sum CFP metric included with at least 73% the target cell, if 3 cells would have been activated simultaneously. However, with

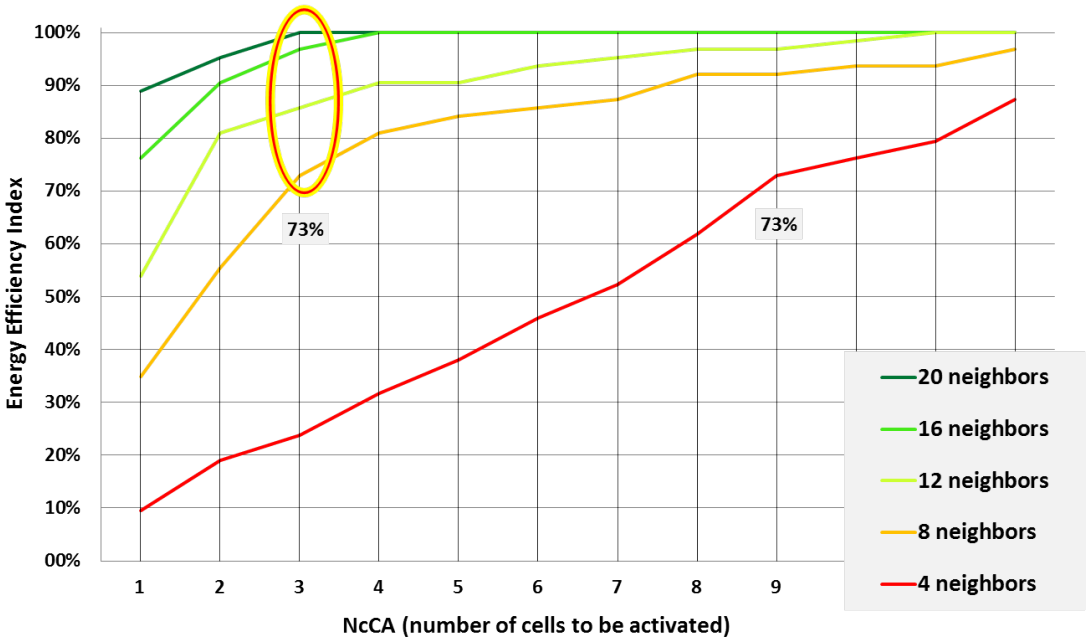

FIGURE 5.14: Energy Efficiency Index: Basic Sum CFP Metric: Successful Target Cell Identifications per Number of Cell to be Activated

the reduction to 4 active neighbors, we observe a major cutback of accuracy, displayed as the red line in figure 5.14.

Interpreting the results, we summarize the major findings below:

- The **minMax metric** was most significantly affected by the reduction of active neighbor cells, mainly due to its wide RSS range (see table 5.1). With each reduction of neighbor cells, corresponding to the number of matching events, respectively scoring gradation, the negative impact was becoming more and more evident. In case of 4 neighbors, the maximum score of any single CFP metric was also restricted to 4.
  For example, if only 4 neighbors are active, most RSS values of the neighbor cells lie within the huge RSS span of minMax, and are therefore scored. Due to the restriction to only 4 matching events, there is a high probability to score minMax 4 times, resulting in many sleeping neighbor cells reaching the highest score of 4. A differentiation between the cells is no longer possible.

- Opposite to minMax, the strong limitation of **Q10** to RSS values closer to the median, was much more resistant against the reduced neighbor cell impact. The strong limitation of Q10 to RSS values closer to the median, resulted in a better selection criteria, i.e. less cells match, but often the target cell was included.

- In line with these observation, **exclOut** benefited from the range limitation caused by the exclusion of outliers, but by a much less degree than Q10. Again, the probability to select too many cells due to the too low number of matching events increased with the decreasing number of neighbors.

- The basic sum metric, however, provided again the most stable and accurate results. However, even the basic sum metric experienced degradation steps, a first minor one for 12 and a second major one for 4 neighbors. Thus, the extended range of the score and thus, finer gradation, stabilizes the results, pointing into the direction to further increased the range i.e. the number of summands to compensate the low number of matching events.

Finally, it should be noted, that the handling of 4 neighbor cells is expected during very low traffic situation. Experiencing overload in one of the few active cells, is often an indication, that the overall traffic situation in the area is going to change, i.e. the start of the business hours in an industrial area. Therefore the activation of multiple cells could be an acceptable approach. Also the activation of any single cell is expected to result in some relieve, as load balancing assists to distribute the load more evenly between the active cells.

5.5 Advanced Cell Fingerprint Metrics

In this section, new CFP metrics are introduced, to justify the basic set of metrics or to further improve the accuracy to identify sleeping cells.

In the next 3 subsections, the simulations for the new single and combined metrics are performed for a highly loaded network, i.e. with 20 active neighbor cells. Any promising enhancements are then evaluated in the last subsection for changing traffic conditions, i.e. also for reduced number of active neighbor cells.

5.5.1 Difference to Median

The analysis of the basic CFP metrics results in the previous sections emphasize the importance of an extended and more detailed range for the scores. Additionally, the higher weighting towards the median of the basic sum metric seems to indicate a better matching for RSS values closer to the median.

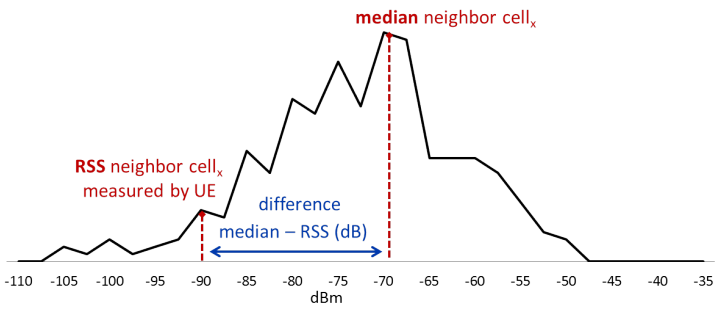

FIGURE 5.15: CFP Metric: Difference to Median

Therefore, instead of upper and lower bound RSS ranges, we pursue the idea to use the absolute difference of UE RSS measure to the median of the corresponding cell fingerprint, presented in figure 5.15. We assume, the closer the received RSS is to the median, the better, i.e. more reliable is the matching result. Eq. (5.3) and Eq. (5.4) calculate the result for the metric diffMedian:

$$\Delta rss(cell_x) = |median(cell_x) - rssUe(cell_x)| \tag{5.3}$$

$$diffMedian = \sum_{x=0}^{X} \Delta rss(cell_x) \tag{5.4}$$

where $\Delta rss(cell_x)$ is calculated as the absolute difference between the median of the cell fingerprint for the neighbor cell $median(cell_x)$ and the RSS as measured by the UE for the same neighbor cell $rssUe(cell_x)$. The $\Delta rss(cell_x)$ are summed up per neighbor cell as indicated in Eq. (5.4). The neighbor cell with the lowest sum of $\Delta rss(cell_x)$ is regarded as best fitting cell to be activated.

The advantage of diffMedian is the very fine gradation of the sum of the RSS differences compared to the scores resulting in the unique identification of 1 single cell.

Figure 5.16 presents the results of the diffMedian metric. The results are based on the standard configuration i.e. with 20 active neighbor cells and averaged UE RSS measurement samples, presenting the ASS.

Unexpectedly, the results indicated with 2.08 ASS significantly less accuracy for diffMedian compared to the metrics minMax and exclOut as well as to the sum of the 3 basic CFP metrics. Only Q10 delivered worse accuracy results. Consequently, we deduce, that the assumed advantage of more detail scores does not produce the desired improvement. The reason is, that the RSS ranges better model the individual cell RSS distributions than 1 single value. Also, the closer distance to the median is just one of many factors to determine the cell. Different to positioning, the validity of a cell area cannot be reduced to one single measure, but is more precisely modeled by ranges of valid measurements. Consequently, we do not pursue the diffMedian metric for cell identification any further.

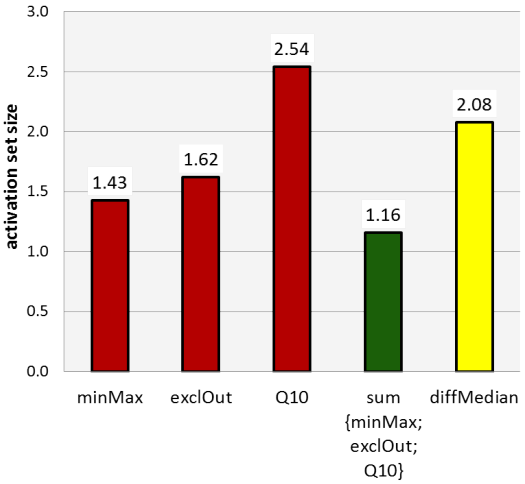

FIGURE 5.16: Activation Set Size: diffMedian (Difference to Median) vs. Basic CFP Metrics

5.5.2 Additional Single Quantile CFP Metrics

In this subsection, we introduce additional single quantile CFP metrics for the cell fingerprints aligned to the 3 single basic CFP metrics minMax, exclOut, and Q10. Some reasons for the introduction of the additional quantile CFP metrics, besides the validation and possible improvement of the basic CFP metrics, are listed below:

1. Few low or very low RSS are expected in the typical shadowing environment of an urban area. If regarded as valid, these measurement may obscure the typical radio conditions of a neighbor cell. Those measurements may be regarded as unreliable and thus, discarded.

2. Also a very strong signal strength may be restricted to very few UEs meeting special conditions. Such measurements may result from very rare events in an urban environment, e.g. from a UE having line of sight to a neighbor cell, that is along the antenna path of maximum gain. In the extreme, if a very high RSS, that occurs only once, is considered as valid, it may skew the result. To achieve more reliable fingerprints, extremely high measurements should be disregarded, although their effects are expected to be lower than those of the very low RSS measurements.

3. In case of multiple very strong RSS values, low percentile CFP metrics may consider even these high RSS as valid. For example, for a quantile metric with the range between the 2nd and 98th percentile, 2% of the strongest RSS would be discarded. In case of 2% or more very strong RSS measurements, these RSS values would be considered as valid.

4. Newly composed combined sum metrics, partly with an increasing number of summands, may improve the accuracy. Possible reasons are the better modeling of the distributions, but also the further increase of the obtained gradation of the scores.

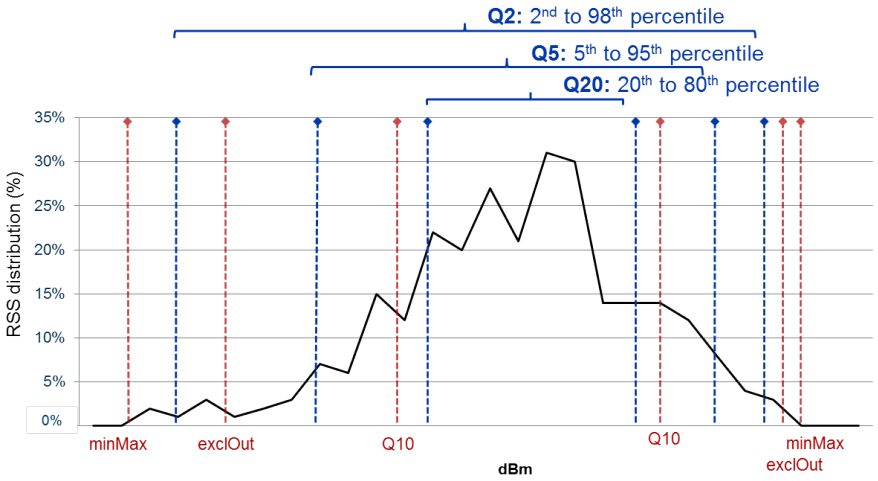

FIGURE 5.17: Example: RSS Distribution with New Percentile Metrics (blue) and Basic CFP Metrics (red)

Therefore, we model the RSS distribution in more details, adding 2 more quantile CFP metrics between minMax and Q10. The third new quantile CFP metric further restricts the narrow Q10 range, assuming possible improvement for the very low traffic scenarios based on the promising results in subsection 5.4 for Q10.

Figure 5.17 presents the new quantiles in blue embedded in the previously introduced metrics in dark red mapped on an exemplary RSS distribution. The following definitions for the newly introduced CFP metrics apply:

- **Range between 2nd and 98th Percentile (Q2)**: valid RSS range between 2nd ($Q_{0.02}$) and the 98th percentile ($Q_{0.98}$)
- **Range between 5th and 95th Percentile (Q5)**; valid RSS range between 5th ($Q_{0.05}$) and the 95th percentile ($Q_{0.95}$); it is also referred to as 20-quantile or vigintile
- **Range between 20th and 80th Percentile (Q20)**: valid RSS range between 20th ($Q_{0.2}$) and 80th percentile ($Q_{0.8}$); it is also referred to as 5-quantile or quintile

The newly proposed percentile CFP metrics are then used in a simulation study with averaged UE measurements, initially for 20 active neighbors. Figure 5.18 presents the new CFP metrics in blue and the basic set in dark red.

Interestingly, Q2 provides the best results, even exceeding minMax. Q5 is substantially better than Q10 and thus, may also be a promising summand. Finally, as expected with 20 active neighbor cells, Q20 experiences the worst accuracy with almost 3 cells required for activation caused by the strictly limited range, resulting in many false positives. However, Q20 may be seen as more promising for reduced numbers of active cells, to be evaluated in section 5.5.4.

Summarizing the findings of this subsections, the basic single CFP metrics did not provide the very optimum accuracy results for the 20 active neighbor cell configuration, but will still be considered as suitable, especially as minMax and exclOut provided

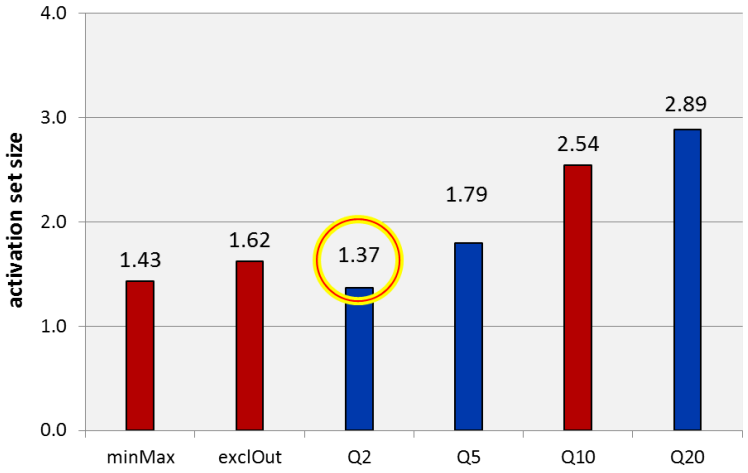

FIGURE 5.18: Activation Set Size: Basic and Newly Defined Percentile Metrics

the second and third best results. The 3 new quantile CFP metrics, especially Q5 and Q10 require further validation in respect to both as summands in new sum CFP metrics as well as in scenarios with reduced numbers of active neighbors performed in the following sections. The new best and very promising metric is Q2. The minor restriction of 2 percentile to the RSS range, excluding RSS values at the very edge, exceeds the accuracy compared to the non-restricted minMax CFP metric, even for multiple neighbors. Considering, that the exclusion of single RSS values at the very cell edge is the originally intended function of the exclOut CFP metric, the outlier exclusion seems not to work adequately, at least not for the given scenario.

5.5.3 Advanced Set of Combined CFP Metrics

From past experience, the combined CFP metric basic sum constantly achieves the highest accuracy. Therefore, additional combined CFP metrics consisting of the single basic and new percentile CFP metrics are introduced, promising further accuracy improvements. For the composition of the new combined CFP metrics, we consider the accuracy results of each single CFP metric. Only the most interesting or promising combinations of combined CFP metrics are selected and listed below:

- sum{minMax, exclOut, Q2, Q5, Q10, Q20}: consisting of all 6 single metrics defined in 4.2.2 and 5.5.2; also referred to as the sum of all 6 single CFP metrics
- sum{Q2; Q5; Q10; Q20}: all quantile CFP metrics exclusively
- sum{Q2; Q5; Q10}: the 3 more accurate quantile CFP metrics
- sum{minMax; exclOut; Q2; Q5; Q10}: the 5 single CFP metrics achieving the most accurate results
- sum{minMax; exclOut; Q2; Q5}: the 4 single CFP metrics achieving the most accurate results

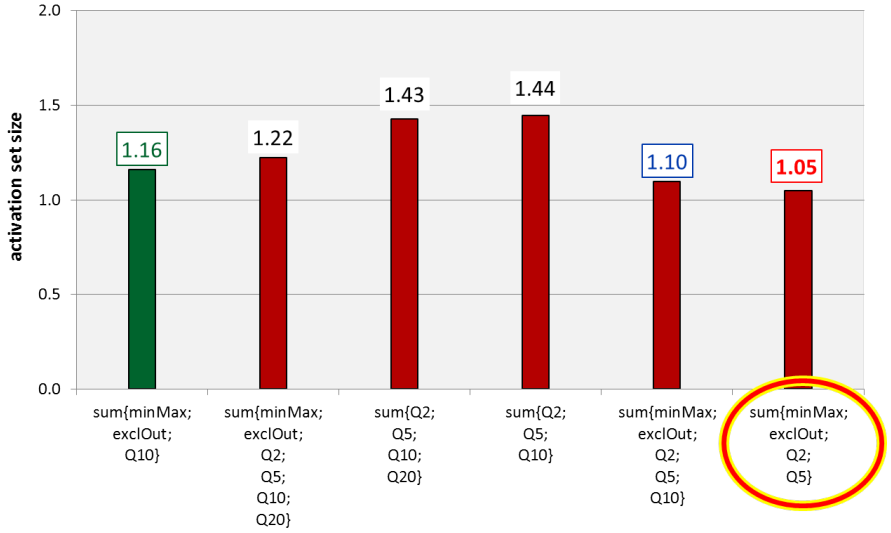

FIGURE 5.19: Activation Set Size: Basic and Newly Defined Combined CFP Metrics

The simulation results, presented in figure 5.19, are based on averaged UE samples for 20 active neighbors. It presents the ASS for the 5 newly defined combined CFP metrics in dark red, whereas the green bar displays the result for the basic sum as the reference to the previous results.

First, we observe, that the resulting accuracy for all presented combined metrics is very close, with an ASS ranging from 1.05 to 1.44 cells. In most cases for any type of combined CFP metric exactly the one best cell would be identified, ensuring the optimum energy saving.
Furthermore, the 2 combined CFP metrics achieving with more than 1.4 ASS the worst results, i.e. the sum of all quantiles and the sum of Q2, Q5, and, Q10, fall marginally below the best single CFP metric, Q2 with an ASS of 1.37. Thus, the combined CFP metrics do not always provide higher accuracy than single CFP metrics, however most of the combined ones do.
Interestingly, the basic sum CFP metric in green provides only the third best results, but with a minor difference compared to the best combined metric.
Obviously, Q20 with the worst single results impact the accuracy of the combined metrics, however with increasing number of summands this is partly compensated as shown by the sum of all 6 single CFP metrics still reaching an ASS of 1.22.
Finally the very best combined metric is composed of the 4 single CFP metrics: minMax, exclOut, Q5 and Q2, the 4 single metrics achieving individually the most accurate results for the configuration with 20 active neighbors. As a consequence, also their sum achieves the best ASS of 1.05, thus approaching the optimum result of 1.0.

Further details of the 3 most accurate sum CFP metrics are visualized in figure 5.20. It presents the Energy Efficiency Index in case NoCA is set to either 1, 2, or 3 cells to be activated. If 3 cells are activated, it is guaranteed, that the target cell is activated using any of the 3 sum CFP metrics presented in figure 5.20. If only 2 cells are activated, a minimum probability of 95% is reached to include the target cell. In the case, however, where operators prefer to activate only 1 cell at a time, the best

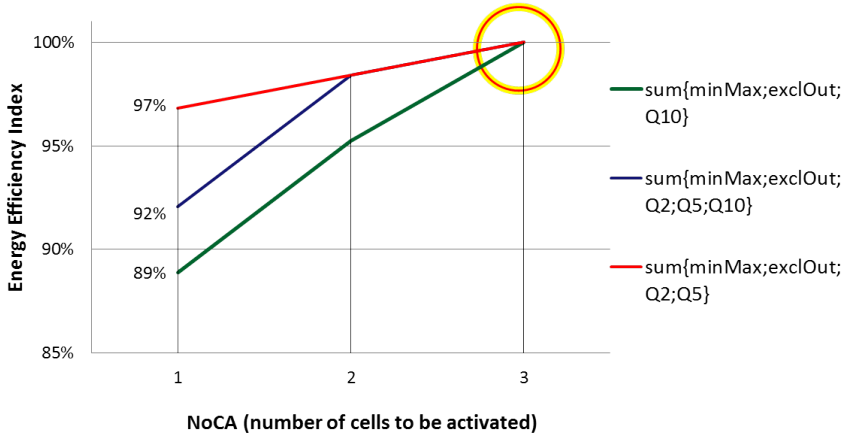

FIGURE 5.20: Energy Efficiency Index: Comparison of Best Combined CFP Metrics for NoCA set to 1, 2, and 3

sum(minMax;exclOut;Q5;Q2) CFP metric should be selected, reaching 97% to instantly activate the target cell.

Overall, the combined CFP metrics met the expectations to further improve the accuracy, confirming the benefits of the finer gradation and increased range of the scores. Interpreting the observation for the combined metrics, we can deduce:

- The CFP metrics model, to a certain degree, the RSS distributions of the neighbor cell. Therefore, considering multiple single CFP metrics, improves the recognition factor of the individual neighbor cell RSS distribution and thus, the cell identification.

- The best result was achieved by the sum of the 4 most accurate single metrics: minMax, exclOut, Q5 and Q2. These single metrics additionally provide the widest range, which is assumed to be one reason for the good accuracy, as only very few false positives are excluded. At least with 20 neighbor cells, resulting in a high number of matching events, considering almost all valid RSS values is expected to increase the accuracy.

5.5.4 Traffic Variation Impact on Advanced Single CFP Metrics

The following simulation study determines and evaluates the best suitable single quantile CFP metrics, introduced in subsection 5.5.2, for the different traffic conditions in a network. We consider the 4 to 20 active neighbor cells as previously described in section 5.4 and apply averaged UE samples.

In figure 5.21, we present as the simulation results, the ASS for all 6 single CFP metrics. The basic CFP metrics minMax, exclOut, and Q10 serve as references for the analysis.

Clearly, Q2 provides nearly consistently the highest accuracy. Two Q2 results are particularly striking: 1) with 16 neighbor cells Q2 is remarkable better than all other cell

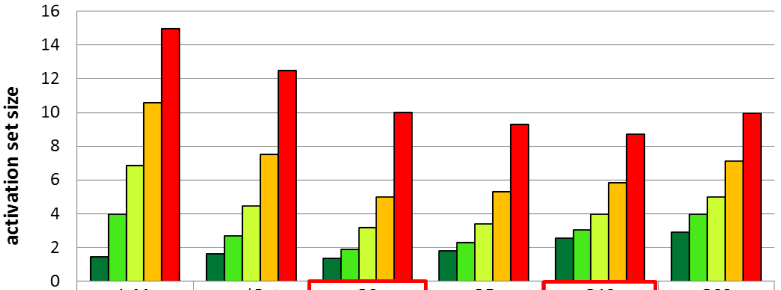

	minMax	exclOut	Q2	Q5	Q10	Q20
All 20 neighbors	1.43	1.62	1.37	1.79	2.54	2.89
16 neighbors	3.97	2.70	1.90	2.27	3.03	3.95
12 neighbors	6.84	4.44	3.16	3.41	3.98	5.00
8 neighbors	10.59	7.54	4.98	5.29	5.84	7.13
4 neighbors	14.98	12.48	10.00	9.29	8.73	9.97

FIGURE 5.21: Activation Set Size for Varying Numbers of Active Neighbors: Single CFP Metrics

single CFP metrics, and 2) for 4 active neighbors, the Q10 metric outperforms Q2, resulting in significantly 1.3 less cells to be activated.

Furthermore, two CFP metrics are throughout all simulation studies far from reaching the best accuracy: Q20 and exclOut. For **Q20** the valid RSS range is limited to values near the median, i.e. too many valid RSS measures are ignored. Although the comparative performance of the results slightly improve with less number of active neighbors, the limitation to accept RSS values as true is too strict. Thus, even with only 4 active neighbors Q10 and Q5 still outperform Q20. Consequently, Q20 should not be considered for fingerprinting as a single CFP metric.

Different to Q20, the **Q5** metric provides reliably, stable and good results. From 4 to 16 active neighbors, Q5 obtains continuously the second best results. We therefore consider Q5 as an important contribution for the combined CFP metrics.

Meanwhile, **Q2** is the CFP metric that produces the most stable and almost always the most accurate results. The reason is the minor restriction of only 2 percentiles as discussed in section 5.5.2. This minor limitation of the full RSS distribution range does not even impact the good accuracy in case of reduced neighbors, until the minimum set of 4 neighbors is reached. Only then, is the number of matching events so low that it can no longer compensate for the wide RSS range, causing frequent scoring of false neighbors. Comparatively, the more limited RSS ranges of Q5, Q10 and Q20 filter out more false positives compared to Q2.

As a conclusion for the single metrics, we observe in the chart of figure 5.21 a concave curve that changes with the changing number of active neighbors. For high and medium traffic, we expect to achieve a optimum accuracy close to Q2. However, for low traffic (4 active neighbors), the expected optimum shifts close to Q10, with a tendency towards Q5.

5.5.5 Traffic Variation Impact on Combined CFP Metrics

Finally, the combined CFP metrics for reduced numbers of active neighbors are presented for the different traffic conditions as the last scenario to be evaluated. We apply the same configuration as in the preceding subsection with 4 to 20 active neighbor cells and averaged UE samples.

Figure 5.22 shows the same selection of combined CFP metrics introduced in section 5.5.3; this time for reduced numbers of active neighbor cells. As a reference the basic sum metric is included as the first sample. To simplify the referencing of the combined metrics, a number is attached to each new combined metric.

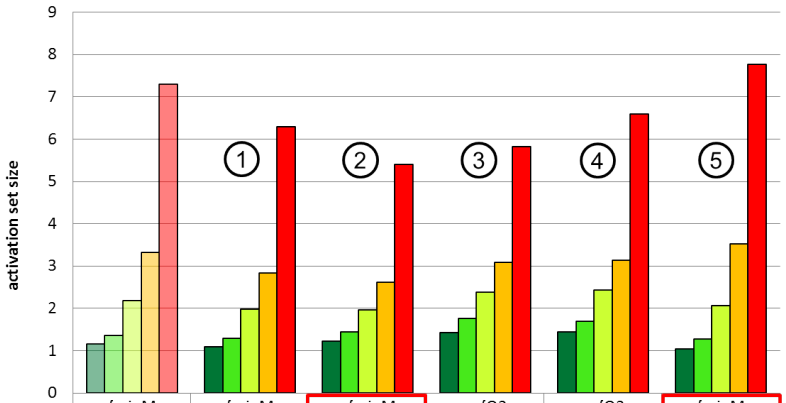

	sum{minMax; exclOut; Q10}	sum{minMax; exclOut; Q2; Q5; Q10}	sum{minMax; exclOut; Q2; Q5; Q10; Q20}	sum{Q2; Q5; Q10; Q20}	sum{Q2; Q5; Q10}	sum{minMax; exclOut; Q2; Q5}
All 20 neighbors	1.16	1.10	1.22	1.43	1.44	1.05
16 neighbors	1.37	1.30	1.44	1.76	1.70	1.27
12 neighbors	2.17	1.98	1.97	2.38	2.43	2.06
8 neighbors	3.32	2.84	2.62	3.10	3.14	3.52
4 neighbors	7.30	6.30	5.40	5.83	6.59	7.78

FIGURE 5.22: Activation Set Size for Varying Number of Active Neighbors: Combined CFP Metrics

The first combined metric with 5 summands (**no. 1**) almost consistently delivers the second best results, only surpassed by the combined metric no. 2 for low traffic situation and no. 5, the sum of the 4 best single metrics for high traffic scenarios. The combined metric **no. 2** (sum of all 6 samples) achieves continuously very good results, and even the best for low traffic scenarios from 4 to 12 active neighbors. The metrics **no. 3 and no. 4** (consisting of quantile only) instead, achieve relatively poor results. Finally, metric **no. 5**, the sum of the 4 most accurate single metrics, deliver the best results in case of high traffic load, with 16 and 20 active neighbors.

Some major observations and interpretations on the combined metrics are listed below:

- With **4 active neighbors**, the best accuracy implied an activation of 5.4 cells. This was not perfect regarding energy saving, but was regarded as sufficient for 2 possible practical approaches: Either the 5 to 6 identified cells could be activated

straight away or just 1 of the best matching cells would be randomly selected and activated, relying on load balancing to distribute the load accordingly. The chosen approach depends on the operators preferences regarding quality or energy resp. cost effectiveness.

- In case of **8 active neighbors**, the ASS reduced to less than half (i.e. ∼2.6) cells compared to 4 active neighbors. For 12 active neighbors, in average less than 2 cells were identifies to match best. Restricting the activation to the identified 2 to 3 cells, improves the energy saving potential, compared to 5 to 6 cells (with 4 active neighbors), to a great extent.

- For **low to medium traffic load**, i.e. mapped to 4 to 12 active neighbor cells, no. 2, the sum of all 6 single metrics, achieved the highest accuracy. One reason was the higher number of metrics, which resulted in a finer gradation and thus, stretched the scores. That compensated, at least partly, the restricted number of matching events caused by the reduced number of active neighbors.
  However, even the extended range of the scores could not fully compensate the reduced number of active neighbor cells, i.e. the lower number of matching events.

- Only in case of **high traffic load**, the accuracy of the single CFP metrics was more important, than the higher number of summands of no. 2. Thus, with 16 and 20 active neighbors, no. 5, i.e. the sum of the 4 most accurate single metrics, provided the highest accuracy, reaching close to the very optimum, i.e. to identify exactly 1 cell with 20 active neighbors.

Finally, also for the combined CFP metrics we observed a concave curve for low and very low traffic conditions, from 4 to 8 neighbors (red and orange bars). The best results were achieved for the combined metric no. 2, composed of the highest number of summands. The inclusion of the more restrictive quantiles, Q10 and Q20, resulted in an increased accuracy. This indicates a tendency to achieve a very good accuracy for the more critical, low traffic situation, with an increasing number of summands, which is further reinforced by the quantiles, restricting the RSS to values close to the median. Conversely, for the high traffic, we observe a less pronounced convex curve for the green bars, achieving the best values for no. 1 and no. 5, which are respectively the sums with the 4 or 5 most accurate single metrics.
The diverging impact of the single metric type and number of single metrics on the accuracy as a function of the changes in the traffic load is discussed in the subsequent chapter.

5.6 Summary

Summarizing the results of the simulation studies, we focus on the more interesting final studies of the combined metrics during changing traffic conditions.

So far, we identified 4 major factors, which influence the accuracy of the combined metrics:

- the number of active neighbor cells impacting both, the single and the combined metrics
- the number of single metrics used as summands in a combined metric
- the achieved accuracy of each single metric used as part of the combined metric
- the degree to which each single metric of the combined metric restricted the RSS distribution. For example, minMax has the widest range without restriction, while Q20 has a very restricted range.

As the impacting factors for the combined metrics differed significantly, depending on the traffic load, we interpret the impact and the corresponding reasons separately:

1. **Low load:** The reduced number of active neighbor cells caused the reduction of matching events. This results in a reduced mapping accuracy of the sleeping cells to the neighbor cell distributions as well as in a decreasing gradation of the score. Conversely, the reasons, why an increasing number of summands improved the accuracy are:

   (a) the more accurate modeling of the RSS distribution, also caused by summands with restricted ranges, improved the matching accuracy

   (b) the increased gradation of the score enabled the matching procedure to better differentiate between the sleeping cells

2. **High load:** With increasing number of active neighbor cells and thus, matching events, the accuracy of the summands, became increasingly important and outweighed the number of summands. One reason was, that the increased scoring range and the accurate mapping of the sleeping cells was already provided by the high number of active neighbors. Thus, the major important factor to further improve the matching accuracy was then the accuracy of each single summand.

As a result, we propose the implementation of an adaptive algorithm for the matching procedure. The number of active neighbors is required as input to determine the most appropriate number and type of the single metrics to be used as summands for the combined metric.

CHAPTER 6

Energy Savings Potential

Contents

6.1 Energy Saving Model 89
6.1.1 Daily Traffic Profile 89
6.1.2 Network Layout 90
6.1.3 Relative Power Saving Potential 90
6.1.4 Assumptions for the Energy Saving Model 91
6.2 Approaches for Cell Identification 92
6.3 Results and Evaluation of the Energy Saving Potential . . . 96
6.4 Limits and Constraints of the Energy Saving Model 98

In this chapter, we evaluate the energy saving potential for temporary deactivating of not needed cells. We use the cell fingerprinting method for cell identification, in comparison with 2 other cell identification approaches. As input for the presented energy saving model, we apply the results of the simulation studies in chapter 5. In particular, considering certain traffic conditions, we use the results that achieved the best performance. The following sections present first the energy saving model for a small cell overlay network, followed by the introduction of 3 different approaches for cell identification, one of which is cell fingerprinting. Subsequently, the saving potential of the 3 approaches is compared and evaluated.

6.1 Energy Saving Model

This section introduces first, a profile of the daily traffic variation and second, an appropriate network layout, both required to set up the energy saving model. Next, we propose a scheme to calculate the power saving and close this section with a summary of assumptions made to determine the energy saving potential using cell fingerprinting.

6.1.1 Daily Traffic Profile

The variation of the daily data traffic volume is a prerequisite for the energy saving by temporary deactivation of currently unused cells. Due to the unavailability of data from operational networks, we propose to use a traffic model frequently referenced in literature. The reference model of the EARTH project [107] provides the European average of the traffic distribution for a dense urban area [33]. The traffic profile, scaling from 0% to 100% on an hourly basis, is presented in figure 6.1, reaching the peak 100% traffic volume between 20 h and 21 h.

Figure 6.2 presents the European daily traffic variation, from which the scaling of the hourly energy consumption in figure 6.1 is deduced. Additionally, figure 6.2 indicates the daily energy waste, i.e. the difference between the available and the requested capacity. The available capacity indicates, that the network capacity is dimensioned for the peak traffic hour, where all cells are activated at any point in time. In case the available and requested capacity converges, the theoretical maximum energy saving can be reached. This implies the implementation of cell deactivation/reactivation procedures to minimize the number of active small cells, where the small cells are still able to process the requested data volume at any point in time.

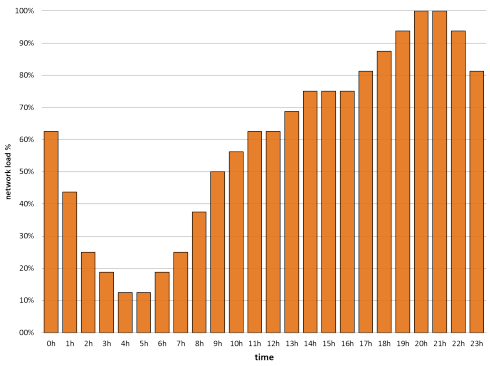

FIGURE 6.1: European Average for a Dense Urban Area: Traffic Distribution on Hourly Basis

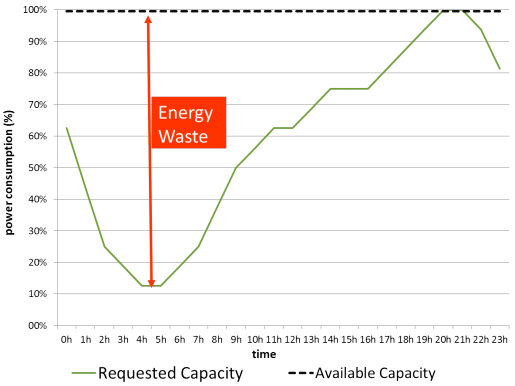

FIGURE 6.2: Daily Traffic Distribution Indicating the Period of Maximum Energy Wastage

6.1.2 Network Layout

The energy saving model requires the definition of a typical network deployed in a dense urban area. Thus, we propose a heterogeneous network, consisting of 2 layers, the network underlay for macrocell, and the network overlay for small cells. The energy saving potential is exclusively determined for the small cell network layer, i.e. only small cells serving as capacity booster for the mobile data traffic are assumed to be activated, or respectively, deactivated. The underlaying macrocells, providing the basic coverage to guarantee the QoE of the users, are assumed to be always active and thus, is not considered for energy saving.

Figure 6.3 presents the HetNet layout for the energy saving model, consisting of 21 small cells and a minimum of 5 sectorized macrocells as network underlay. For cell fingerprinting, the 5 macrocells are required as the minimum number of active cells (see 5.4.2), in case all small cells are sleeping. Then, in case one macrocell is in overload, the remaining 4 neighbors provide the minimum number of cells required for the matching procedure.

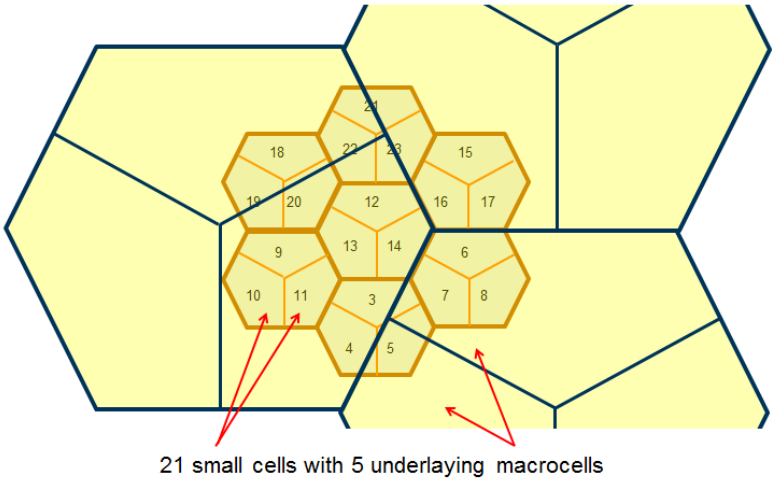

FIGURE 6.3: Energy Saving Model: Network Layout

For determining of the saving potential of the fingerprinting approach, we reuse the accuracy results from the simulation studies, presented in the previous chapter. Accordingly, the 21 small cells in figure 6.3 represent the network setup of the LTE system simulator as presented in chapter 3, with the difference of the macrocell underlay.

6.1.3 Relative Power Saving Potential

For the proposed energy saving model, energy saving is restricted to the small cells overlay. Depending on e.g. the cell type, RAT, and configuration, the small cell power consumption varies significantly as presented in table 2.1 in section 2.2.2. Thus, energy consumption and saving expressed in absolute values would be incomparable.

To overcome this issue and provide valid results independent of the cell type, we propose to use the relative saving in percent of the maximum assumed power consumption of

the complete 21 small cell overlay network. The maximum power consumption of 100% is assumed, when all 21 small cells presented in figure 6.3 are active. Each small cell is assumed to consume the same amount of power, resulting in a share of 21 hundredth (i.e. 4.76%) of the total 100% small cell power consumption.

Furthermore, the load dependent power variation of small cells is ignored in the proposed energy saving model. This assumption can be justified from the details given in section 2.2.2, indicating an almost constant power consumption of active small cells, i.e. the impact of the traffic load on the small cell power consumption is almost negligible.

Finally, in case of periods with no or minor traffic within the given area, the small cells are assumed to be deactivated, i.e. they transit into a "deep" sleep mode with an energy consumption close to zero Watt as described in section 2.2.3 and [16]. For simplification reason the power consumption of deactivated small cell is therefore set to zero.

6.1.4 Assumptions for the Energy Saving Model

For the correct interpretation of the energy saving by temporary cell deactivation of a small cell network overlay, we describe all assumptions concerning the energy saving model below:

1. **Restriction to network overlay:** The energy saving potential is calculated exclusively for the overlaying small cell network layer, i.e. only small cells are assumed to be activated respectively deactivated.

2. **Candidates for deactivation:** All small cells can be switched off in case the data traffic does not exceed 20% of the total maximum data volume achievable, if all macro and small cells would be active. As long as traffic volume remain below 20% of the maximum capacity, macrocells are able to provide the requested data rate.

3. **Small cell power consumption:** In addition, the energy consumption of small cells is simplified. We assume that small cells continuously consume the maximum power, while active, but they consume zero Watt, while sleeping.

   Note that assumptions 2 and 3 do not fit to all types of small cells. Especially, the (close to) zero Watt power consumption during sleep mode, requires a deep sleep mode for small cells, which is not yet supported by all small cells. However, both assumptions may compensate each other, as the first assumption is too negative and the second one too positive for small cell power consumption, as indicated in 2.2.2.

4. **Time periods with increasing or constant traffic load:** Once a cell is activated, even if not used, i.e. without any UE connection, it remains activated as long as the overall request for traffic volume does not start to decrease. This differs from the assumption in chapter **4**, when cells are automatically deactivated after a defined guard period without any connection setup. This simplification applies for all evaluated approaches introduced in the following section. Overall, the restricted deactivation has a negative impact on the energy saving potential.

5. **Load distribution between cells:** MLB is assumed to distribute the traffic load onto the active cells. In case of further traffic load increase in the subsequent hour, additional cells are only activated, if the given overall cell capacity is less than the overall requested traffic volume. Realistically, in case of an additional data volume request in a coverage area with sleeping small cells, additional cell activation might be required. However, as the previous activation of small cells unloads the macrocells, the macrocell load relieves, providing capacity to take over e.g. short term traffic peak from coverage areas of sleeping small cells.

6. **Macro and microcell fingerprint significance and accuracy:** Cell fingerprinting works for any type of cell. Using multiple CFP metrics (e.g. quantiles) for the evaluation enables the detection of characteristic RSS distributions for each type of neighbor cell, also for small cells with macrocell neighbors. As the matching requires a minimum set of 4 neighbors and the use of combined CFP metrics, we assume that the matching procedure is able to distinguish between the sleeping small cells, even if the only active neighbors are macrocells.

6.2 Approaches for Cell Identification

For the evaluation of the energy saving potential, we assume that the provided network capacity has to at least meet or exceed the demanded capacity of the UEs. The closer the provided capacity meets the actual demanded capacity, the more energy can be saved. Cells are activated, whenever the requested capacity of the UEs exceeds the provided network capacity.

For cell activation, we investigate 3 different approaches to determine the minimum number of cells to be activated, to meet the user's capacity request. Cell fingerprinting, as 1 of the 3 approaches, is compared with 2 reference cell identification approaches, a very optimistic and a very pessimistic. All 3 approaches are introduced below:

I. **Theoretical Optimum**

   The best cell(s) to take over the increasing traffic demand is always correctly identified. Consequently, this very optimistic approach assumes that the most appropriate cell to be activated is always known, i.e., only the minimum number of required cells is active at each point in time to satisfy the user's traffic demand.

II. **Best Cell Unknown**

   The appropriate sleeping cell to take over the increasing traffic demand is unknown. The implication is that the correct cell cannot be identified, which results in a very pessimistic approach.

III. **Cell Fingerprinting Approach**

   We use the cell fingerprinting procedure for cell identification as defined in chapter 4 and evaluated in chapter 5. The impact of cell fingerprinting on energy saving

should be evaluated, by means of the accuracy to identify the minimum number of appropriate cell(s).

All 3 approaches follow the same hourly-performed procedure presented in figure 6.4, to determine the number of small cells to be activated in response to an increasing traffic demand.

```
FOR each hour of the day
  IF ((any small cell IS sleeping) AND
    (demanded network capacity > (20% of max. network capacity +      // covered by macrocells
                                  capacity of activated small cells))
    CASE approach OF
      Theoretical optimum:
        activate minimum no. of small cells to match the demand;
      Best cell unknown:
        activate all sleeping small cells;
      Cell fingerprinting:
        cell matching with best CFP metric for given no. of active neighbors;
        activate best matching cell(s);
        // no. of cells to be activated depends on no. of active neighbors and CFP metrics
    ENDCASE
  ENDIF
ENDFOR
```

FIGURE 6.4: Energy Saving Model: Hourly Cell Activation Procedure for the 3 Approaches

At any hour of the day, the provided average network capacity is matched with the average demanded capacity. The provided network capacity consists of the capacity provided by the macrocells and by the active small cell, where the (always active) macrocells are assumed to contribute up to a maximum of 20% to the total network capacity. For the demanded network capacity, the traffic indicated in the daily traffic profile presented in figure 6.1 is used. If the demanded capacity exceeds the provided capacity, the number of sleeping cells to be activated is determined separately for each of the 3 approaches.

For the **Theoretical Optimum** approach, the best matching cell is known, i.e. it always corresponds to the target cell. Therefore, the number of cells to be activated is directly proportional to the current traffic load as presented in green in figure 6.5. In case the demanded capacity exceeds the provided capacity, the minimum number of cells is activated. The demanded capacity is always met as precisely as possible, to ensure the user's QoE and to obtain the optimum energy saving.

For the **Best Cell Unknown** approach, the cell to be activated cannot be identified. Therefore, in case a cell experiences overload, all sleeping, small neighbor cells will be activated. The result is displayed in yellow in figure 6.5 indicating, that all cells will be activated at 7am, when the traffic demand raises and thus, exceeds the provided capacity drastically. Due to the missing cell identification capability, all cells will remain active until the traffic demand starts to decrease at 10pm (22h).

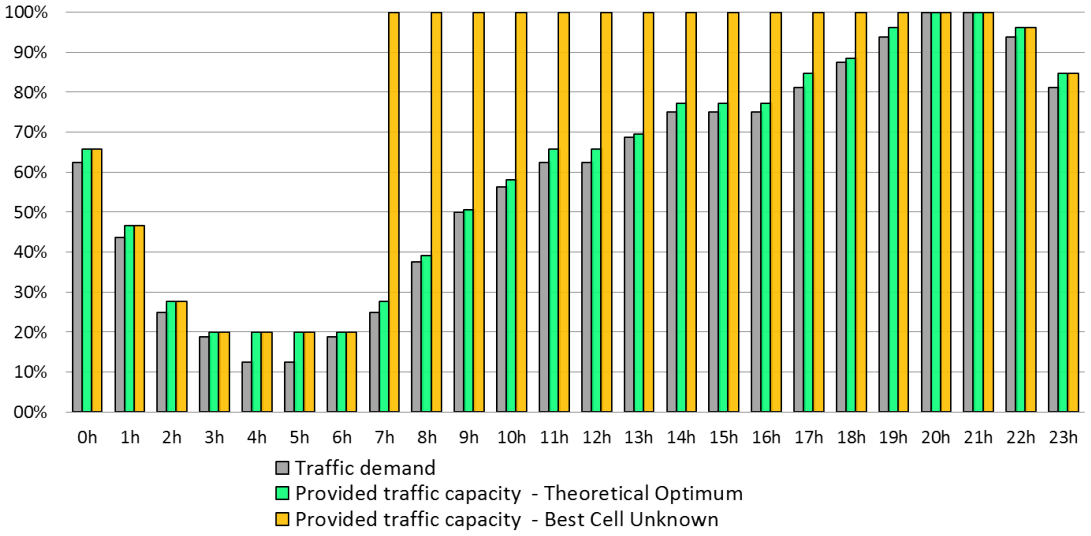

FIGURE 6.5: Reference Cell Identification Approaches: Relation to Traffic Demand for Theoretical Optimum and Best Cell Unknown - on Hourly Basis for One Day

For the third approach, **Cell Fingerprinting**, the number of cells to be activated depends additionally on the number of active neighbors as well as on the CFP metrics, presented in figure 5.22 of chapter 5.5.4. We propose to use the 2 combined CFP metrics, which were identified to provide the highest accuracy for defined traffic conditions. These 2 combined metrics are presented in figure 6.6, providing the ASS for the defined set of active neighbor cells. For the hourly activation procedure in figure 6.4, the corresponding best combined metric for a given number of active cells is selected.
The selected 2 CFP metrics are described below:

1. **Sum of all single CFP metrics** - Sum{minMax, exclOut, Q2, Q5, Q10, Q20}

   The sum of all single CFP metric adds up all single CFP metrics, which are: minMax, exclOut, and all implemented quantiles, i.e. 2nd, 5th, 10th and 20th quantile, as defined and evaluated in the sections 5.5.3 and 5.5.4. The best results are achieved for low and median traffic scenarios, i.e. for 12, 8, or 4 active neighbors. For example, in case of only 4 active neighbors, an average of 5.4 cells are identified as the best matching cells. The numbers of cells to be activated, corresponds for 5.4 cells in the worst case to 6 cells or to 5 cells, if rounded as presented in figure 6.7.

2. **Sum of the best 4 single CFP metrics** - Sum{minMax; exclOut; Q2; Q5}

   This combination of best single CFP metrics achieves the best results in case of 16 or 20 active neighbors, see figure 6.6. If 16 or 20 neighbor cells are active, for the most times the activation of 1 cell is sufficient, while 2 cells need to be activated in the worst case as presented in figure 6.7.
   Particularly, in case of 20 neighbors, the activation of just 1 cell is assumed as adequate. The reason is, that the average of 1.05 ASS in figure 6.6, results in a 5% probability to activate the second best matching cell with almost similar RSS conditions, which is typically expected to take over the expanding traffic demand.

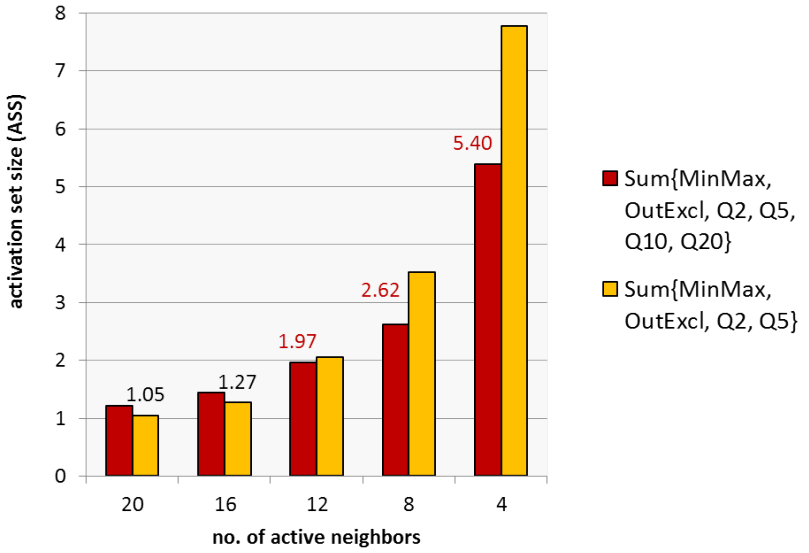

FIGURE 6.6: Cell Fingerprinting: Relation of Best Combined CFP Metrics to Number of Active Neighbors

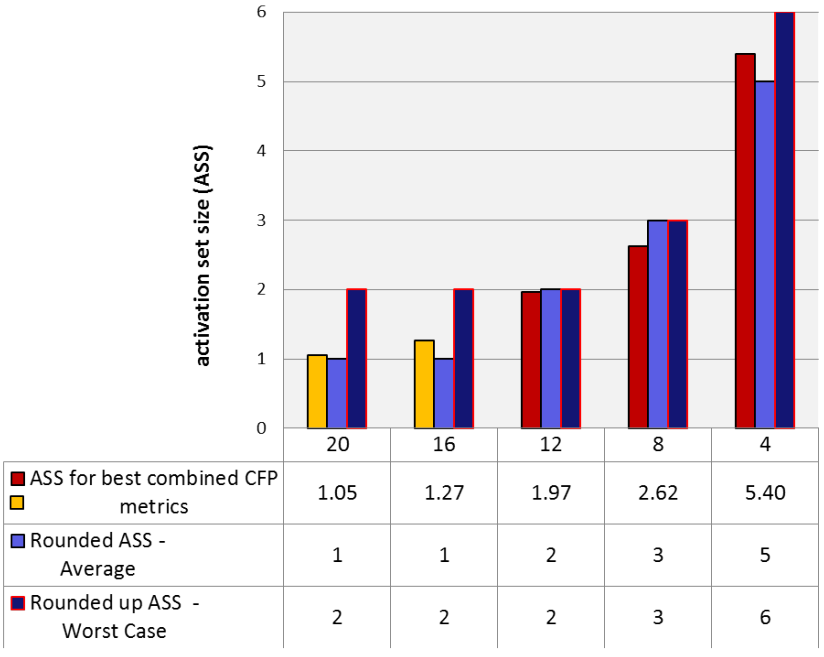

FIGURE 6.7: Cell Fingerprinting: ASS for 2 Best CFP Metrics Mapped on Number of Cells to be Activated 1) Rounded and 2) Rounded up (Worst Case)

In figure 6.7, the ASS for the 2 best combined CFP metrics is presented, i.e. the sum of all single CFP metrics (in red) and the sum of the best 4 single CFP metrics (in yellow). Using the ASS, the number of cells to be activated distinguishes between 2 cases: 1) the ASS is rounded, which results in the activation of the averaged ASS. For 4, 16, and 20 active neighbors there is a risk, that the target cell is not be activated. 2) the ASS is rounded up to ensure at any point in time the activation of the target cell. Both cases are separately considered for the evaluation of the energy saving potential.

The final result using cell fingerprinting on an hourly basis is presented in figure 6.8. The daily basis has to be split into 2 phases: during the night phase from 8pm to 6am (i.e. 20h until 6h in figure 6.8) with no increasing traffic demand, the resulting number of active small cells matches with the 2 reference approaches, presented in figure 6.5. During the day time interval, the provided traffic capacity mostly follows closely the traffic demand. There are few exceptions, e.g. at 7h, much more cells are activated than actually required. This is caused by the small number of active neighbors, resulting in a higher inaccuracy and therefore forcing more cells to be activated. But, whenever the traffic demand is overcompensated, the increasing number of active neighbors results in a improved accuracy and thus, reduced overcapacity for the subsequent cell activation procedure. The results of the worst case CFP slightly exceeds the average, especially during increasing traffic. The increased number of cells to be activated, compared to the "averge" case, depends on the number of active neighbors as illustrated in figure 6.7.

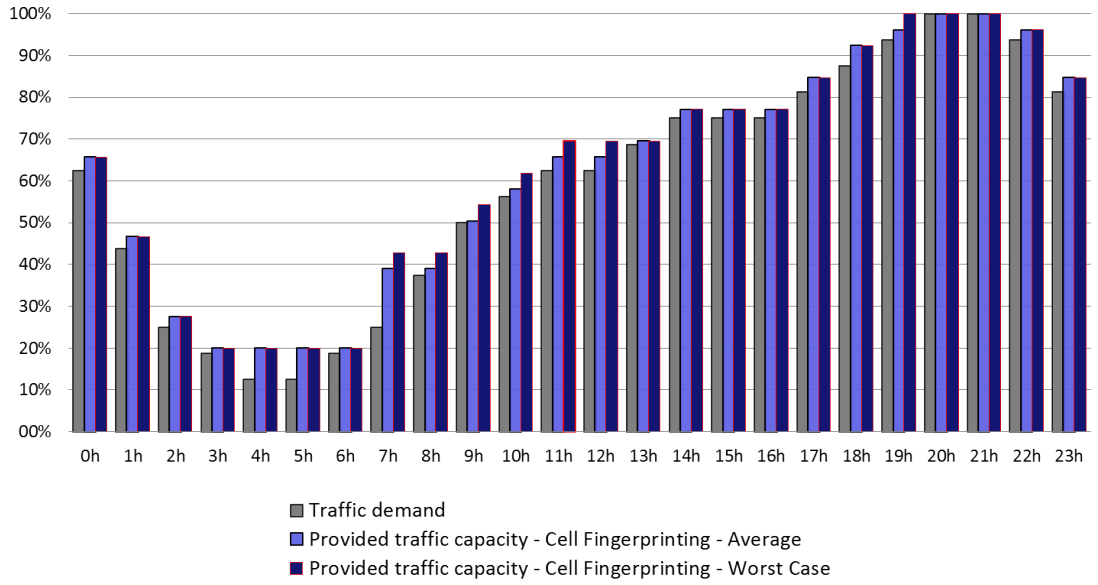

FIGURE 6.8: Cell Fingerprinting Approach: Daily Traffic Demand vs. Traffic Capacity on Hourly Basis

6.3 Results and Evaluation of the Energy Saving Potential

For the presentation and evaluation of the energy saving results, we focus on the cell fingerprinting method and the extent it converges with the theoretical optimum, one of the reference methods introduced in the previous section.

Figure 6.9 presents the number of active cells for the 3 approaches, limited to the relevant time period cells are activated, from 6 am to 8 pm (20 h). Additionally, cell fingerprinting is further split into 2 cases: the average and maximum (worst case) number of cells needed for activation.
We observe, that all small cells are still sleeping at 6 am, as the macrocells are able to provide the needed capacity. At 7 am, when additional capacity of small cells is required,

the very different number of active cells per approach is apparent. Obviously, there is a significant differences between the "Best Cell Unknown" approach, and the other 2 approaches, the theoretical optimum and cell fingerprinting. The optimum approach follows the traffic demand, whilst the "Best Cell Unknown" approach has to activate all small cells immediately. Cell fingerprinting, however, suffers from the small number of active neighbor cells resulting in the activation of 5 or 6 cells, where 2 cells would be sufficient. Until reaching the peak traffic hour at 8 pm, when the capacity of all small cells is required, the cell fingerprinting accuracy improves with the increasing number of neighbors, closely following the theoretical optimum.

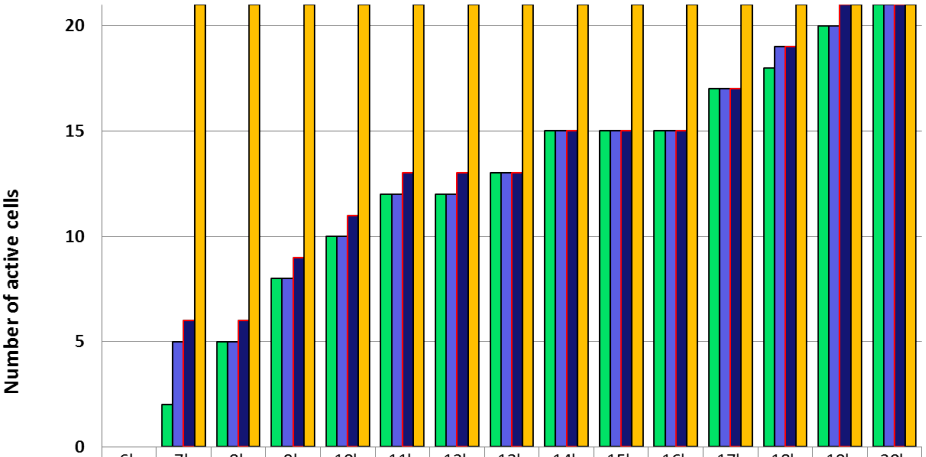

	6h	7h	8h	9h	10h	11h	12h	13h	14h	15h	16h	17h	18h	19h	20h
Theoretical Optimum	0	2	5	8	10	12	12	13	15	15	15	17	18	20	21
Cell Fingerprinting - Average	0	5	5	8	10	12	12	13	15	15	15	17	19	20	21
Cell Fingerprinting - Worst Case	0	6	6	9	11	13	13	13	15	15	15	17	19	21	21
Best Cell Unknown	0	21	21	21	21	21	21	21	21	21	21	21	21	21	21

FIGURE 6.9: Number of Active Cells per Approach: Hourly from 6 am to 8 pm

Both figures 6.10 and 6.11 provide a summary of the approaches for a 24 h period, i.e. the daily average number of active cells per approach in figure 6.10 as well as the saving percentage in figure 6.11. Although both figures provide the results for a day, the focus is on the periods with growing traffic demand. Only then, cell activation occurs, asking for cell identification, while periods with constant or decreasing traffic are irrelevant for the comparison between the 3 approaches. Additionally, a prerequisite to achieve the presented result for all 3 approaches, is the implementation of an optimal cell deactivation algorithm.

According to the achieved saving percentage in figure 6.11, temporary deactivation of currently unused cells can **save up to 48% of the total small cell power consumption** in a dense urban network overlay. The 48% saving is restricted to the theoretical optimum approach, allowing to map the growing data traffic volume 100% accurately on the best fitting cell. However, even in case all smalls are activated at once, as soon as additional cell capacity is needed, i.e. the "Best Cell Unknown" approach, still up to 26% of the total small cell power consumption can be saved.

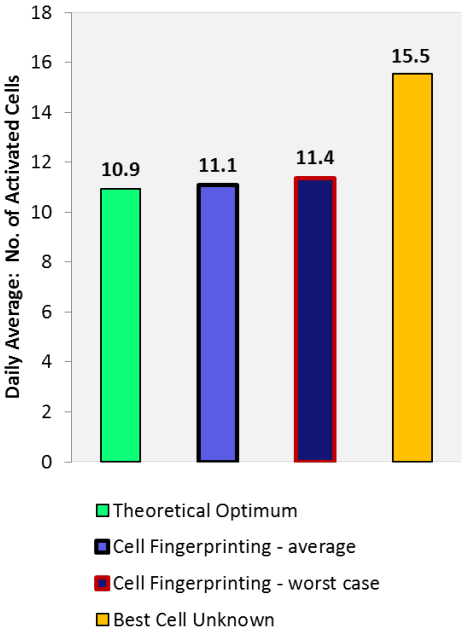

FIGURE 6.10: Daily Average: No. of Activated Cells (max. 21)

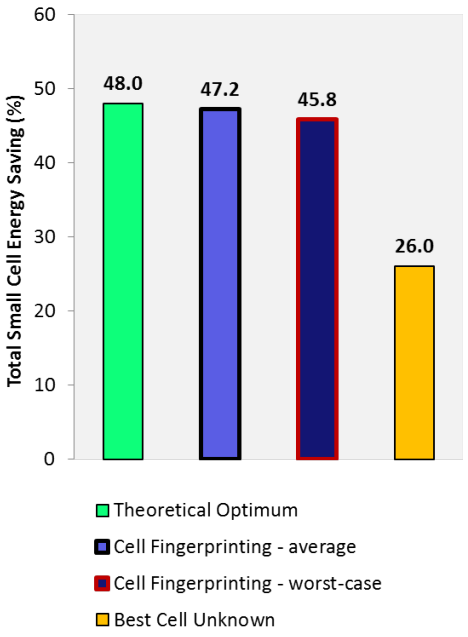

FIGURE 6.11: Saving Percentage of the Total Power Consumption

Most important, the **cell fingerprinting approach can save up to 47.2%** of the power consumed by small cells, in case fingerprinting is used for cell identification when the traffic volume increases. Even, if the maximum number of cells identified by cell fingerprinting is activated, still 45.8% less power is consumed as presented in figure 6.11.

When comparing the saving percentage of cell fingerprint and the theoretical optimum in figure 6.11, it results in less power saving for cell fingerprinting of 0.8% for the average and 2.2% for the maximum number of cell activations. Thus the energy saving using cell fingerprinting closely approaches the theoretical optimum, which indicates cell fingerprinting as a valid approach to identify the most appropriate sleeping cell to be activated.

6.4 Limits and Constraints of the Energy Saving Model

For the presented energy saving model certain limits and constraints should be considered, which are discussed below.

The focus of the energy saving evaluation is the effect of the cell fingerprinting method on the saving potential. As cell fingerprinting is only applicable for periods with increasing traffic demand, the **deactivation procedure** is not considered. Therefore, in case of decreasing traffic, the capacity is adjusted by deactivation of cells proportionally to the given traffic load. This approach reflects the theoretical optimum approach for cell deactivation. Several more realistic cell deactivation approaches are described in chapter 2.3.1.

For the energy saving model, the **average hourly traffic load** is derived from the reference data of the EARTH-project, [107]. It presents an average of the daily traffic load in Europe in an urban environment, but may not represent the traffic behavior of a local section in an urban environment.

A prerequisite for cell fingerprinting, as used in this chapter, is that the cell experiencing the overload situation has a **minimum of 4 active neighbors**, regardless of macro- or small cells. Although an operational cellular network requires multiple active neighbors, e.g. for mobility and reliability reasons, alternatives may be considered for the unlikely case of less than 4 active neighbors. One option could be, the use of fingerprinting with a result of more than 6 best matching cells to be activated. Cells would return to sleep mode after a defined guard period, resulting in an increased power consumption due to the unnecessary temporary activation of not needed cells. Instead, or better, in addition to cell fingerprinting, periodic traffic pattern can be used for cell identification, see chapter 2.4.4. Then, in case cell fingerprinting identifies multiple best matching cells, only those cells, whose traffic pattern indicate traffic during the same time period in the previous days, are activated.

Only the radio access part of the network is considered by the energy saving model. Deactivation of small cells, however, may also negatively **impact the UE power consumption**. Caused by forced handover or radio link setup to more distant macrocells, as the close small cells is sleeping or transitioning to sleep mode, may force the UE to use a higher signal strength and thus, consume more power. Additionally, there is, albeit minimum, an expected BS power increase caused by the additional signaling exchange required for cell fingerprinting as explained in chapter 4.

CHAPTER 7

Conclusion and Future Work

Contents

7.1 Contributions and Constraints 100
7.2 Energy Saving in Operational Networks 102
7.3 Use of Cell Fingerprinting for Future Applications 103

After having investigated energy saving in cellular networks, self-organizing network procedures, and fingerprinting, this final chapter brings it all together. Starting with a short overview, we continue with the major findings and achievements in the first section. The likelihood that operators will implement the energy saving SON and cell fingerprinting in operational networks is briefly discussed in the second section. Obviously, not all ideas and approaches coming up during the creation of this work could be pursued or implemented. To keep them in mind, the possible enhancements and new ideas are put into the ultimately final section about the future work.

7.1 Contributions and Constraints

This thesis studied energy saving in radio access networks with focus on cell fingerprinting as the means of identifying sleeping cells. As a first step, we studied and evaluated the relevant topics in literature, including fingerprinting, self-organization, triggers for cell activation and deactivation as well as the energy saving potential in operational networks. The next steps concentrated on energy saving and the cell fingerprint method, where the major contributions are made in the following 3 areas:

1. **Framework for cell fingerprinting and the design of cell fingerprints:** Starting with a comprehensive concept for the temporary cell deactivation procedures, we continued with the details for cell fingerprinting as the essential approach of this thesis. The implementation of the framework for cell fingerprinting was split into the generation and the consecutive matching part. For the design of the cell fingerprints, we defined CFP metrics, which modeled the RSS distributions of the neighbor cells as measured by the UE. These CFP metrics were derived from the analysis of a huge number of recorded RSS measurements. During cell fingerprint generation, the CFP metrics were calculated, and subsequently used for cell identification in the matching process. As a next step, a simple scoring system for the matching algorithm was designed and implemented, to determine the best matching cell. The implemented basic cell fingerprint procedures reliably delivered reasonable results, which justified the CFP approach.

2. **Evaluation of the cell fingerprinting accuracy:** We implemented the proposed framework in the LTE system simulator, to determine the accuracy of identifying the target cell. Multiple parameter settings and different scenarios were evaluated, from which the major important ones were, 1) the single and combined CFP metrics and 2) the traffic conditions, which were mapped on corresponding numbers of active cells.
   The achieved accuracy varied strongly, mostly depending on the number of active neighbor cells. For example, with 20 active neighbors the best solution identified an average of 1.05 cells to be activated, which is close to the optimum of 1 cell. On the contrary, for 8 active neighbors the best solution identified an average of 2.6 cells, and even 5.4 cells if only 4 (the minimum) neighbors were active.
   However, even the rather high 5.4 cells to be activated may be considered sufficient for many cases. As the 4 active neighbors reflect a very low loaded traffic scenario, an overloaded cell may indicate an overall rising traffic demand, requiring the activation of several cells. If this is not the case, the cells would return to sleep mode, if no connection is established. Even, if just one of the 5.4 cells is activated, it was found to be virtually always an adjacent neighbor of the target cell, which is known to relieve the overloaded cell.

   Some major finding were:

   1. Averaged UE measurement samples from different UEs resident in the same cell improved the accuracy compared to single UE measurement sample. We assume that samples from UEs located at different positions of the cell, better map the RSS conditions of a cell.

   2. The accuracy strongly increased with the number of active neighbor cells, which indicated the traffic load.

   3. Typically, the accuracy also increased, if multiple single CFP metrics were summed in a combined metric. Obviously, the combination of several metrics reflects the RSS distribution of a neighbor cell better.

4. For different traffic load situations, different metrics performed best, i.e. we could not identify one best metric, which provided the best accuracy for all scenarios.

5. For low traffic situations: combined metrics with a higher number of summands mostly outperformed metrics with less summands.

The finer the gradation of the scores, which increased in line with the number of summands of a combined metric, the better is the differentiation between the sleeping cells. This is of utmost importance in case of very few matching events caused by a very low number of active neighbor cells.

3. **Evaluation of the power saving potential:** For temporarily deactivated cells of an overlaying small cell network, the energy saving potential was evaluated. The cell identification accuracy resulting from the simulation studies served as input for the model. Using cell fingerprinting, up to 47% power could be saved for the small cell overlay, which approaches closely the optimum of 47.8% power reduction.

Besides these findings and achievements of the cell fingerprint approach, also few **constraints** need to be considered:

1. Prior to the use of cell fingerprinting for cell identification, a preparation phase for the initial generation of cell fingerprints is required.

2. The BSs used for temporary cell deactivation require not only the implementation of the sleep mode, but also a fast wake-up time. Inevitably, a short delay is expected until a BS is fully up and running i.e. until the mobile users can actually transmit/receive data to/from the BS.

3. An additional approval in operational networks is recommended. Especially, the topology and the type of area, but also the countless network configurations caused by, e.g., different radio access technologies and network layouts may require different sets of metrics to achieve the optimum accuracy for cell fingerprinting.

7.2 Energy Saving in Operational Networks

Despite the world-wide concern about the carbon footprint and the environmental challenges, network operators primarily have to focus on the network quality and the costs to install and run the network. Besides the operators, also the majority of the mobile users primarily focus on their costs for network usage, but also on the perceived network quality. Therefore, the future effort in low energy consuming networks depends to the most part on the savings potential. With the installation of a huge number of additional cells to deal with the data traffic explosion, the proportion of the energy costs to the total costs to run a network is definitely expected to increase. But also the limited organic resources, e.g. oil, gas and coal, will further increase the energy price on the

medium or long term, despite short-term drops in the energy price caused by, e.g., oil overproduction or the emerging fracking industry.

Therefore, we assume that operators are very motivated to take measures for energy saving in their networks. Besides less energy consuming hardware and radio equipment, the adaption of the capacity to the changing traffic demand seems to be a rather promising approach. Especially, the strong increase of small cells and the continuously improving energy saving SON definition in the standardization work, makes the SON approach more attractive. The use of cell fingerprinting for cell identification, however, is still unclear at present.

7.3 Use of Cell Fingerprinting for Future Applications

In conclusion, we present a future outlook on possible enhancements, additional applications and new ideas for the cell fingerprinting approach. Besides procedural enhancements regarding the generation and matching of cell fingerprints, new applications for cell fingerprinting are proposed, which may not be restricted to cell level. Finally, cell fingerprinting is not limited to energy saving, but may be re-used for further radio network applications.

Self-Learning and Standardization Progress for Temporary Cell Deactivation Procedures

A future enhancement of the cell fingerprinting approach introduced in this thesis could be the implementation of a self-learning capability to avoid the repeated activation of an inappropriate cell. Erroneously activated cells can easily be determined as they return to sleep mode, if no link is established within a given monitoring time. To improve the accuracy over time, the relevant data related to each matching event (e.g. number, ID and RSS of active neighbor cells; number and ID of best matching cell; and time of day) would be recorded, appending the positive or negative associated result. Thus, the network is able to learn from the past experience, and to react appropriately, whenever a similar or identical scenario occurs.

More progress and support for future network generations is expected from the standardization group 3GPP for energy saving SON itself, as well as its integration into a unified self-management system as proposed by [69].

Update of Generated Cell Fingerprints

For the generation of cell fingerprints, we used in the simulation studies of this work, the currently received signal strength of the neighbor cells. In operational networks however, the RSS of the neighbor cells to a greater extent, but even the neighbor cells themselves, may change over time, e.g. new buildings may impact the received signal strength or new cells may be deployed. Therefore, the cell fingerprints require continuous updates to reflect the most current RF conditions. Updates are expected to be performed continuously, but also on a periodical or event driven basis. The update procedure may use the newly received samples and reprocess the cell fingerprints by overwriting the

oldest measurements. Alternatively, the latest measurements may be combined with the currently recorded measurements, whereas the most recent measures may have a higher weight. Thus, depending on the update procedure, the measurements may require time stamps. In case of network expansion or strongly changing RF conditions, the current cell fingerprints may no longer apply. Then, a completely new set of cell fingerprints may be required.

Matching Enhancements

Although cell fingerprinting is performed and evaluated in this work for several parameter setting and scenarios, still multiple additional configurations would need to be investigated. Especially very low traffic scenarios may achieve significant improvement.

Promising enhancements could be achieved by introducing further single CFP metrics, especially when used as summands for the combined CFP metrics. Also, adding a higher weight to the more accurate single CFP metrics may increase the accuracy of the combined CFP metrics.

Introducing a different type of metric, where only week RSS signals would be disregarded, i.e. the all strong RSS signals would be considered as valid, would be another promising case study.

Another area for improvement is the preprocessing of the UE samples. Besides a single sample or an average of the 2 latest received samples, further approaches could be evaluated. Examples are averaged samples from the same UE or the averages of more than 2 samples from the same or different UEs. Additionally, a higher weight for the more recent samples could be considered.

Furthermore, the impact of different radio technologies, network layouts and different topologies on cell fingerprinting could be evaluated. For example, an interesting future scenarios could be the transition from outdoor to indoor environment.

Cell Fingerprinting Accuracy beyond Cell Level

While cell fingerprinting pursues the objective to localize a cell, measurement analysis of multiple simulation studies clearly indicated an accuracy beyond cell level. Obviously, this is restricted to samples retrieved from a single UE. On the contrary, averaged samples from multiple UEs within a serving cell represent the cell characteristics more precisely. For example, using the measurements from 1 UE, which is close to the cell edge, typically the most nearby neighbor cell gets the highest scores. If a UE is located in the cell center, all adjacent neighbor cell are scored similarly. Although the energy saving SON does not require the more detailed localization information within the cell, it may be beneficial for applications, some of which are described in the next subsection.

Cell Fingerprinting Usage for Other Applications

The cell fingerprinting method is not limited to the energy saving functionality, but could also be a valid enhancement for several further cell identification or localization sensitive applications.

Temporary deactivation of cells reduces not only the energy consumption, but also the **inter-cell interference**. This may result in an increased SINR, leading to a gain in throughput. Just like for energy saving, cells would need to be activated with growing traffic demand, re-using cell fingerprinting to identify the appropriate cell.

Additionally, cell fingerprinting may contribute to the enhancement of the **handover** procedures, at least for the following 2 scenarios. Firstly, for handover optimization from a macrocell to a small cell overlay, cell fingerprinting may be used to better identify the most appropriate small cell, as proposed in [19]. Secondly, cell fingerprinting may be used to avoid repeated handover failures. Depending on the UE position, neighbor cells may provide good RSS conditions, but the HO may fail, i.e. due to very quickly changing radio conditions. A self-learning algorithm based on the relation between UE fingerprint localization information and the previous experienced handover failures may prevent future handovers to cells marked as highly risky to fail.

The feature "**minimization of drive tests**" is another example for a location sensitive application. The very cost-intensive drive tests are required for network optimization and trouble shooting. Whenever possible, they are substituted by applications, that retrieve remotely the UE measurements. Required are also reliable location information associated to the measurements on cell level or beyond, which could also be provided by cell fingerprinting.

Finally, cell fingerprinting may be used for **UE positioning**. An improved localization is expected by the decreasing cell size of future small cells, and additionally, by a possibly further enhanced accuracy beyond cell level. Then, cell fingerprinting could be used as the simple and effective, but less accurate positioning method by itself or as one additional method within a global localization procedure combining multiple localization relevant data.

Glossary

AI - the Accuracy Index - is the probability that the target cell is activated, given only the highest scoring cells are activated; i.e. it indicates how often the target cell is among the cells reaching the highest score.

ASS - the Activation Set Size - is the minimum number of cells that must be activated, if the target cell is to be activated first.

basic sum is a combined CFP metric considering the results of the single CFP metrics minMax, exclOut and Q10.

best matching cell achieved the best results (i.e. the highest score) in the matching algorithm and is therefore assumed to provide the best radio conditions to unload the overloaded cell, if activated. At best, it is identical to the target cell.

CFP - the cell fingerprint - is assumed to uniquely identify a cell. It consists of the list of neighbor cells and their associated results for each CFP metric.

CFP metric is a part of the cell fingerprint, which maps characteristics of the neighbor cell RSS distribution. Examples are the minimum and maximum (minMax) RSS and the upper and lower outlier fence (exclOut).

deactivate changes the cell state from active to sleep mode. The terms "switch off" or "put into sleep mode" are synonyms found in literature.

diffMedian is a single CFP metric derived from the absolute difference of UE RSS measure to the median of the corresponding cell fingerprint.

EEI - the Energy Efficiency Index - is the probability that the target cell is activated in case the number of cells to be activated is restricted, e.g. for energy saving reason.

ES SON is the self-organized network procedure to save energy in cellular networks. Cells are deactivated, whenever their capacity is temporarily not required to cover the capacity needs and reactivated on a need basis.

exclOut is a single CFP metric providing the range of the retrieved RSS values excluding outliers from a neighbor cell.

minMax is a single CFP metric providing the range of the retrieved RSS values from a neighbor cell.

NoCA is number of cells to be simultaneously activated; the cells with highest scores are activated first. Different to the Activation Set Size (ASS), the NoCA may exclude the target cell.

reactivate changes the cell state from sleep to active mode after a preceding cell deactivation. The terms "wake up" and "switch on" are synonyms found in literature.

sExclOut is the score of the exclOut (excluding outlier) metric, incremented during the matching procedure, whenever the RSS of the UE sample lies in the exclOut range of the cell fingerprint for the corresponding neighbor cell.

sleeping cell(s) are not able to receive or transmit any radio signal. These cells were previously deactivated and are currently in a low-power sleep mode. They can be triggered by active neighbor cells.

sMinMax is the score of the minMax metric, incremented during the matching procedure, whenever the RSS of the UE sample lies in the minMax range of the cell fingerprint for the corresponding neighbor cell.

sQ10 is the score of the Q10 (decile) metric, incremented during the matching procedure, whenever the RSS of the UE sample lies in the Q10 range of the cell fingerprint for the corresponding neighbor cell.

target cell is the sleeping cell known to be the best cell to take over the traffic from the cell in overload. The measurement sample used for the matching procedure originates from a UE resident in this cell. If the matching algorithm exclusively identifies the target cell, the optimum result is achieved.

List of Acronyms

2G	Second Generation
3G	Third Generation
4G	Fourth Generation
5G	Fifth Generation
3GPP	Third Generation Partnership Project
ASS	Activation Set Size
BS	Base Station
CCO	Coverage and Capacity Optimization
CFP	Cell Fingerprint
CI	Cell Identification
CIO	Cell Individual Offset
DRX	Discontinuous Reception
DTX	Discontinuous Transmission
EARTH	Energy Aware Radio and NeTwork TecHnologies
ES	Energy Saving
ES SON	Energy Saving Self-Organizing Networks
eNB	E-UTRAN NodeB
eNodeB	E-UTRAN NodeB
E-UTRAN	Evolved Universal Terrestrial Radio Access Network
GPS	Global Positioning System
GSM	Global System for Mobile communication
HetNet	Heterogeneous Network
HO	Handover

HSPA	High Speed Packet Access
ID	Identifier
ICIC	Inter-Cell Interference Coordination
IP	Internet Protocol
IoT	Interference over Thermal
IQR	Interquartile Range
LTE	Long Term Evolution
LTE-A	LTE Advanced
MBSFN	Multicast-broadcast single-frequency network
MAC	Media Access Control
MIMO	Multiple Input Multiple Output
MLB	Mobility Load Balancing
MRO	Mobility Robustness Optimization
NGMN	Next Generation Mobile Networks
OAM	Operation, Administration and Maintenance
OFDMA	Orthogonal Frequency Division Multiple Access
PA	Power Amplifier
Q2	Range between 2nd and 98th Percentile
Q5	Range between 5th and 95th Percentile
Q10	Range between 10th and 90th Percentile
Q20	Range between 20th and 80th Percentile
QoS	Quality of Service
QoE	Quality of Experience
OPEX	Operational Expenditure
RAN	Radio Access Network
RAT	Radio Access Technology
RF	Radio Frequency
RSS	Received Signal Strength
SINR	Signal to Interference and Noise Ratio
SNR	Signal to Noise Ratio
SON	Self-Organizing Networks
TDoA	Time Difference of Arrival
ToA	Time of Arrival
TP	True Positive
Tx	Transmit
UC	Use Case
UE	User Equipment
UML	Universal Modeling Language

UMTS Universal Mobile Telecommunications System

WCDMA Wideband Code Division Multiple Access

WLAN Wireless Local Area Network

Bibliography

[1] J. Randers, *2052: A Global Forecast for the Next Forty Years*. Chelsea Green Publishing, 2012.

[2] M. Olsson, C. Cavdar, P. Frenger, S. Tombaz, D. Sabella, and R. Jantti, "5GrEEn: Towards Green 5G Mobile Networks," in *IEEE 9th International Conference on Wireless and Mobile Computing, Networking and Communications (WiMob)*, 2013, pp. 212–216.

[3] G. Fettweis and S. Alamouti, "5G: Personal Mobile Internet beyond what Cellular did to Telephony," *IEEE Communications Magazine*, vol. 52, no. 2, pp. 140–145, February 2014.

[4] Cisco, "Cisco VNI Mobile. Cisco Visual Networking Index: Global Mobile Data Traffic Forecast Update 2013–2018," 2014. [Online]. Available: www.cisco.com/c/en/us/solutions/collateral/service-provider/visual-networking-index-vni/white_paper_c11-520862.html [Accessed: 2015-10-19]

[5] ICT Facts and Figures: The World in 2014. [Online]. Available: www.itu.int/en/ITU-D/Statistics/Pages/facts [Accessed: 2015-10-19]

[6] Z. Zheng, X. Zhang, L. Cai, R. Zhang, and X. Shen, "Sustainable Communication and Networking in Two-tier Green Cellular Networks," *IEEE Wireless Communications*, vol. 21, no. 4, pp. 47–53, 2014.

[7] J. Hoydis, M. Kobayashi, and M. Debbah, "Green Small-Cell Networks," *IEEE Vehicular Technology Magazine*, vol. 6, no. 1, pp. 37–43, 2011.

[8] Virtual Excellence in Mobile and Personal Communications Ltd (VCE) – Green Radio. [Online]. Available: www.mobilevce.com/green-radio [Accessed: 2015-10-19]

[9] B. Lannoo, S. Lambert, W. Van Heddeghem, M. Pickavet, F. Kuipers, G. Koutitas, H. Niavis, A. Satsiou, M. Till, A. F. Beck *et al.*, "Overview of ICT Energy Consumption," EINS Project, Public Deliverable D8.1, 2013.

[10] P. Frenger, P. Moberg, J. Malmodin, Y. Jading, and I. Gódor, "Reducing Energy Consumption in LTE with Cell DTX," in *IEEE 73rd Vehicular Technology Conference (VTC Spring)*, 2011, pp. 1–5.

[11] Centre for Energy-Efficient Telecommunication; Bell Labs and University of Melbourne, "The Power of Wireless Cloud," *White Paper*, 2013.

[12] H. Klessig, A. Fehske, G. Fettweis, and J. Voigt, "Cell Load-Aware Energy Saving Management in Self-Organizing Networks," in *IEEE 78th Vehicular Technology Conference (VTC Fall)*, Sept 2013, pp. 1–6.

[13] A. Fehske, G. Fettweis, J. Malmodin, and G. Biczok, "The Global Footprint of Mobile Communications: The Ecological and Economic Perspective," *IEEE Communications Magazin*, vol. 49, 2011.

[14] J. Manner, M. Luoma, J. Ott, and J. Hämäläinen, "Mobile Networks Unplugged," in *ACM Proceedings of the 1st International Conference on Energy-Efficient Computing and Networking*, 2010, pp. 71–74.

[15] 3GPP TR 36.927, v12.0.0, "Evolved Universal Terrestrial Radio Access (E-UTRA); Potential Solutions for Energy Saving for E-UTRA (Release 10)," September 2014.

[16] M. Ajmone Marsan, L. Chiaraviglio, D. Ciullo, and M. Meo, "On the Effectiveness of Single and Multiple Base Station Sleep Modes in Cellular Networks," *Computer Networks*, vol. 57, no. 17, pp. 3276–3290, 2013.

[17] E. Roth-Mandutz, S. S. Mwanje, and A. Mitschele-Thiel, "RSS based Cell Fingerprint Patterns and Algorithms for Cell Identification in the Context of Self-organized Energy Saving," in *ICST (Institute for Computer Sciences, Social-Informatics and Telecommunications Engineering) Proceedings of the 11th International Conference on Mobile and Ubiquitous Systems: Computing, Networking and Services*, 2014, pp. 397–400.

[18] ——, "Cell Identification based on Received Signal Strength Fingerprints: Concept and Application towards Energy Saving in Cellular Networks," *EAI Endorsed Transactions on Mobile Communications and Applications*, vol. 14, no. 1, 9 2014.

[19] A. Prasad, O. Tirkkonen, P. Lunden, O. N. Yilmaz, L. Dalsgaard, and C. Wijting, "Energy-Efficient Inter-Frequency Small Cell Discovery Techniques for LTE-Advanced Heterogeneous Network Deployments," *IEEE Communications Magazine*, vol. 51, no. 5, pp. 72–81, 2013.

[20] E. Roth-Mandutz and A. Mitschele-Thiel, "LTE Energy Saving SON using Fingerprinting for Identification of Cells to be Activated," in *IEEE Proceedings of Future Network and Mobile Summit (FutureNetworkSummit), Lisbon, Portugal*, July 2013, pp. 1–8.

[21] GreenTouch, 2010-2015. [Online]. Available: www.greentouch.org [Accessed: 2015-10-19]

[22] EIT-ICT Labs Project, "5GrEEn - Towards Green 5G Mobile Networks," Tech. Rep., 2013-2015. [Online]. Available: www.eitictlabs.eu/news-events/news/article/toward-green-5g-mobile-networks-5green-new-project-launched/ [Accessed: 2015-10-19]

[23] M. Olsson, C. Cavdar, P. Frenger, S. Tombaz, D. Sabella, and R. Jantti, "5GrEEn: Towards Green 5G Mobile Networks," in *IEEE 9th International Conference on Wireless and Mobile Computing, Networking and Communications (WiMob)*, Oct 2013, pp. 212–216.

[24] Towards Real Energy-efficient Network Design (TREND), 2010-2013. EU Seventh Framework Programme for Research and Technological Development (FP7) project INFSO-ICT-257740. [Online]. Available: cordis.europa.eu/project/rcn/95446_en.html [Accessed: 2015-10-19]

[25] G. Biczók, J. Malmodin, and A. Fehske, "Economic and Ecological Impact of ICT," ICT-EARTH; EARTH Project Work Package: Public Deliverable D2.1(2.0), 2011.

[26] D. Zeller, M. Olsson, O. Blume, A. Fehske, D. Ferling, W. Tomaselli, and I. Gódor, *Sustainable Wireless Broadband Access to the Future Internet - The EARTH Project*. Springer, 2013.

[27] 3GPP TR 36.902, v9.3.1, "Evolved Universal Terrestrial Radio Access Network (E-UTRAN); Self-Configuration and Self-Optimizing Network Use Cases and Solutions (Release 9)," March 2011.

[28] 3GPP Release 12, v0.2.0, "Overview of 3GPP Release 12," September 2015.

[29] A. De Domenico, E. Calvanese Strinati, and A. Capone, "Enabling Green Cellular Networks: A Survey and Outlook," *Computer Communications*, vol. 37, pp. 5–24, 2014.

[30] Y. Zhang, L. Budzisz, M. Meo, A. Conte, I. Haratcherev, G. Koutitas, L. Tassiulas, M. A. Marsan, and S. Lambert, "An Overview of Energy-Efficient Base Station Management Techniques," in *IEEE 24th Tyrrhenian International Workshop on Digital Communications-Green ICT (TIWDC)*, 2013, pp. 1–6.

[31] M. Olsson, A. Fehske, L. Hevizi, O. Blume, A. Vidacs, I. Godor, P. Fazekas, M. A. Imran, and Y. Qi, "Integration Strategy of EARTH Energy Efficiency Enablers," in *IEEE Future Network & Mobile Summit (FutureNetw)*, 2012, pp. 1–8.

[32] C. R. Murthy and D. C. Kavitha, "A Survey of Green Base Stations in Cellular Networks," *ISSN IRACST–International Journal of Computer Networks and Wireless Communications (IJCNWC)*, pp. 2250–3501, 2012.

[33] M. A. Imran, E. Katranaras, G. Auer, O. Blume, V. Giannini, I. Godor, Y. Jading, M. Olsson, D. Sabella, P. Skillermark *et al.*, "Energy Efficiency Analysis of the Reference Systems, Areas of Improvements and Target Breakdown," ICT-EARTH; EARTH Project Work Package: Public Deliverable D2.3, 2012.

[34] T. Chen, Y. Yang, H. Zhang, H. Kim, and K. Horneman, "Network Energy Saving Technologies for Green Wireless Access Networks," *IEEE Wireless Communications*, vol. 18, no. 5, pp. 30–38, 2011.

[35] Z. Hasan, H. Boostanimehr, and V. K. Bhargava, "Green Cellular Networks: A Survey, some Research Issues and Challenges," *IEEE Communications Surveys & Tutorials*, vol. 13, no. 4, pp. 524–540, 2011.

[36] 3GPP TR 23.866, v12.0.0, "Study on System Improvements for Energy Efficiency (Release 12)," June 2012.

[37] I. Godor *et al.*, "Most Promising Tracks of Green Network Technologies," ICT-EARTH; EARTH Project Work Package: Public Deliverable D3.1, 2010.

[38] L. M. Correia, D. Zeller, O. Blume, D. Ferling, Y. Jading, I. Gódor, G. Auer, and L. Van Der Perre, "Challenges and Enabling Technologies for Energy aware Mobile Radio Networks," *IEEE Communications Magazine*, vol. 48, no. 11, pp. 66–72, 2010.

[39] L.-C. Wang and S. Rangapillai, "A Survey on Green 5G Cellular Networks," in *International Conference on Signal Processing and Communications (SPCOM)*, July 2012, pp. 1–5.

[40] K. Abdallah, I. Cerutti, and P. Castoldi, "Energy-Efficient Coordinated Sleep of LTE Cells," in *IEEE International Conference on Communications (ICC)*, 2012, pp. 5238–5242.

[41] J. Gong, J. Thompson, S. Zhou, and Z. Niu, "Base Station Sleeping and Resource Allocation in Renewable Energy Powered Cellular Networks," *IEEE Transactions on Communications*, vol. 62, no. 11, pp. 3801–3813, Nov 2014.

[42] K. Son, H. Kim, Y. Yi, and B. Krishnamachari, "Base Station Operation and User Association Mechanisms for Energy-Delay Tradeoffs in Green Cellular Networks," *IEEE Journal on Selected Areas in Communications*, vol. 29, no. 8, pp. 1525–1536, 2011.

[43] M. H. Alsharif, R. Nordin, and M. Ismail, "A Review on Intelligent Base Stations Cooperation Management Techniques for Greener LTE Cellular Networks," *Journal of Communications*, vol. 9, no. 12, 2014.

[44] J. Meseguer Llopis, Ł. Rajewski, and S. Kuklinski, "Reinforcement Learning based Energy Efficient LTE RAN," in *ACM Proceedings of the 2014 Conference Companion on Genetic and Evolutionary Computation Companion*, 2014, pp. 1197–1204.

[45] E. Ternon, P. Agyapong, L. Hu, and A. Dekorsy, "Energy Savings in Heterogeneous Networks with Clustered Small Cell Deployments," in *IEEE 11th International Symposium on Wireless Communications Systems (ISWCS)*, 2014, pp. 126–130.

[46] Z. Niu, Y. Wu, J. Gong, and Z. Yang, "Cell Zooming for Cost-Efficient Green Cellular Networks," *IEEE Communications Magazine*, vol. 48, no. 11, pp. 74–79, November 2010.

[47] Y. Zhu, T. Kang, T. Zhang, and Z. Zeng, "QoS-aware User Association based on Cell Zooming for Energy Efficiency in Cellular Networks," in *IEEE 24th International Symposium on Personal, Indoor and Mobile Radio Communications (PIMRC Workshops)*, 2013, pp. 6–10.

[48] 3GPP, "LTE." [Online]. Available: www.3gpp.org/LTE [Accessed: 2015-10-19]

[49] D. Ferling *et al.*, "Final Report on Green Radio Technologies," ICT-EARTH; EARTH Project Work Package: Public Deliverable D4.3, 2012.

[50] G. Auer, V. Giannini, I. Gódor, P. Skillermark, M. Olsson, M. A. Imran, D. Sabella, M. J. Gonzalez, C. Desset, and O. Blume, "Cellular Energy Efficiency Evaluation Framework," in *IEEE 73rd Vehicular Technology Conference (VTC Spring)*, 2011, pp. 1–6.

[51] NTT-DOCOMO, Alcatel-Lucent, Alcatel-Lucent Shanghai Bell, Ericsson and Telecom Italia, "Base Station Power Model," *TSG-RAN WG1 #66bis, R1-11 3495*, 2011.

[52] J. Lorincz, T. Garma, and G. Petrovic, "Measurements and Modelling of Base Station Power Consumption under Real Traffic Loads," *Sensors*, vol. 12, no. 4, pp. 4281–4310, 2012.

[53] A. Fehske, "How Much Energy is Needed to Run a Wireless Network?" *IEEE Wireless Communications*, p. 41, 2011.

[54] 4G Americas, "Self-Optimizing Networks in 3GPP Release 11: The Benefits of SON in LTE," *White Paper*, October 2013.

[55] R. Bendlin, V. Chandrasekhar, R. Chen, A. Ekpenyong, and E. Onggosanusi, "From Homogeneous to Heterogeneous Networks: A 3GPP Long Term Evolution Rel. 8/9 Case Study," in *IEEE 45th Annual Conference on Information Sciences and Systems (CISS)*, 2011, pp. 1–5.

[56] A. Damnjanovic, J. Montojo, Y. Wei, T. Ji, T. Luo, M. Vajapeyam, T. Yoo, O. Song, and D. Malladi, "A Survey on 3GPP Heterogeneous Networks," *IEEE Wireless Communications*, vol. 18, no. 3, pp. 10–21, 2011.

[57] 3GPP TS 22.220, v12.0.0, "Service Requirements for Home NodeBs and Home eNodeBs (Release 12)," October 2014.

[58] A. Roessler and M. Kottkamp, "LTE-Advanced (3GPP Rel.11) - Technology Introduction," *White Paper*, 2013.

[59] P. Dini, M. Miozzo, N. Bui, and N. Baldo, "A Model to Analyze the Energy Savings of Base Station Sleep Mode in LTE HetNets," in *IEEE International Conference on Green Computing and Communications (GreenCom) and IEEE Internet of Things(iThings) and IEEE Cyber, Physical and Social Computing(CPSCom)*, 2013, pp. 1375–1380.

[60] A. Prasad, A. Maeder, and C. Ng, "Energy Efficient Small Cell Activation Mechanism for Heterogeneous Networks," in *IEEE Globecom Workshops (GC Wkshps)*, 2013, pp. 754–759.

[61] E. Ternon, P. Agyapong, L. Hu, and A. Dekorsy, "Database-Aided Energy Savings in Next Generation Dual Connectivity Heterogeneous Networks," in *IEEE Wireless Communications and Networking Conference (WCNC)*, 2014, pp. 2811–2816.

[62] O. Fratu, A. Vulpe, R. Craciunescu, and S. Halunga, "Small Cells in Cellular Networks: Challenges of Future HetNets," *Wireless Personal Communications*, vol. 78, no. 3, pp. 1613–1627, 2014.

[63] T. Q. Quek, G. de la Roche, I. Güvenç, and M. Kountouris, *Small Cell Networks: Deployment, PHY Techniques, and Resource Management*. Cambridge University Press, 2013.

[64] D. T. Ngo and T. Le-Ngoc, *Architectures of Small-Cell Networks and Interference Management*. Springer, 2014.

[65] NTT DOCOMO, 3GPP TSG RAN WG1, R1-133456, "Views on Small Cell On/Off Mechanisms," August 2013.

[66] Next Generation Mobile Networks, "Use Cases related to Self Organising Network, Overall Description," 2007. [Online]. Available: www.ngmn.org [Accessed: 2015-10-19]

[67] SOCRATES (Self-Optimisation and self-ConfiguRATion in wirelEss networkS), 2008-2010. EU Seventh Framework Program, INFSO-ICT-216284. [Online]. Available: www.fp7-socrates.eu [Accessed: 2015-10-19]

[68] 3GPP TR 37.822, v12.1.0, "Study on Next Generation Self-Optimizing Network (SON) for UTRAN and E-UTRAN (Release 12)," March 2015.

[69] Self-Management for Unified Heterogeneous Radio Access Networks (SEMAFOUR), 2012-2015. EU Seventh Framework Programme for Research and Technological Development (FP7). [Online]. Available: www.fp7-semafour.eu [Accessed: 2015-10-19]

[70] 3GPP TS 32.511, v12.0.0, "Automatic Neighbour Relation (ANR) Management; Concepts and Requirements (Release 12)," September 2014.

[71] 3GPP TR 32.522, v11.7.0, "Self-Organizing Networks (SON) Policy Network Resource Model (NRM) Integration Reference Point (IRP); Information Service (IS) (Release 11)," September 2013.

[72] 3GPP TR 32.551, v12.0.0, "Energy Saving Management (ESM); Concepts and Requirements (Release 12)," September 2014.

[73] 3GPP TR 36.300, v13.1.0, "Evolved Universal Terrestrial Radio Access (E-UTRA) and Evolved Universal Terrestrial Radio Access Network (E-UTRAN); Overall Description; Stage 2 (Release 13)," September 2015.

[74] 3GPP TR 32.834, v11.0.0, "Study on Operations, Administration and Maintenance (OAM); Aspects of Inter-Radio-Access-Technology (RAT) Energy Saving (Release 11)," January 2012.

[75] 3GPP TS 36.423, v13.1.0, "Evolved Universal Terrestrial Radio Access Network (E-UTRAN); X2 Application Protocol (X2AP) (Release 13)," September 2015.

[76] S. Hämäläinen, H. Sanneck, and C. Sartori, *LTE Self-Organising Networks (SON): Network Management Automation for Operational Efficiency*. John Wiley & Sons, 2012.

[77] C. Peng, S.-B. Lee, S. Lu, H. Luo, and H. Li, "Traffic-Driven Power Saving in Operational 3G Cellular Networks," in *ACM Proceedings of the 17th Annual International Conference on Mobile Computing and Networking*, 2011, pp. 121–132.

[78] E. Oh, B. Krishnamachari, X. Liu, and Z. Niu, "Toward Dynamic Energy-Efficient Operation of Cellular Network Infrastructure," *IEEE Communications Magazine*, vol. 49, no. 6, pp. 56–61, 2011.

[79] A. Yildiz, T. Girici, and H. Yanikomeroglu, "A Pricing Based Algorithm for Cell Switching Off in Green Cellular Networks," in *IEEE 77th Vehicular Technology Conference (VTC Spring)*, June 2013, pp. 1–6.

[80] GreenTouch Consortium and others, "GreenTouch Green Meter Research Study: Reducing the Net Energy Consumption in Communications Networks by up to 90% by 2020," June 2013.

[81] European Commission. (2015) Digital Agenda for Europe; A Europe 2020 Initiative - Broadband Strategy & Policy. [Online]. Available: ec.europa.eu/digital-agenda/en/broadband-strategy-policy [Accessed: 2015-09-15]

[82] J. Seitz, T. Vaupel, S. Haimerl, S. Meyer, J. G. Boronat, G. Rohmer, and J. Thielecke, "Wi-Fi Attitude and Position Tracking," in *Microelectronic Systems*. Springer, 2011, pp. 173–185.

[83] T. Vaupel, J. Seitz, F. Kiefer, S. Haimerl, and J. Thielecke, "Wi-Fi Positioning: System Considerations and Device Calibration," in *IEEE Proceedings of International Conference on Indoor Positioning and Indoor Navigation (IPIN), Zurich, Switzerland*, September 2010, pp. 1–7.

[84] V. Honkavirta, T. Perälä, S. Ali-Löytty, and R. Piché, "A Comparative Survey of WLAN Location Fingerprinting Methods," in *6th Workshop on Positioning, Navigation and Communication, WPNC 2009, Leibniz Universität Hannover, Hannover, Germany, March 19, 2009*, 2009, pp. 243–251.

[85] M. Quan, E. Navarro, and B. Peuker, "Wi-Fi Localization using RSSI Fingerprinting," 2010.

[86] Y. Mo, Z. Cao, and B. Wang, "Occurrence-Based Fingerprint Clustering for Fast Pattern-Matching Location Determination," *IEEE Communications Letters*, vol. 16, no. 12, 2012.

[87] N. Al Khanbashi, N. Al Sindi, S. Al-Araji, N. Ali, Z. Chaloupka, V. Yenamandra, and J. Aweya, "Real Time Evaluation of RF Fingerprints in Wireless LAN Localization Systems," in *IEEE 10th Workshop on Positioning Navigation and Communication (WPNC)*, 2013, pp. 1–6.

[88] P. Rao and P. Siccardo, "Location Determination using RF Fingerprinting," Jul. 31 2001, US Patent 6,269,246. [Online]. Available: www.google.de/patents/US6269246 [Accessed: 2015-10-19]

[89] H. Laitinen, S. Ahonen, S. Kyriazakos, J. Lähteenmäki, R. Menolascino, and S. Parkkila, "Cellular Location Technology," *Public Deliverable of IST/CELLO Project*, 2001.

[90] M. Ibrahim and M. Youssef, "CellSense: A Probabilistic RSSI-Based GSM Positioning System," in *IEEE Global Telecommunications Conference (GLOBECOM 2010)*, Dec 2010, pp. 1–5.

[91] E. Roth-Mandutz, "Use of GSM Devices for Stand-alone Localization Including Differentiation to WLAN Fingerprinting," Master's Thesis, Fraunhofer Institut IIS and Georg Simon Ohm University of Applied Sciences, 2010.

[92] M. Laaraiedh, L. Yu, S. Avrillon, and B. Uguen, "Comparison of Hybrid Localization Schemes using RSSI, TOA, and TDOA," in *11th European Wireless Conference 2011 - Sustainable Wireless Technologies (European Wireless)*, April 2011, pp. 1–5.

[93] S. Fischer, "Observed Time Difference of Arrival (OTDOA) Positioning in 3GPP LTE," *White Paper*, 2014.

[94] L. Xin-Di, H. Wei, and T. Zeng-Shan, "The Improvement of RSS-based Location Fingerprint Technology for Cellular Networks," in *IEEE Proceedings of International Conference on Computer Science & Service System (CSSS), Nanjing, China*, August 2012, pp. 1267–1270.

[95] K. Hiltunen, "Improving the Energy-Efficiency of Dense LTE Networks by Adaptive Activation of Cells," in *Proceedings of IEEE International Communications Workshops (ICC), Budapest, Hungary*, June 2013, pp. 1150–1154.

[96] ——, "Utilizing eNodeB Sleep Mode to Improve the Energy-Efficiency of Dense LTE Networks," in *Proceedings of IEEE 24th International Symposium on Personal Indoor and Mobile Radio Communications (PIMRC), London, United Kingdom*, September 2013, pp. 3249–3253.

[97] 3GPP TR 32.826, v10.0.0, "Study on Energy Saving Management (ESM) (Release 10)," March 2010.

[98] 4G Americas, "Self-Optimizing Networks: The Benefits of SON in LTE," *White Paper*, July 2011.

[99] T. Beitelmal and H. Yanikomeroglu, "A Set Cover Based Algorithm for Cell Switch-Off with Different Cell Sorting Criteria," in *IEEE International Conference on Communications Workshops (ICC)*, June 2014, pp. 641–646.

[100] IKR Simulation and Emulation Library. Institute of Communication Networks and Computer Engineering (IKR); University of Stuttgart. [Online]. Available: http://www.ikr.uni-stuttgart.de/en/Content/IKRSimLib/ [Accessed: 2015-09-15]

[101] S. S. Mwanje, "Coordinating Coupled Self-Organized Network Functions in Cellular Radio Networks," Ph.D. Dissertation, Ilmenau University of Technology, 2015.

[102] M. Naseer-ul Islam, "Self-Organized Coverage and Capacity Optimization for Cellular Mobile Networks," Ph.D. Dissertation, Ilmenau University of Technology, 2013.

[103] 3GPP TR 36.814, v9.0.0, "E-UTRA; Further Advancements for E-UTRA Physical Layer Aspects (Release 9)," March 2010.

[104] M. Gudmundson, "Correlation Model for Shadow Fading in Mobile Radio Systems," *Electronics Letters*, vol. 27, no. 23, pp. 2145–2146, 1991.

[105] Z. Yang, L. Jian, C. Wu, and Y. Liu, "Beyond Triangle Inequality: Sifting Noisy and Outlier Distance Measurements for Localization," *ACM Transactions on Sensor Networks (TOSN)*, vol. 9, no. 2, p. 26, 2013.

[106] J. W. Tukey, "Exploratory Data Analysis," Reading, Mass.: Addison Wesley Pub Co Inc, 1977.

[107] Energy Aware Radio and neTwork tecHnologies (EARTH), 2010-2012. EU Seventh Framework Programme for Research and Technological Development (FP7) project INFSO-ICT-247733. [Online]. Available: www.ict-earth.eu [Accessed: 2015-10-19]

Erklärung

Ich versichere, dass ich die vorliegende Arbeit ohne unzulässige Hilfe Dritter und ohne Benutzung anderer als der angegebenen Hilfsmittel angefertigt habe. Die aus anderen Quellen direkt oder indirekt übernommenen Daten und Konzepte sind unter Angabe der Quelle gekennzeichnet.

Weitere Personen waren an der inhaltlich-materiellen Erstellung der vorliegenden Arbeit nicht beteiligt. Insbesondere habe ich hierfür nicht die entgeltliche Hilfe von Vermittlungs- bzw. Beratungsdiensten (Promotionsberater oder anderer Personen) in Anspruch genommen. Niemand hat von mir unmittelbar oder mittelbar geldwerte Leistungen für Arbeiten erhalten, die im Zusammenhang mit dem Inhalt der vorgelegten Dissertation stehen.

Die Arbeit wurde bisher weder im In- noch im Ausland in gleicher oder ähnlicher Form einer Prüfungsbehörde vorgelegt.

Ich bin darauf hingewiesen worden, dass die Unrichtigkeit der vorstehenden Erklärung als Täuschungsversuch bewertet wird und gemäß § 7 Abs. 10 der Promotionsordnung den Abbruch des Promotionsverfahrens zur Folge hat.

Ilmenau, 05.11.2015 Elke Roth-Mandutz